

**DEVELOPMENT OF NATURAL DYE COATING FROM
ANTHOCYANIN MIXED WITH WATER-BASED POLYMER**

LEE SU VEI

**DISSERTATION SUBMITTED IN FULFILMENT OF
THE REQUIREMENTS FOR THE DEGREE OF
MASTER OF SCIENCE**

**DEPARTMENT OF PHYSICS
FACULTY OF SCIENCE
UNIVERSITY OF MALAYA
KUALA LUMPUR**

2013

ABSTRACT

In this work, anthocyanin dye extracted from roselle (*Hibiscus sabdariffa* L.) has been used as colourant in poly(vinyl alcohol) coating. Various additives were individually introduced into the aqueous anthocyanin. Coating was formulated by mixing the aqueous anthocyanin containing additive with PVA. Stability and properties of anthocyanin dye in aqueous as well as in coating were studied. In study of UV stability of aqueous anthocyanin, addition of hydrochloric acid enhanced UV stability of anthocyanin with a lower degradation rate of 0.0033 h^{-1} . In study of storage stability of the aqueous anthocyanin, zinc nitrate was found to inhibit fungi growth, with no fungi colony visible and high colour stability as shown with a low total colour change (ΔE) of 13.60. Hydrochloric acid has also caused a shift in the degradation temperature to $305.37 \text{ }^\circ\text{C}$, considerably the highest among other samples. In UV degradation study of PVA coating, addition of acetic acid and hydrochloric acid has individually enhanced colour stability of the coating, with a total colour change of 8.95 and 16.89 respectively, lower compared to other samples. Addition of nitrate salts, on the other hand, caused a structural change in the coating. Formation of hydrogen bonding can be deduced from infrared spectroscopy. Shifts in the O-H stretching and bending, CH_2 , and CH_3 vibrations can be observed. Increase in relative intensities of these groups due to presence of nitrate indicates hydrogen bonding between PVA and nitrate. Presence of hydrogen bonding can also be reflected on the increase in glass transition temperature of PVA samples. This indicated that the coating became glassy. Structural change in the coating was also supported by XRD study. Broadness of the diffraction halo has increased upon addition of nitrate salt. This subsequently reduced the size of the ordered domains as indicated by a shorter Scherrer column length.

ABSTRAK

Dalam kerja ini, pewarna antosianin diekstrak daripada rosel (*Hibiscus sabdariffa* L.) telah digunakan sebagai pewarna dalam saduran poli(vinil alkohol). Pelbagai bahan tambahan telah ditambah secara individu ke dalam antosianin akueous. Saduran telah dirumuskan dengan mencampurkan antosianin akueous mengandungi bahan tambahan dengan PVA. Kestabilan dan ciri-ciri pewarna antosianin dalam akueous dan dalam saduran telah dikaji. Dalam kajian kestabilan UV antosianin akueous, penambahan asid hidroklorik telah meningkatkan kestabilan UV antosianin dengan kadar degradasi yang lebih rendah iaitu 0.0033 h^{-1} . Dalam kajian kestabilan penyimpanan antosianin akueous, zink nitrat ditemui merencatkan pertumbuhan fungi, dengan tiada koloni fungi dinampak dan kestabilan warna yang tinggi seperti yang ditunjuk oleh jumlah perubahan warna (ΔE) yang rendah, iaitu 13.60. Asid hidroklorik telah menyebabkan peralihan dalam suhu degradasi kepada $305.37 \text{ }^\circ\text{C}$, boleh dianggap paling tinggi antara sampel-sampel lain. Dalam kajian degradasi UV saduran PVA, tambahan asid asetik dan asid hidroklorik telah secara individu meningkatkan kestabilan warna saduran tersebut, dengan jumlah perubahan warna 8.95 dan 16.89 masing-masing, lebih rendah dibandingkan sampel-sampel lain. Tambahan garam nitrat, sebaliknya, menyebabkan perubahan struktur dalam saduran. Pembentukan ikatan hidrogen boleh disimpulkan daripada spektroskopi infra merah. Peralihan dalam getaran O-H regangan dan bongkokan, CH_2 , and CH_3 dapat diperhatikan. Peningkatan dalam intensiti relatif kumpulan ini kesan daripada kehadiran nitrat menunjukkan ikatan hidrogen antara PVA dan nitrat. Kehadiran ikatan hydrogen boleh juga diperhatikan daripada peningkatan suhu peralihan kaca sampel PVA. Ini menunjukkan saduran menjadi lebih bersifat kaca. Perubahan struktur dalam saduran juga disokong oleh kajian XRD. Kelebaran halo

belauan telah meningkat dengan penambahan garam nitrat. Ini seterusnya mengurangkan saiz domain tersusun seperti yang ditunjukkan oleh Sherrer panjang lajur yang lebih pendek.

ACKNOWLEDGEMENTS

First of all, I would like to express warmest gratitude for my supervisor Dr. Zul Hazrin bin Zainal Abidin and co-supervisor Prof. Dr. Abdul Kariem bin Mohd Arof for their dedicated efforts in aiding and contributing not only ideas and suggestions but energy, time and financial support without which this work would not have come into completion. It is noble what they have contributed and sacrificed not only for this work but for the whole scientific community as well. I would like to also thank all colleagues and lab mates who have extended their hands to me at the most demanding hour, and such are Dr. Norhana Abdul Halim, Dr. Vengadaesvaran, Dr. Rameh Kasi, Dr. Siti Rohana, Ghassan, Nisa, Umai, Mira, Ramis Rau and all others at the Center for Ionics, UM. Last but not least, I would like to extend my heartiest appreciation and thanks to my family, parents, siblings, and family relatives who have garnered and rallied their support behind me and believe in me for so many years, and for many years yet to come.

LIST OF PUBLICATIONS

1. **Lee, S.V.**, Vengadaesvaran, B., Arof, A.K. and Abidin, Z.H.Z. (2013). Characterisation of poly(acrylamide-co-acrylic acid) mixed with anthocyanin pigment from *Hibicus sabdariffa* L. *Pigment and Resin Technology*, 42 (2), 103-110.
2. **Lee, S.V.**, Halim, N.A., Arof, A.K. and Abidin, Z.H.Z. (2013). Characterisation of poly(vinyl alcohol) coating mixed with anthocyanin dye extracted from roselle flower with different nitrate salt. *Pigment and Resin Technology*, 42 (2), 146-151.
3. Abidin, Z.H.Z., Naziron, N.N., Nasir, K.M., Rusli, M.S., **Lee, S.V.**, Kufian, M.Z., Majid, S.R., Vengadaesvaran, B., Arof, A.K., Taha, R.M. and Yahya, R. (2013). Influence of curcumin natural dye colorant with PMMA-acrylic polyol blended polymer. *Pigment and Resin Technology*, 42 (2), 95-102.
4. Abidin, Z.H.Z., Nasir, K.M., Jamari, S.K.M., Saidon, N., **Lee, S.V.**, Halim, N.A. and Yahya, R. (2013). The characteristics of a coating system containing lawsone dye colorant and PMMA-acrylic polyol blended resin. *Pigment and Resin Technology*, 42 (2), 128-136.

LIST OF CONTENTS

	Page
Abstract	i
Abstrak	ii
Acknowledgements	iv
List of Publications	v
List of Contents	vi
List of Figures	ix
List of Tables	xii
CHAPTER 1: INTRODUCTION	
1.1 Research Background	1
1.2 History of Coatings	2
1.3 Coatings in Industry	3
1.4 Scope of Thesis	3
CHAPTER 2: LITERATURE REVIEW	
2.1 Coating and Its Composition	5
2.2 Binder	5
2.2.1 Poly(Vinyl Alcohol) (PVA)	6
2.2.2 Synthesis	6
2.2.3 Physical and Chemical Properties	8
2.2.4 Applications	9
2.3 Pigment and Dye	9
2.3.1 Anthocyanin Pigment	11
2.3.2 Structure of Anthocyanin	12
2.3.3 Anthocyanin Stability	14
2.3.4 <i>Hibiscus sabdariffa</i> L. Plant	16
2.4 Solvent	18
2.5 Additives	20

CHAPTER 3: METHODOLOGY

3.1	Sample Preparation	22
3.2	Characterisation on Anthocyanin Extract	23
3.2.1	UV-Visible Absorption Spectroscopy	23
3.2.2	The pH Differential Method	26
3.2.3	Test for UV Stability	28
3.2.4	Test for Fungal Degradation	28
3.3	Characterisation on PVA Coatings	29
3.3.1	Fourier Transform Infrared (FTIR) Spectroscopy	29
3.3.2	Thermogravimetric Analysis (TGA)	32
3.3.3	Glass Transition Temperature by DSC	34
3.3.4	CIELAB Colourimetry	38
3.3.5	X-Ray Diffraction Measurement	40

CHAPTER 4: CHARACTERISATION ON AQUEOUS ANTHOCYANIN

4.1	The pH Differential Method	42
4.2	UV-Visible Absorption Spectroscopy	43
4.3	UV Stability of Anthocyanins with Additives	46
4.4	Degradation of Anthocyanins by Fungi	53

CHAPTER 5: CHARACTERISATION ON PVA-ANTHOCYANIN COATINGS

5.1	Fourier Transform Infrared (FTIR) Spectroscopy	61
5.2	Thermogravimetric Analysis (TGA)	69
5.3	Glass Transition Temperature by DSC	77
5.4	UV Degradation by CIELAB Colourimetry	83
5.5	X-Ray Diffraction (XRD)	89

CHAPTER 6: DISCUSSION	92
------------------------------	-----------

CHAPTER 7: CONCLUSIONS AND SUGGESTIONS FOR FUTURE WORKS	96
REFERENCES	99

LIST OF FIGURES

	Page
Figure 2.1: Repeating unit of poly(vinyl alcohol).	7
Figure 2.2: Hydrolysis of poly(vinyl acetate) into poly(vinyl alcohol).	8
Figure 2.3: General structure of anthocyanin and anthocyanidin.	12
Figure 2.4: Structural transformation of anthocyanins in solution.	15
Figure 2.5: Roselle calyxes.	16
Figure 2.6: Delphinidin-3-sambubioside.	17
Figure 2.7: Cyanidin-3-sambubioside.	17
Figure 3.1: Shifts in the absorption spectrum.	25
Figure 3.2: Spectral characteristics of anthocyanins in pH 1.0 and pH 4.5.	26
Figure 3.3: FTIR spectra of different compositions of silicone and polyester resins (range of wave number: 2000-4000 cm ⁻¹).	31
Figure 3.4: TGA of silicone/acrylic blends.	33
Figure 3.5: Specific volume as a function of temperature for amorphous material.	35
Figure 3.6: Typical DSC curve.	36
Figure 3.7: DSC thermogram of the silicone/polyester binder system.	38
Figure 3.8: 3-D L*a*b* colour space.	39
Figure 4.1: UV-visible absorption spectra of anthocyanins at pH 1.0 and pH 4.5.	43
Figure 4.2: Effect of acid on the absorption peak of aqueous anthocyanins.	45
Figure 4.3: Effect of nitrate salt on the absorption peak of aqueous anthocyanins.	46
Figure 4.4: UV degradation of Antho.	47
Figure 4.5: UV degradation of AAce.	48
Figure 4.6: UV degradation of ACit.	48
Figure 4.7: UV degradation of AHyd.	49

Figure 4.8:	UV degradation of ACal.	49
Figure 4.9:	UV degradation of AMag.	50
Figure 4.10:	UV degradation of AZin.	50
Figure 4.11:	Fitted first order kinetics of anthocyanin samples with acid.	51
Figure 4.12:	Fitted first order kinetics of anthocyanin samples with salt.	51
Figure 4.13:	Colour degradation of Antho sample by fungi.	55
Figure 4.14:	Colour degradation of AAce sample by fungi.	55
Figure 4.15:	Colour degradation of ACit sample by fungi.	56
Figure 4.16:	Colour degradation of AHyd sample by fungi.	56
Figure 4.17:	Colour degradation of ACal sample by fungi.	57
Figure 4.18:	Colour degradation of AMag sample by fungi.	57
Figure 4.19:	Colour degradation of AZin sample by fungi.	58
Figure 5.1:	FTIR spectra of PVA coatings with acid as additive: (i) PurePVA, (ii) PAntho, (iii) PAAce, (iv) PACit, and (v) PAHyd.	62
Figure 5.2:	FTIR spectra of PVA coatings with nitrate salt as additive: (i) PurePVA, (ii) PAntho, (iii) PACal, (iv) PAMag, and (v) PAZin.	63
Figure 5.3:	Thermogram and DTG of PurePVA sample.	71
Figure 5.4:	Thermogram and DTG of PAntho sample.	71
Figure 5.5:	Thermogram and DTG of PAAce sample.	72
Figure 5.6:	Thermogram and DTG of PACit sample.	72
Figure 5.7:	Thermogram and DTG of PAHyd sample.	73
Figure 5.8:	Thermogram and DTG of PACal sample.	73
Figure 5.9:	Thermogram and DTG of PAMag sample.	74
Figure 5.10:	Thermogram and DTG of PAZin sample.	74
Figure 5.11:	Overlapped thermograms of all coating samples.	77
Figure 5.12:	Glass transition temperature of PurePVA sample.	79
Figure 5.13:	Glass transition temperature of PAntho sample.	79
Figure 5.14:	Glass transition temperature of PAAce sample.	80
Figure 5.15:	Glass transition temperature of PACit sample.	80
Figure 5.16:	Glass transition temperature of PAHyd sample.	81
Figure 5.17:	Glass transition temperature of PACal sample.	81

Figure 5.18:	Glass transition temperature of PAMag sample.	82
Figure 5.19:	Glass transition temperature of PAZin sample.	82
Figure 5.20:	Colour change of PAntho sample upon exposure to UV for 24 hours.	85
Figure 5.21:	Colour change of PAAce sample upon exposure to UV for 24 hours.	86
Figure 5.22:	Colour change of PACit sample upon exposure to UV for 24 hours.	86
Figure 5.23:	Colour change of PAHyd sample upon exposure to UV for 24 hours.	87
Figure 5.24:	Colour change of PACal sample upon exposure to UV for 24 hours.	87
Figure 5.25:	Colour change of PAMag sample upon exposure to UV for 24 hours.	88
Figure 5.26:	Colour change of PAZin sample upon exposure to UV for 24 hours.	88
Figure 5.27:	X-ray diffractograms of coating samples (i) PurePVA, (ii) PAntho, (iii) PAAce, (iv) PACit, (v) PAHyd.	90
Figure 5.28:	X-ray diffractograms of coating samples (i) PurePVA, (ii) PAntho, (iii) PACal, (iv) PAMag, (v) PAZin.	91

LIST OF TABLES

		Page
Table 2.1:	Sources and average amount of anthocyanins.	11
Table 2.2:	Common anthocyanidins and their corresponding substituents, λ_{max} and colour.	13
Table 2.3:	Characteristics of some organic solvents.	19
Table 2.4:	Examples and function of some additive types.	21
Table 3.1:	Designation for pure anthocyanin extract and extract with additive.	22
Table 3.2:	Composition of coating system containing poly(vinyl alcohol), anthocyanin, and additive.	23
Table 4.1:	Relative intensities of maximum peaks at UV and visible range.	45
Table 4.2:	Degradation rates and half-lives of aqueous samples.	52
Table 4.3:	Visual comparison of samples on day 0 and day 35.	54
Table 4.4:	Colour parameters of samples on 0th day and 35th day and fungi dry weight.	58
Table 5.1:	Band assignment of peaks in pure PVA sample.	61
Table 5.2:	Relative peak intensities between sample PurePVA and PAntho.	64
Table 5.3:	Relative peak intensities between sample PAntho and PAAce.	64
Table 5.4:	Relative peak intensities between sample PAntho and PACit.	65
Table 5.5:	Relative peak intensities between sample PAntho and PAHyd.	65
Table 5.6:	Relative peak intensities between sample PAntho and PACal.	66
Table 5.7:	Relative peak intensities between sample PAntho and PAMag.	66
Table 5.8:	Relative peak intensities between sample PAntho and PAZin.	67
Table 5.9:	Percent weight of all coating samples at 300 °C.	76
Table 5.10:	Temperature of coating samples at 70% weight.	76
Table 5.11:	CIELAB parameters of all samples upon UV irradiation for 24 hours.	85

Table 5.12:	FWHM values from XRD diffraction halo for all PVA coating samples.	90
-------------	--	----

CHAPTER 1: INTRODUCTION

1.1 Research Background

In this research, emphasis is on the development of a coating system by mixing poly(vinyl alcohol), a water soluble polymer with anthocyanin extracted from *Hibiscus sabdariffa* L. plant as dye in the coating, with various additives. Coatings or paints refer to liquid, paste or powder materials which are applied to a substrate and form films on the surface. The terms *coating* and *paint* have always been used interchangeably. However, it is now common to use coatings as a more general term, including the electroplated copper, zinc coatings, inner and outer surface of a can, printing inks, paper and fabrics coatings, kitchen finish etc., while paint refers to architectural, household and internal design decoration. In modern days, polymeric materials have gained much attention as coating materials compared to phenolic resins and alkyd resins in the 1930's. Among the common are polyurethane, polyester, polyol acrylic and vinyl coatings. In this work, coating is developed from mixture of poly(vinyl alcohol) as binder with anthocyanin as dye. Effect of additives to both the anthocyanin dye and the coating is studied.

Poly(vinyl alcohol) was first synthesized by Hermann and Haehnel in 1924 through hydrolysis of poly(vinyl acetate) in ethanol with potassium hydroxide [Saxena, 2004]. It has found many uses in various areas such as food industry, paper industry and biomedical field. Poly(vinyl alcohol) is chemically stable, biodegradable and non-toxic, hence the various applications. In this work, potential of poly(vinyl alcohol) as coating material is assessed.

Anthocyanin has been an interesting subject of research in biochemistry, food science and technology and medical science. It is the most abundant natural pigment after chlorophyll. To date, more than 539 anthocyanins have been identified in nature [Andersen & Jordheim, 2006]. The word anthocyanin is derived from two Greek words: *anthos* (meaning flower) and *kyanos* (meaning blue). Anthocyanins have been used in art and decoration in early civilization. Use of anthocyanin as food colourant can be traced back to 1500BC in Egypt, where the Egyptians used wine as colourant for candies. Early industrial use of anthocyanin was as dye for fabrics [Deroles, 2009]. In recent days, there has been increasing interest in anthocyanin as natural food colourant [Bridle & Timberlake, 1997]. It was estimated that sales of anthocyanins obtained from grape skin reached S\$200 million worldwide [Deroles, 2009]. Some of the earlier works regarding anthocyanins were done by Robert Robinson and Richard Willstatter, and both were awarded Nobel Prize in Chemistry. In this work, potential use of anthocyanin as colourant for coating is explored.

Research on integration of natural plant pigments in coating has been scarce. Abidin *et al.* (2006) has studied the potential use of curcumin, carotenoid, and lawsonia pigment as colourant in acrylic coating. Use of natural pigment as colourant in coatings is environmental friendly and cost effective. Being natural pigment, anthocyanin is obtained from plant sources and does not contribute to pollution of environment, which is in line with “green” concept that industries and authorities have been trying to achieve.

1.2 History of Coatings

History of coatings started in the ancient days as paints. Ancient people decorated walls in the cave with oil paints mixed with pigments such as ochre, manganese ore, and

chalk. In early civilization such as Egypt, Babylon and Greece, paint was made from the mixtures of gummy substances and colour component from various sources. Linseed oil was used as paint in fine arts during the Renaissance. Until early 1900s, vegetable oils and wood resins remained as important materials for paint production. Synthetic resins were introduced after that. Phenolic resins were the first synthetic binders produced in the 1920s, followed by alkyd resins in the 1930s. However, introduction of solvent-borne synthetic resins brought along VOC (volatile organic compound), which became a source of environmental pollution. Beginning late 1960s, emphasis has been more on the development of new renewable coating material and natural products which use water as solvent.

1.3 Coatings in Industry

Use of paint is not only fuelled by domestic demand, but also industrial demand. It is a lucrative business product in areas such as automobiles, building, and oil & gas industries. In 2003, global coatings market was estimated at US\$70 billion [Tullo, 2004]. For architectural coating alone, it accounted for 58% of total volume of coating in the United States in 2003 [Wicks *et al.*, 2007]. Architectural coatings include paint used for building protection, either inside or outside, and also include household furniture. On the other hand, industrial coatings accounted for 29% of total volume of coating in the same year and these included automobile, appliances, aircraft, metal cans etc.

1.4 Scope of Thesis

In the coating industry, majority of the coating materials used are solvent-based and involve the use of organic solvent with high volatility such as xylene, toluene, acetone, methyl ethyl ketone, etc. However, this poses a potential danger to the coating applicator and also the environment. An issue concerning the selection of pigments for

coating is the cost of the pigment materials. Synthetic pigments cost relatively higher than natural pigments which are obtainable from plant sources. In this work, new coating systems containing water soluble poly(vinyl alcohol) as binder and anthocyanins dye derived from roselle are developed. Various additives are added into the system and the effects of additive on both the aqueous anthocyanins and PVA coatings are studied.

Information regarding primary components of a coating, properties of poly(vinyl alcohol), and stability of anthocyanins are given in Chapter Two. Chapter Three deals with methodology which covers preparation and characterisation techniques for both aqueous anthocyanins and coatings. In Chapter Four, results of characterisation on aqueous anthocyanins including the pH differential method, UV-Vis absorption spectroscopy, UV stability and stability to fungal attack are presented.

Chapter Five presents results of characterisation on poly(vinyl alcohol) coating systems, such as the Fourier Transform Infrared spectroscopy, thermogravimetric analysis, glass transition temperature by DSC, UV-induced colour degradation, and X-ray diffraction. In Chapter Six, discussion regarding the properties and performance of the anthocyanins dye and coating systems with addition of various additives is presented. Conclusions of this work as well as suggestions for improvement and for further works are given in Chapter Seven.

CHAPTER 2: LITERATURE REVIEW

2.1 Coating and Its Composition

Coatings are essentially made up of four major components: binder, pigment, solvent and additive.

2.2 Binder

Binder, also called resin or polymer, is the main component of a coating. It acts as “glue” that binds other components together in a coating and forms the matrix of the coating. It is also responsible for adhesion of the coating to the substrate. Examples of binders are: alkyd, epoxy, acrylics, silicone, polyurethane, polyesters, and phenolic resin, to name a few. Binders can be classified into thermoplastics or thermosets, depending on the curing mechanism. Curing can occur physically or chemically. Physical curing is known as drying, which involves evaporation of solvent from the coating. Binders that cure this way are called thermoplastics. Chemical curing occurs when a chemical reaction occurs between the components of a binder, which leads to polymerization and cross-linking between the components. In this way, the binder is “set” and cures, and is known as thermoset.

Molecular weight of binders can range from 500 to 200000 or higher. Low molecular weight binders have low viscosity while high molecular weight binders have high viscosity. Binders with high molecular weight exhibit better properties such as elasticity, hardness and impact deformation than that with low molecular weight [Heiling, 1998]. However, viscosity of these binders will be high. For ease of application, binders should have low viscosity. Solvents can be used to adjust the viscosity, but this will pose an

issue to the environment as the VOC contributes to the pollution of environment. Hence, a compromise is often inevitable.

Even though some binder materials exhibit exceptional properties and performance, some of them are potentially dangerous to handle. Polyurethane, for example, is produced from cross-linking between polyol and polyisocyanate. Raw materials for polyisocyanate are isocyanates, such as toluene diisocyanate (TDI), and diphenylmethane diisocyanate (MDI), which are toxic and potentially carcinogenic. Another example is epoxy, some of which contains bisphenol A, a potential irritant, and epichlorhydrin, a suspected carcinogen in animals [Gempeler & Schneider, 1998]. A balance has to be achieved in choosing binder materials depending on the functions of the coating. Poly(vinyl alcohol) has proven to be a non-toxic, biodegradable and significantly safe and easy to handle, that leads to its many popular applications in the coating industry such as paper coating.

2.2.1 Poly(Vinyl Alcohol) (PVA)

Poly(vinyl alcohol) is a water soluble, biodegradable, hydrophilic, non-toxic synthetic polymer. It was first synthesized by Hermann and Haehnel in 1924 through hydrolysis of poly(vinyl acetate) in ethanol with potassium hydroxide [Saxena, 2004]. Properties of poly(vinyl alcohol) are dependent on the degree of polymerization, degree of hydrolysis and molecular weight. It can be classified into two categories: partially hydrolysed and fully hydrolysed. Monomer unit of poly(vinyl alcohol) is vinyl alcohol. Structure of poly(vinyl alcohol) is $[\text{CH}_2\text{CH}(\text{OR})]$ depicted below, where R is H or COCH_3 :

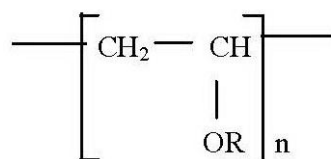


Figure 2.1 Repeating unit of poly(vinyl alcohol).

2.2.2 Synthesis

Poly(vinyl alcohol) is commercially synthesized from poly(vinyl acetate) by a continuous process. The acetate groups are hydrolysed by ester interchange with methanol in the presence of aqueous sodium hydroxide [Saxena, 2004]. Raw material used in manufacturing poly(vinyl alcohol) is vinyl acetate. Poly(vinyl acetate) is first formed from polymerization of vinyl acetate monomer, after which it undergoes hydrolysis reaction with methanol in the presence of aqueous sodium hydroxide. In hydrolysis of poly(vinyl acetate), ester group of the vinyl acetate is replaced by the hydroxyl group. Aqueous saponification agent is gradually added in the reaction. Poly(vinyl alcohol) is precipitated, washed and dried. Degree of hydrolysis is controlled by the time when saponification reaction is stopped [Saxena, 2004]. Poly(vinyl alcohol) with different amount of hydroxyl groups and hence different properties can be produced. Hydrolysis reaction of poly(vinyl acetate) into poly(vinyl alcohol) is depicted in Figure 2.2.

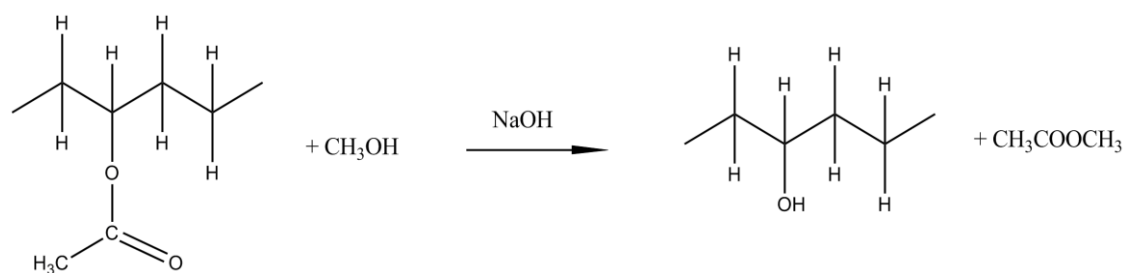


Figure 2.2: Hydrolysis of poly(vinyl acetate) into poly(vinyl alcohol).

2.2.3 Physical and Chemical Properties

Poly(vinyl alcohol) in granular powder form is odourless, tasteless and white or creamy in colour. It is soluble in water and slightly soluble in ethanol. Its solubility in water decreases with increase in molecular weight and decrease in hydrolysis. Poly(vinyl alcohol) containing up to 20 wt% vinyl acetate is insoluble in organic solvents [Heiling, 1998]. A typical 5% poly(vinyl alcohol) solution exhibits pH range of 5.0-6.5. Melting point of poly(vinyl alcohol) can range from 180 °C to 190 °C.

Poly(vinyl alcohol) films are clear and colourless. The polymer films exhibit good mechanical properties, crack resistance and good lightfastness [Heiling, 1998]. It is resistant to oils, fats, greases and waxes. It has good pigment binding capacity and good compatibility with pigment and extenders used in the industry. However, disadvantage of poly(vinyl alcohol) is its weak water and electrolyte resistance.

There is no quantitative method available to determine poly(vinyl alcohol). It has been suggested that filter paper treated with potassium iodide and iodine solutions be used to measure poly(vinyl alcohol) concentration in wastewater in the range of 1000-

20000mg/l [Saxena, 2004]. Colours of poly(vinyl alcohol) in various solvents have been used to identify its presence.

2.2.4 Applications

There are various applications of poly(vinyl alcohol) in domestic sector as well as in industry, and its potentials are being currently explored and expanded to many other fields. Poly(vinyl alcohol) has been used as adhesive and in the paper industry as paper coating [Schuman *et al.*, 2004]. It is also used in the food industry as binding and coating agent for food supplement tablets and capsules [Saxena, 2004]. Poly(vinyl alcohol) has also many applications in the pharmaceutical and biomedical field [Pourciel *et al.*, 2003]. It has been used for controlled drug release tests due to its biodegradable and non-toxic properties [Peppas *et al.*, 2000]. It has also been used in many biomaterial applications such as in artificial pancreas [Young *et al.*, 1996], haemodialysis [Paul *et al.*, 1997], and implantable biomaterials [Chuang *et al.*, 1999]. Poly(vinyl alcohol) is also used in wastewater treatment as encapsulation material [Chang *et al.*, 2005]. Recent researches indicated that poly(vinyl alcohol) has potential as polymer electrolyte for energy devices such as fuel cell and battery [Kadir *et al.*, 2010].

2.3 Pigment and Dye

Pigments are finely divided solids of uniform size that are dispersed and suspended in the binder after curing. Primary function of a pigment is to provide colour, gloss and opacity to the system and subsequently hide the substrate. Some pigments are also used to improve corrosion properties of the coating. Colour pigments that are soluble are referred to as dyes or colourants.

Pigments can be classified into two types: organic and inorganic. Organic pigments are generally complicated organic molecules which main function is to provide colour [Weldon, 2009]. They are seldom used in heavy-duty industrial coatings. Inorganic pigments consist of discreet crystalline particles, which are dispersed in coatings with special additives to improve compatibility [Weldon, 2009]. Two of the most common inorganic pigments are titanium dioxide and iron oxide. Titanium dioxide is a white colour inorganic pigment most widely used. It provides clean white colour and high refractive index. Its commercial products include Bayertitan (Bayer), Kemira (Kemira Pigments Oy), and Hombitan (Sachtleben) [Kohler, 1998]. Iron oxide pigment is an inorganic red pigment with good heat resistance suitable for aggressive environments [Fuller, 1973]. Its commercial products are Bayferrox (Bayer), Harcros (Harrison & Crosfield), and Ferrofin (Laporte PLC) [Kohler, 1998].

A major concern about synthetic pigments is their toxicity. Heavy metal pigments such as lead, chromium, cadmium and barium pose serious health and environmental problems [Forsgren, 2006]. Another issue regarding synthetic pigment is their escalating cost, including raw material cost, synthesis and production cost. A viable alternative to synthetic pigment is natural pigment derived from plant sources. Abidin *et al.* (2006) has studied the potential of yellow and brown natural pigment extracted respectively from turmeric and Henna as dye in the coating system. Potential usage of carotenoid natural pigment as dye in coating has also been studied by Omar and Ahmad (2009). Natural red pigment can also be obtained from plant sources as an alternative to synthetic pigment. Red colour in nature can be found in anthocyanin, a natural chromophore capable of giving colours ranging from red to blue.

2.3.1 Anthocyanin Pigment

Anthocyanins are the largest and most important group of water soluble natural pigments. They belong to a larger group of phenolic compounds called flavonoids [Britton, 1983]. Anthocyanins are distributed in vacuole of a plant cell. They are found primarily in fruits, flowers, roots and other parts of higher plants. They are responsible for a wide range of colours, such as blue, violet, red and orange in many plants and vegetables. There are many sources of anthocyanins, some of the common are listed in Table 2.1. To date, there are more than 539 anthocyanins identified in nature [Andersen & Jordheim, 2006].

Table 2.1: Sources and average amount of anthocyanins.

Anthocyanin source	Amount (mg.kg ⁻¹)
Blueberry	825-4200
Chokeberry	506-10000
Red Grapes	300-7500
Blood Orange	2000
Eggplant	7500
Red Cabbage	250

Source: Mateus & de Freitas (2009).

In the past few decades, anthocyanin has gained much attention both from scientific research community and industry. There have been researches in biological activities and effects of anthocyanin to human in medical applications. Among the interesting researches in medical and pharmaceutical applications are the antioxidant and antiradical properties of anthocyanin [Igarashi *et al.*, 2006; Tsai *et al.*, 2002; Kong *et al.*,

2003], anti-inflammatory and anti-oedema properties [Wagner, 1985]. Anthocyanin has also shown promising potential as natural dye to replace artificial colourant in food industry [Bridle & Timberlake, 1997; Melo *et al.*, 2009]. Zhu *et al.* (2008) has reported the use of anthocyanin as dye in dye-sensitised solar cells.

2.3.2 Structure of Anthocyanin

Anthocyanins are glycosides of anthocyanidins, the aglycones having the characteristic $C_6C_3C_6$ carbon skeleton [Harborne, 1998]. The base structure is 2-phenylbenzopyrylium, or known as flavylium cation. The structure of anthocyanidin and anthocyanin is given in Figure 2.3. Anthocyanidin does not occur naturally due to the instability of the structure [Melo *et al.*, 2009]. Upon glycosylation, it is known as anthocyanin, the stable form that exists in nature. In both anthocyanidin and anthocyanin, position 7 of A ring and position 4' of B ring are bonded with hydroxyl group (OH). In anthocyanidin, position 5 of A ring and position 3 of C ring are bonded with hydroxyl group, while in anthocyanin, position 3 is glycosylated and position 5 is occasionally glycosylated. Figure 2.3 shows the general structures of anthocyanidin and anthocyanin.

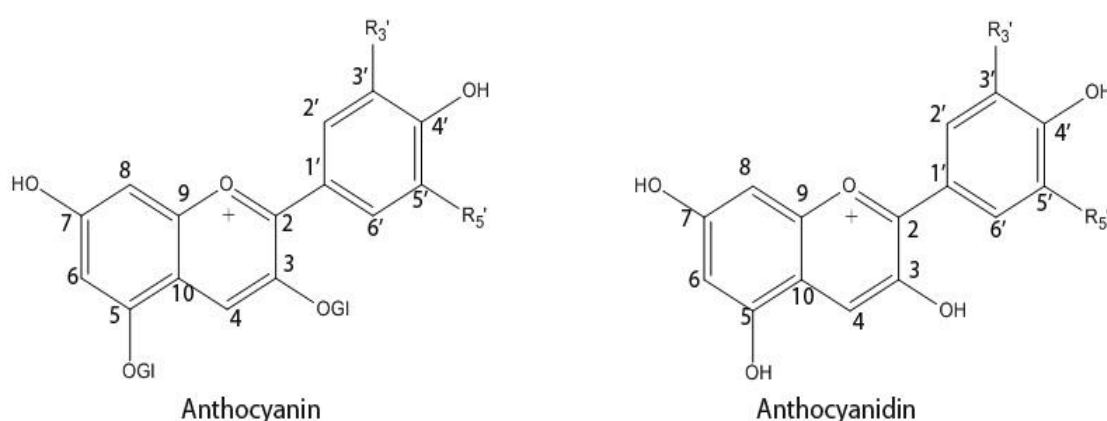


Figure 2.3: General structure of anthocyanin and anthocyanidin.

Glycosylation increases water solubility while acylation decreases water solubility [He & Giusti, 2010]. It improves anthocyanin stability by forming intramolecular hydrogen bonding network within the molecule [Borkowski *et al.*, 2005]. Some common sugar moieties attached to the anthocyanins are glucose, galactose, rhamnose, arabinose, xylose, rutinose, and sambubiose. The sugar moieties can be further acylated with organic aromatic or aliphatic acids such as cinnamic acid, caffeic acid, malonic acid, acetic acid, p-coumaric acid, ferulic acid and succinic acid.

There are 25 different anthocyanidins that have been identified. However, 90% of all anthocyanins are based on only six common aglycones (anthocyanidins): cyanidin (30%), delphinidin (22%), pelargonidin (18%), peonidin, malvidin and petunidin (altogether 20%) [Andersen & Jordheim, 2006]. Variety in the types of anthocyanins is due to the different substituents at position 3' and 5' of B ring of anthocyanin, and whether they are hydroxylated or methylated. This leads to changes in the maximum absorption wavelength and colour of the anthocyanins. Table 2.2 [Melo *et al.*, 2009] lists the six common anthocyanidins and corresponding substituents at the B ring.

Table 2.2: Common anthocyanidins and their corresponding substituents, λ_{\max} and colour.

Name	R _{3'}	R _{5'}	λ_{\max} (nm)	Colour
Cyanidin	OH	H	535	Red orange
Delphinidin	OH	OH	545	Violet
Pelargonidin	H	H	520	Orange
Peonidin	OCH ₃	H	532	Red
Malvidin	OCH ₃	OCH ₃	542	Violet
Petunidin	OCH ₃	OH	543	Violet

Source: Melo *et al.* (2009).

2.3.3 Anthocyanin Stability

Natural pigments are generally unstable and the same applies to anthocyanins. Anthocyanins are sensitive to various factors such as pH, light, temperature, and oxygen. Anthocyanins are reported to undergo structural transformation at different pH [Brouillard & Dubois, 1977]. Colour of anthocyanins also changes along with the change of the molecular structure at different pH.

Four major forms of anthocyanins occur in equilibria: flavylium cation, quinonoidal bases, carbinol (hemiacetal) base and chalcone. At pH below 2, anthocyanins exist dominantly as the flavylium cation - a weak acid, which is red in colour. In less acidic medium (pH 4-6), deprotonation of the flavylium cation to water readily occurs to generate quinonoidal bases, which are bluish. This is a very fast process. However, at this pH range, the flavylium cation also readily undergoes nucleophilic attack by water at position C-2, forming the colourless carbinol or hemiacetal base [Quina *et al.*, 2009]. This process (hydration) is also moderately fast. The reversible processes for deprotonation and hydration are also fast. The carbinol pseudobase can further equilibrate to an open ring form, the colourless chalcone, at a slower rate [He & Giusti, 2010]. Likewise, reconversion from chalcone to flavylium cation is also a very slow process [Francis, 1989]. The process is illustrated in Figure 2.4.

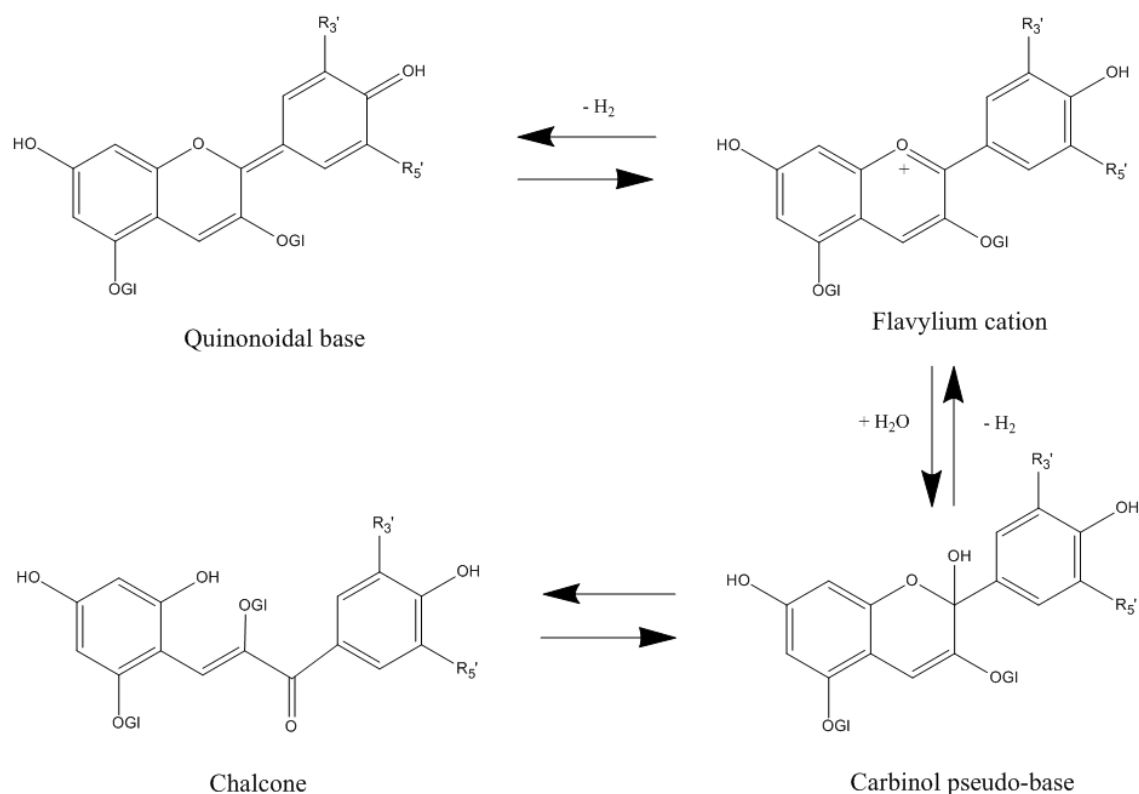


Figure 2.4: Structural transformation of anthocyanins in solution.

Light has a profound influence on anthocyanin stability [Giusti & Wallace, 2009]. It accelerates degradation of anthocyanins. Anthocyanins are susceptible to degradation due to the lack of structural stability and tinctorial strength. Anthocyanins with hydroxyl-substituted C-5 are more susceptible to light than unsubstituted anthocyanins. Anthocyanin stability is also affected by heat. It was reported that anthocyanin undergoes first order degradation kinetics [Patras *et al.*, 2010]. First step in thermal degradation of anthocyanin is conversion to colourless chalcone which eventually produces α -diketone [Wrolstad, 2004]. Anthocyanin is also susceptible to oxidative degradation by oxygen. Reaction of anthocyanin with oxygen yields yellow-brown oxidized product.

2.3.4 *Hibiscus sabdariffa* L. Plant

Hibiscus sabdariffa L. is in the family Malvaceae. It is commonly known as roselle. It is a tropical plant mainly found in Asia and Tropical Africa [Mahadevan, 2009]. It is estimated at about 3.5m tall and has a deep penetrating taproot. It has smooth and cylindrical, typically dark green to red stems. Its leaves are alternate, green with red veins and petioles. Its red calyxes consist of 5 large sepals with a collar of 8-12 slim [Mahadevan, 2009]. Its fruit is a capsule containing 5 valves encapsulating seeds. The seeds are kidney-shaped and light-brown in colour. Roselle propagates by seed.



Figure 2.5: Roselle calyxes.

Roselle has found various domestic and biomedical uses. It is commonly used to make jellies, jams and beverages in Egypt and Sudan [Mahadevan, 2009], in Taiwan [Tsai & Huang, 2004], and in Thailand [Chumsri *et al.*, 2008]. It has also been traditionally used as antiseptic, aphrodisiac, astringent, chlogagueee, demulcent, digestive and tonic [Mahadevan, 2009]. Calyx extracts of roselle have been found to exhibit strong in vitro

and in vivo antioxidant properties [Prenci *et al.*, 2007]. It also exhibits strong antihypertensive action in human [Mojiminiyi *et al.*, 2007] and cardioprotective effects in rats [Odigie *et al.*, 2003].

Calyxes of roselle are bright red in colour and rich in anthocyanins. Du and Francis (1973) have reported 2 major: delphinidin-3-sambubioside and cyanidin-3-sambubioside, and 2 minor anthocyanins: delphinidin-3-glucoside and cyanidin-3-glucoside in the calyxes of roselle. Chemical structures of the major anthocyanins found in roselle are illustrated in Figure 2.6 and Figure 2.7. Wong *et al.* (2002) has studied the physico-chemical properties of roselle calyxes. Roselle was reported as highly acidic with low sugar content. Major sugars identified in roselle were glucose, fructose and sucrose.

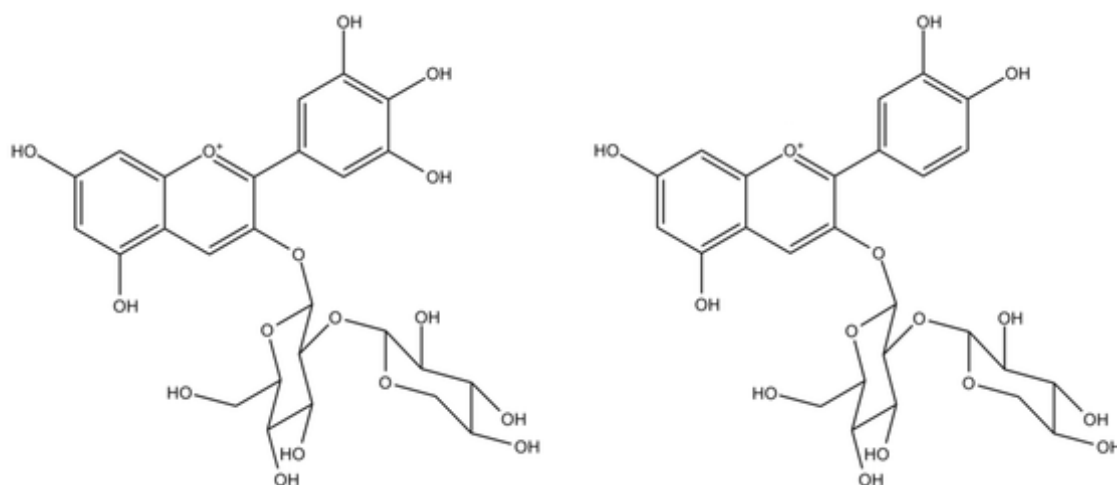


Figure 2.6: Delphinidin-3-sambubioside. Figure 2.7: Cyanidin-3-sambubioside.

2.4 Solvent

Solvents or volatile organic compounds are volatile liquids that dissolve the binder. They modify the viscosity of the binder system and enhance flow and uniformity of the mixture. This will ease difficulty during application so that the paint can be applied as a uniform, thin film on the substrate. Solvents also act as carrier for non-volatile components. After application, the solvents evaporate, forming coating film on the substrate. Solvents significantly affect not only the application characteristics of paint, but also the appearance, physical properties, and durability of coating [Yuhas, 1995]. Two important performance requirements that must be considered in choosing the types of solvents are solvency and evaporation rate. These characteristics control the initial paint viscosity during application, coating viscosity at various stages of drying, and final coating appearance [Yuhas, 1995]. Solvent for a particular binder must be capable of dissolving the binder particles to form coating. Evaporation rate of a solvent used in coatings cannot be too high or too low. Slow rate of evaporation would lead to blistering, trapped liquid or air in the coating that makes it fail. On the other hand, if the evaporation rate is high, the coating may not have the chance to form a smooth, continuous film, leaving the surface rough [Weldon, 2009]. Examples of solvents are alcohols, ketones, esters and ethers. Some characteristics of solvents are listed in Table 2.3 [Schweitzer, 2006].

Table 2.3: Characteristics of some organic solvents.

Solvent	Strength/Solvency	Polarity	Specific gravity	Evaporation rate
Toluene	High	Intermediate	0.87	4.5
Xylene	High	Intermediate	0.87	9.5
Methyl ethyl ketone	Strong	High	0.81	2.7
Ethyl acetate	Intermediate	Intermediate	0.90	2.7
Ethanol	Weak	Intermediate	0.79	6.8

Source: Schweitzer (2006).

The main concern regarding use of solvents is that after application, solvents enter the atmosphere as pollutant during evaporation or drying, causing hazards to environment and also the personnel in work. Among some of the environmental effects caused by solvents or VOC are ozone holes, summer smogs, green house effects, and acid rain [Warnon, 2004]. Effects of solvents on human may vary under different circumstances. Short term exposure to high solvent doses may cause acute damage, whereas absorption of smaller amounts over a prolonged period leads to chronic damage and sensitization [Ortelt, 1998]. Due to concern over solvent emissions, alternatives to solvent are of great interest to the coating industry, and these include radiation cured coating, powder coating and water-borne coating.

Water appears to be a potential candidate as vehicle for water soluble binder materials. It has been used as vehicle in water-reducible coatings, which have either carboxylic acid or amine groups that are at least partially neutralized with low molecular weight amines or acids, respectively [Wicks, 2007]. Examples of water-reducible coatings

include water reducible polyester, alkyds, and urethanes. Besides, water has also been used as vehicle for emulsion coatings. The water-based emulsions are usually formulated with high-molecular-weight resins such as copolymers of poly(vinyl chloride), or poly(vinyl acetate), styrene-butadiene, acrylic ester etc. [Schweitzer, 2006]. In water-based coating, curing is usually by physical drying or evaporation of water.

2.5 Additives

Additives are often added to the coating system in small amount to perform specific functions. Even though they are in minute amount, they give significant effects on the properties of the coating. Effects of additive depends on their types, they perform specific functions to enhance application characteristics and properties of the cured coating. These include surfactants, wetting agents, coalescing agents, anti-skinning agents, catalysts, thickening agents, anti-fungal biocides and hardener. For instance, zinc oxide is used to prevent deterioration of resin by heat of the actinic sun rays. Cobalt and manganese naphthanates act as dryers for alkyds and oil-based paint. Further information about the types and functions of some of the additives is tabulated in Table 2.4 [Weldon, 2009].

Table 2.4: Examples and function of some additive types.

Additive	Function	Example
Anti-settling agent	Break down and disperse large agglomerates of pigments in the resin/solvent system.	Waxes, chemically treated clays, low molecular weight polyethylenes.
Viscosity modifier	Increase viscosity so that excessive flow does not occur after application	Cellulose ethers, micronized silica.
Surfactant	Alter the surface tension of resins or polymers so that they become compatible with water	Salts of fatty acids, quarternary ammonium compounds.
Anti-skinning agent	To prevent surface skin formation caused by contact with atmospheric oxygen	Methyl ethyl ketoxime, butyraldehyde oxime.
Plasticizer	Increase flexibility of the coating films	Diocetyl phthalate, chlorinated parafins, organic phosphate.

Source: Weldon (2009).

CHAPTER 3: METHODOLOGY

3.1 Sample Preparation

There are two parts in the sample preparation. In the first part, anthocyanin pigment is extracted from calyxes of *Hibiscus sabdariffa* L. (roselle) by using water extraction method, where calyxes were soaked in distilled water for 3 hours. The extract was then filtered by Whatman filter paper (110mm diameter) to remove insoluble impurities and foreign particles. After that, pH differential method was employed to estimate the total anthocyanin content in the crude extract. Two types of additives were introduced into the extracts: acids and salts. The acids were 5wt% acetic acid, 5wt% citric acid, and 1wt% hydrochloric acid. Hydrochloric acid was fixed at 1wt% to avoid excessive acidity of the aqueous solution. The added salts were 5wt% calcium nitrate, 5wt% magnesium nitrate, 5wt% zinc nitrate. Table 3.1 lists the designation of anthocyanin extract samples. Characterisation conducted on anthocyanin and samples with additives were UV-Vis absorption spectroscopy, UV degradation, and fungal degradation.

Table 3.1: Designation for pure anthocyanin extract and extract with additive.

Designation	Extract	Additive
Antho	100wt% Anthocyanin	-
ACal	95wt% Anthocyanin	5wt% Calcium nitrate
AMag	95wt% Anthocyanin	5wt% Magnesium nitrate
AZin	95wt% Anthocyanin	5wt% Zinc nitrate
AAce	95wt% Anthocyanin	5wt% Acetic acid
ACit	95wt% Anthocyanin	5wt% Citric acid
AHyd	99wt% Anthocyanin	1wt% Hydrochloric acid

In the second part, crude extract and extracts containing additive were mixed with poly(vinyl alcohol), PVA. The ratio was 75wt% extract to 25wt% PVA. It was found that other ratio would cause inhomogeneous mixtures, leading to inapplicable paint system. Pure PVA was dissolved with distilled water as solvent without anthocyanin and additives to be used as control. All coating samples were coated on glass slide for approximately 1 day to dry. Poly(vinyl alcohol) (80% hydrolysed) was obtained from Sigma Aldrich Malaysia. Compositions of the coating system are tabulated in Table 3.2. Fourier Transform Infrared (FTIR) spectroscopy, thermogravimetric analysis, differential scanning calorimetry, UV degradation by CIE colourimetry, and X-ray diffractometry (XRD) analysis were conducted on the coating samples.

Table 3.2: Composition of coating system containing poly(vinyl alcohol), anthocyanin, and additive.

Designation	Binder	Extract/Solvent
PurePVA	25wt% PVA	75wt% H ₂ O
PAntho	25wt% PVA	75wt% Antho
PACal	25wt% PVA	75wt% ACal
PAMag	25wt% PVA	75wt% AMag
PAZin	25wt% PVA	75wt% AZin
PAAce	25wt% PVA	75wt% AAce
PACit	25wt% PVA	75wt% ACit
PAHyd	25wt% PVA	75wt% AHyd

3.2 Characterisation on Anthocyanin Extract

3.2.1 UV-Visible Absorption Spectroscopy

When a transparent material is illuminated by visible light, it absorbs some wavelengths of the light while some other wavelengths are transmitted. When atoms or molecules absorb an electromagnetic radiation, they are excited from ground state to excited state.

In the case of excitation by UV and visible light, the transition corresponds to the electronic transition between energy levels. For an atom, transition between two discrete energy levels results to a sharp line in the UV-visible spectrum. For a molecule, due to the small difference in the vibrational levels of ground and excited states, which results in many possible transitions between the ground and excited states, the spectrum becomes continuous band. Electronic transition in the UV and visible ranges are $n \rightarrow \pi^*$ transition [Valeur, 2002].

UV-visible absorption spectroscopy is governed by Beer-Lambert Law, which states that absorbance is directly proportional to the molar absorptivity and concentration of the absorbing species, and pathlength of radiation through the species. Beer-Lambert law is given as in Equation 3.1.

$$A = \epsilon cl \quad (3.1)$$

Where, A is absorbance, ϵ is molar absorptivity, c is concentration and l is optical pathlength. However, the law may not be obeyed if solute and solvent form complexes, when thermal equilibrium exists between the ground state and low-lying state, or when fluorescent compounds are present [Pavia *et al.*, 2009].

UV-visible absorption spectrum can be generally related to the colour appearance of a material. Materials that absorb strongly in the long wavelengths (red) region appear blue, since short wavelengths (blue region) are reflected or transmitted. Likewise, materials that absorb strongly in the short wavelengths (blue) region appear red. Shifting in the peak of absorption spectrum is of most concern in the study of stability. Bathochromic shift refers to shift to longer wavelengths, while hypsochromic shift refers to shift to

shorter wavelengths. On the other hand, hyperchromic shift refers to increase in absorbance whereas hypochromic shift refers to decrease in absorbance value. Bathochromic shift of absorption peak to the red region causes the material to appear bluer, whereas hypsochromic shift causes the material to appear redder. Hyperchromic and hypochromic shifts can also affect colour appearance of a material. Figure 3.1 shows the shifts in the absorption spectrum.

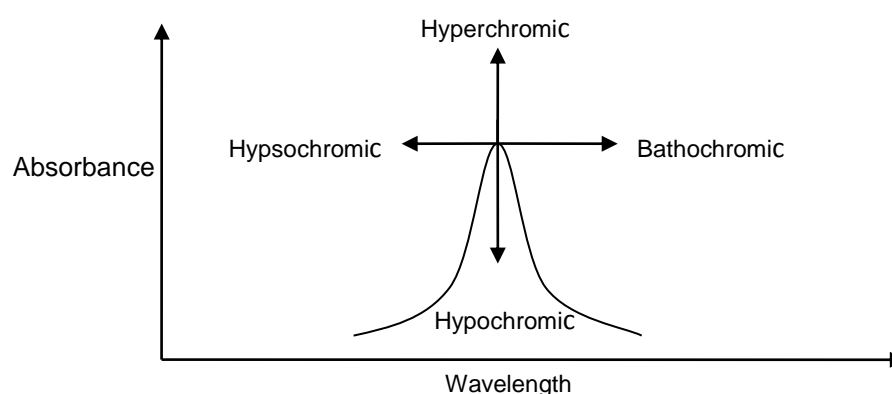


Figure 3.1: Shifts in the absorption spectrum.

Instrument usually used in UV-visible absorption spectroscopy is the double beam UV-Vis spectrophotometer. It measures absorption of light by a substance at a specific wavelength. The spectrophotometer uses deuterium and hydrogen lamps as source of UV radiation and tungsten filament lamp as a source of visible radiation. It has a monochromator to select wavelength which is radiated once at a time. Quartz or fused silica cuvettes are used as the container for the sample. Detector of the transmitted radiation is a photomultiplier tube.

3.2.2 The pH Differential Method

The pH differential method is a method for measurement of total anthocyanin content in a sample. It is based on the structural transformation of anthocyanins between pH 1.0 and 4.5. At pH 1.0, anthocyanin exists predominantly as red-coloured flavylium cation, while at pH 4.5, the colourless hemiacetal or carbinol form [Lee *et al.*, 2005]. Hence, difference in the absorbance of the $\lambda_{\text{vis-max}}$ is proportional to the concentration of the pigment. Figure 3.2 depicts the absorption spectra of anthocyanins in pH 1.0 and pH 4.5.

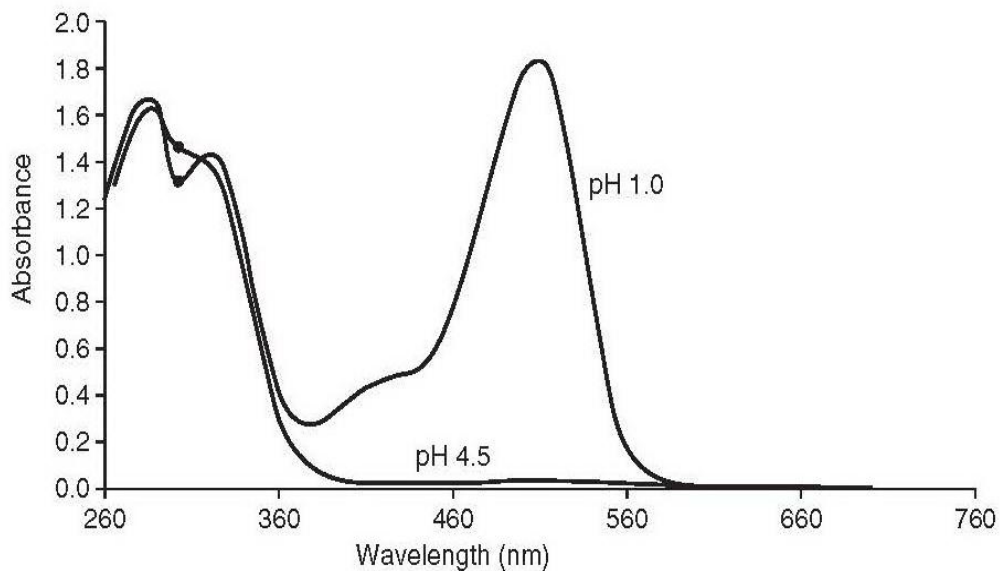


Figure 3.2: Spectral characteristics of anthocyanins in pH 1.0 and pH 4.5.

Source: Giusti and Wrolstad (2001).

The total anthocyanin concentration is given as:

$$\text{Total anthocyanin content (mg/l)} = \frac{A \times MW \times DF \times 1000}{\epsilon \times l} \quad (3.2)$$

and

$$A = (A_{\lambda_{vis-max}} - A_{700})_{pH\ 1.0} - (A_{\lambda_{vis-max}} - A_{700})_{pH\ 4.5} \quad (3.3)$$

where MW is molecular weight in g/mol, DF is dilution factor, ϵ is molar absorptivity in $l \times \text{mol}^{-1} \times \text{cm}^{-1}$, and A is the difference in absorbance value for the maximum absorption peak in visible range at two different pH value after correcting for haze. Equation 3.2 is actually a modified form of Beer-Lambert's equation for absorbance.

Molecular weight and molar absorptivity values of the identified anthocyanin present in the sample should be used in calculating the concentration of that anthocyanin. It has been reported that molar absorptivity of anthocyanins is different with different extraction method and solvent [Giusti & Wrolstad, 2001]. In pH differential method, for a specific anthocyanin, extraction method and solvent used should be same as that used by the researcher who reported the molar absorptivity of that anthocyanin, so that the reported molar absorptivity value, ϵ can be used. In the event that the anthocyanin is not identified, or lack of literature for molar absorptivity value, it is more appropriate to express the anthocyanin as cyanidin-3-glucoside [Lee *et al.*, 2005].

Buffer solutions used are 0.025M potassium chloride for pH 1.0 and 0.4M sodium acetate for pH 4.5. The absorbance value should be corrected for haze at 700nm. Haze is cloudy appearance due to scattering of light by sediments or colloidal materials. This scattering of light can be corrected at 700nm, where no absorbance of sample occurs. A comprehensive methodology was published by Giusti and Wrolstad (2001).

3.2.3 Test for UV Stability

UV radiation causes photodegradation, a reaction where energy (in the form of absorbed photon) is transferred into a substance. The photochemical reaction will occur if the incoming photons have sufficient energy to break or form new bond [Koutchma, 2009]. UV radiation is a non-ionising radiation and its energy is lower than ionising radiation such as X-ray and gamma rays. However, UV radiation is capable of promoting electronic transitions in atoms and molecules, and hence causing photochemical reaction to occur. The effect of UV radiation on anthocyanins has also been studied before by Bakowska *et al.* (2003), Marco *et al.* (2011) and Setareh *et al.* (2007).

In the test for UV stability of anthocyanin extract and extracts containing additive, the samples were kept in air tight laboratory bottles and exposed to UV radiation of wavelength 312nm and illuminance of 17.55lx continuously for 8 hours. Absorption spectra were obtained before exposure and at 4th, 6th, and 8th hour of exposure. Changes in the absorption spectra, such as shifting in the peak are used as indication of anthocyanin degradation.

3.2.4 Test for Fungal Degradation

It has been known that natural products such as juice extracts and plant materials are susceptible to infestation by atmospheric fungi for their nutrients. Anthocyanin crude extract is also susceptible to attack by fungi for its nutrients. However, sterilization of anthocyanin extract is impractical for coating applications. For anthocyanin extracted with water to be used as colourant in coating, it is therefore important to assess its stability and inhibition of fungi activity.

Three approaches were employed in the test. Visual observation was required to detect any fungi growth. CIELAB colourimetry was conducted to detect change in colour of the samples, as it was reported that anthocyanins are readily decolourised by fungi [Huang, 1955]. Measurement of fungi dry weight is another approach used to indicate fungi activity. It has been utilised by many researchers as a conventional approach of indication of fungi growth rate [Reeslev & Kjoller, 1995; Sutton & Starzyk, 1973; Priyadarshini & Tulpule, 1978]. In this approach, the extracts with fungi were filtered with Whatman filter paper (110mm diameter), and stored in oven at 40 C overnight to remove moisture. Weight of dry fungi was taken, minus the weight of the filter paper. Amount of samples used in this characterisation was 10.0g. All three methods were conducted at the 35th day of storage.

3.3 Characterisation on PVA Coatings

3.3.1 Fourier Transform Infrared (FTIR) Spectroscopy

Infrared spectroscopy has been used for material analysis for over seventy years. The main principle in infrared spectroscopy is absorption and transmission of infrared radiations by molecules and their functional groups which are infrared-active. Wavelengths in vibrational infrared region of an electromagnetic spectrum correspond to energy of vibration of chemical bonds [Smith, 1996]. When an infrared radiation passes through a material, radiation with wavelength matching the natural vibrational frequency of a chemical bond will cause an increase in the vibrational amplitude [Pavia *et al.*, 2009]. A decrease in the infrared intensity is detected at wavelength which absorption occurs. Covering the vibrational infrared region, the resulting spectrum will be either spectrum of transmission or absorption of the sample. As with UV-Vis absorption spectroscopy, Beer-Lambert Law can also be applied in infrared spectroscopy.

Typical practical useful range of infrared radiation lies between $400\text{-}4000\text{cm}^{-1}$. An important aspect for infrared absorption is that the molecular vibration must cause a change in the dipole moment of the molecule [Larkin, 2011]. Molecules that satisfy this condition are said to be infrared active. Homonuclear diatomic molecules such as N_2 and O_2 do not possess infrared spectra since there is no dipole moment [Smith, 1999]. These are infrared inactive. Infrared spectroscopy also cannot be used to detect atoms, monoatomic ions or noble gases such as argon and helium since they do not possess vibration motion.

The main use of infrared spectroscopy is to determine structural information and identify functional groups of molecules present in a sample. Different types of chemical bonds and functional groups exhibit different vibrational normal frequencies. This is due to the difference in bond strength and mass of atoms in different bond. For example, triple bond, which is stronger than single bond, vibrates at higher frequency. Infrared spectroscopy can also be used to do fingerprinting of molecules [Kendall, 2006]. This is due to the fact that different materials have different molecular structures.

Infrared spectroscopy uses dispersive material like prism or grating to separate different wavelengths in the infrared region before being illuminated on the sample. However, this process is time-consuming, since the individual wavelength has to be separated first. Modern type infrared spectrometers are usually Fourier transform infrared (FTIR) spectrometers. In this method, all the infrared wavelengths pass through the sample simultaneously. The resultant spectrum is the overlap and superposition of all the absorbed or transmitted wavelengths. Fourier transform is applied to resolve and separate each individual mode or frequency. In this work, acquisition of infrared spectra

was conducted in transmission mode from $650\text{-}4000\text{cm}^{-1}$ with resolution 2points/cm using the Thermo Scientific Nicolet iS10 Spectrometer.

Infrared spectroscopy has been employed for characterisation of coating. An important application of infrared spectroscopy in coating industry is the chemical analysis and determination of composition of a coating [Kendall, 2006]. Vengadaesvaran (2003) has applied FTIR spectroscopy technique to study blending of acrylic resin with silicone resin in coating. It was reported that reaction has taken place between acrylic and silicone intermediate, and can be observed from the appearance of new peaks and shifted peaks. Ramesh *et al.* (2008) has employed the infrared spectroscopy to identify the compositions of silicone-polyester resin, and also the changes in the infrared spectra with different silicone/polyester composition as shown in Figure 3.3.

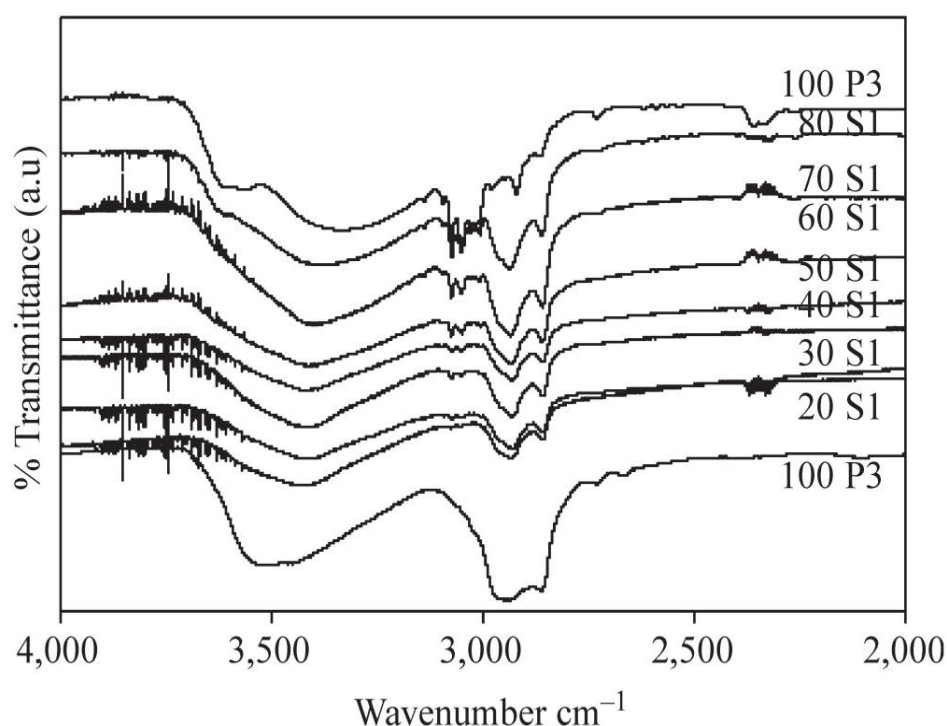


Figure 3.3: FTIR spectra of different compositions of silicone and polyester resins (range of wave number: $2000\text{-}4000\text{ cm}^{-1}$).

Source: Ramesh *et al.* (2008).

3.3.2 Thermogravimetric Analysis (TGA)

Thermogravimetric analysis is a technique in which mass of a material is measured as a function of temperature. This requires heating the material in a controlled environment. Polymers generally exhibit mass loss upon heating. Mass loss may be categorised as volatile components such as moisture, residue solvents, or low molecular mass additives that generally evaporate between ambient and 300 °C [Bruce Prime *et al.*, 2009].

TGA is used to determine polymer thermal stability. Polymers that can withstand higher temperature without decomposing are more thermally stable than those which decompose at lower temperature. In general, degradation mechanisms of polymers are free-radical processes initiated by bond dissociation at the temperature of pyrolysis [Wampler, 2007]. The three specific modes are random scission, unzipping to monomer, and sidegroup elimination. TGA is also used for compositional analysis. In a multicomponent material, the individual component can be separated by temperature, due to different thermal properties. For instance, low molecular weight solvent which evaporates and boils at low temperature can be separated from inorganic materials which are thermally stable up to 900 °C. When a low boiling point material decomposes, a change in mass is noticeable, and detectible from the TGA thermogram. There has also been report that TGA can be utilised in forensic applications [Ihms and Brinkman, 2004].

Derivative TGA (DTG) is an important technique in providing useful information in TGA experiments. It is able to distinguish overlapping mass loss events, identify shapes and maxima of mass loss processes and identify minor mass loss steps [Bruce Prime *et al.*, 2009]. The maximum derivative peak indicates maximum gradient of mass loss, and

hence, each peak indicate separate events. However, DTG should not be used for kinetic analysis due to the larger amount of noise [Bruce Prime *et al.*, 2009].

Nonvolatiles and thermal stability determinations are usually conducted in coating analysis. Compositional analysis may also be applied in coating analysis, where weight loss at different temperatures and modes could indicate differences in materials [Gilman, 2006]. Chew *et al.* (2007) used TGA to study thermal stability of silicone/acrylic resin blends and thermal stability of 30% silicone showed best performance as in Figure 3.4. Vengadaesvaran (2003) has also used TGA method to study thermal decomposition of blending of two types of silicone resins with acrylic resin, and it was reported that mass loss decrease with the increase in silicone concentration.

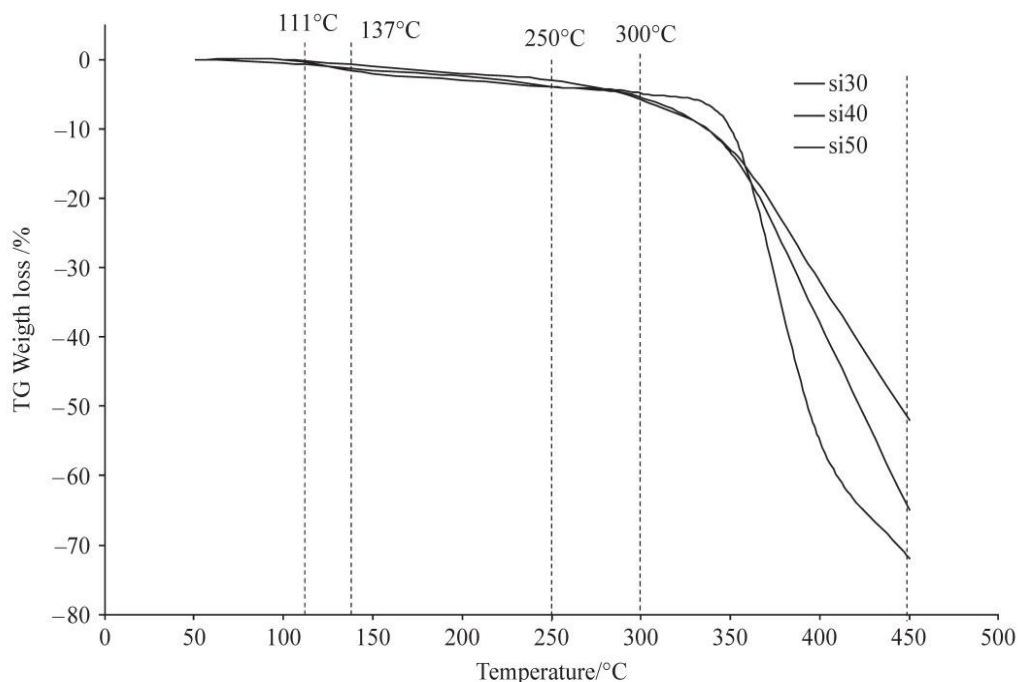


Figure 3.4: TGA of silicone/acrylic blends.

Source: Chew *et al.* (2007).

Comparison of thermal stability of materials can be assessed in thermogravimetric analysis by drawing horizontal line and vertical line across the thermogram. In vertical line comparison, materials with higher weight percentage are more thermally stable than materials with lower weight percentage at a particular temperature, as the latter degraded more. Likewise, in horizontal line analysis, materials with a higher temperature at a particular weight percentage are more stable than materials with lower temperature. This is because the former degraded at a higher temperature at the same weight percent.

In TGA experiment conducted on the coating samples, Hi-Res mode was used. In Hi-Res mode, heating rate is varied in response to changes to the sample's rate of mass loss. This enables better separation of closely overlapped degradation steps. Heating range was from room temperature up to 900 °C and purge gas used was nitrogen.

3.3.3 Glass Transition Temperature by DSC

Glass transition temperature, T_g is defined as the temperature at which an increase in thermal expansion coefficient occurs in an amorphous material [Wicks, 2007]. In amorphous material, its specific volume increases when its temperature increases. There is no sharp change in volume and hence no melting point. Rather, there is an increase in gradient of specific volume with respect to temperature. Temperature at which this change occurs is the glass transition temperature. The phenomenon was first observed in glass, hence the name glass transition. Glass is non-crystalline, mechanically solid and rigid. In molten state, its motion is mainly translational, while in glassy state, its segmental motion is mainly vibrational [Menczel *et al.*, 2009]. Therefore, for polymer above T_g , it is in rubbery state while below T_g , it is in rigid glassy state.

Glass transition temperature can be considered the lowest temperature at which segments of polymer molecules can move with some facility relative to neighbouring segments [Wicks, 2007]. When an amorphous polymer is heated, atoms in the polymer vibrate more vigorously and collide with neighbouring polymer molecule more frequently. At T_g , empty spaces or free volume between adjacent molecules are large enough that adjacent molecule or segment of a polymer molecule can fit into the spaces. Greater increase in thermal expansion coefficient above T_g gives the higher degree of freedom of polymer molecules. This results in higher volume increase with the increase in temperature. For a given molecule, the increased degrees of freedom represent additional ways of absorbing energy, hence the increase in specific heat [Gabbott, 2008]. Figure 3.5 shows the increase in gradient of specific volume with respect to temperature above T_g .

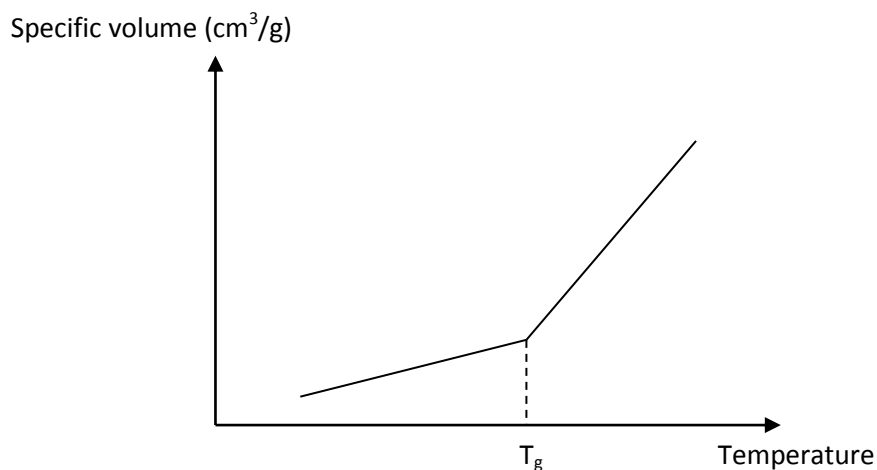


Figure 3.5: Specific volume as a function of temperature for amorphous material.

Glass transition temperature can be measured using differential scanning calorimetry (DSC) method. Differential scanning calorimetry is a thermoanalytical method in which

difference in amount of heat required to raise the temperature of a sample and a reference is measured as a function of their temperature. Figure 3.6 shows typical DSC curve of heat flow to the sample against its temperature.

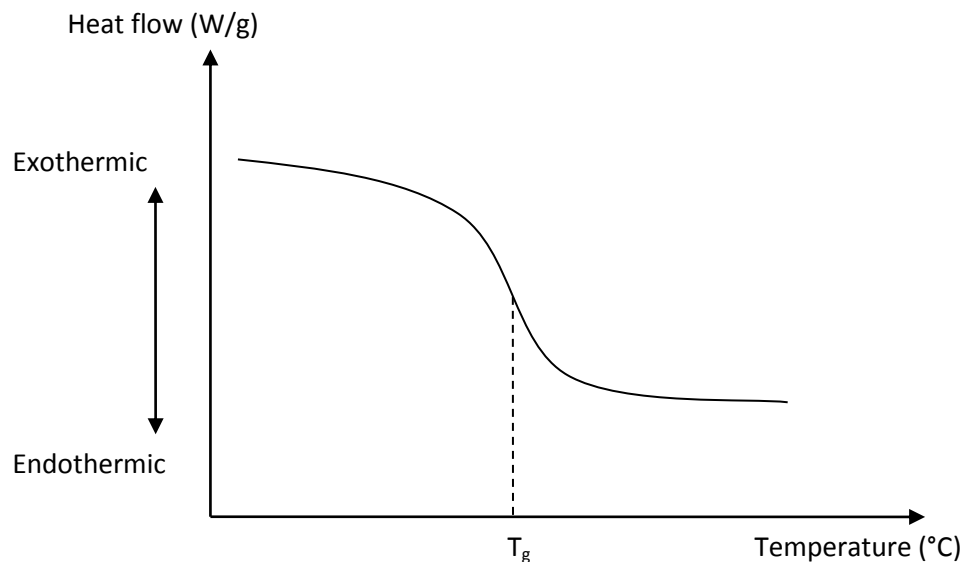


Figure 3.6: Typical DSC curve.

Endothermic part of the curve means the sample absorbs heat or releases less heat relative to the upper part whereas exothermic part of the curve means the sample releases heat or absorbs less heat relative to the lower part [Brown, 2004]. Glass transition temperature, T_g , often taken to be the mid-point of the drop, indicates the increase in energy supplied to the sample to maintain it at the same temperature as the reference material. There is an increase in heat capacity in the sample as it undergoes glass transition and goes into the rubbery form. Above T_g , the sample has higher heat capacity due to larger free volume in it, hence being able to absorb more heat to raise the temperature by the same amount.

The sample pan which contains sample material and the reference pan which is empty are kept in a heating chamber, where heat is supplied to them electrically. Temperature of each pan is measured by a thermocouple and is kept to be the same. Due to the extra polymer material contained in the sample pan, the sample needs to absorb more heat to keep the temperature of the sample increase at the same rate as the reference. The heater will then put more heat to the sample to keep its temperature same as the reference. The difference of heat is measured and plotted against the temperature of the polymer sample.

DSC method has been used to determine glass transition temperature of coating materials which can be used to predict flexibility and hardness of coating [Abidin, 2006; Ramesh *et al.*, 2007; and Vengadaesvaran, *et al.*, 2010]. Abidin (2006) reported that increasing dammar content in the acrylic resin increases its T_g value which leads to higher cross-linking and more brittle characteristics. Ramesh *et al.* (2007) reported an increase in T_g value with addition of silicone into polyester matrix, as shown in Figure 3.7. It was reported that network density was increased, caused by silica cluster formation around the end groups of polyesters.

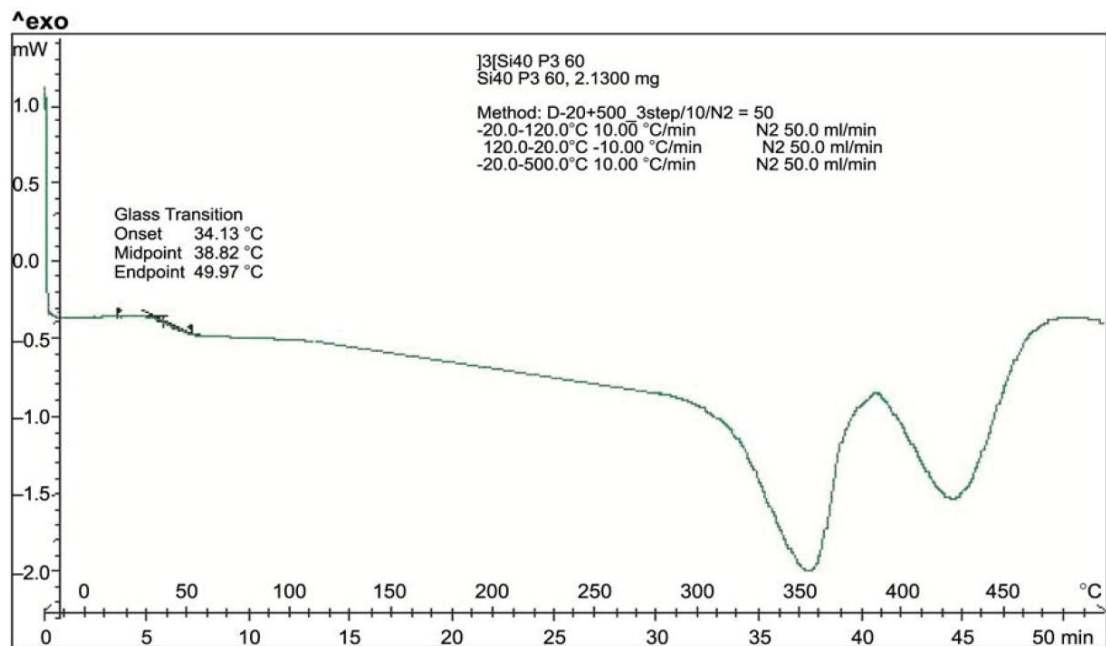


Figure 3.7: DSC thermogram of the silicone/polyester binder system.

Source: Ramesh *et al.* (2007).

3.3.4 CIELAB Colourimetry

Colour is a perspective of human eye and not measurable. The parameters measured are colour stimuli. Appearance of colour to human is limited to visible range of the electromagnetic spectrum. In 1931, Commission Internationale de l'Eclairage (CIE) recommended a standard colourimetric system including colour matching functions for a standard colourimetric observer, standard illuminants, standard light sources, and a chromaticity diagram [Ohta & Robertson, 2005]. Hence, the 1931 RGB colourimetric system was introduced. In 1964, CIE introduced a new colourimetric system with addition of second standard observer. In 1976, CIE recommended two new uniform colour spaces: CIELAB and CIELUV [Schanda, 2007].

To date, CIELAB remains the most common used colourimetric system. In CIELAB system, colour space is three dimensional and is represented by three parameters: L^* , a^* , and b^* . L^* means lightness or brightness, with values range from 0 (total dark) to 100

(total bright). The positive a^* value represents red colour stimuli, while negative a^* represents green colour stimuli. The positive b^* value represents yellow colour, whereas negative b^* value represents blue colour. Figure 3.8 shows the three dimensional L^* , a^* , b^* colour space.

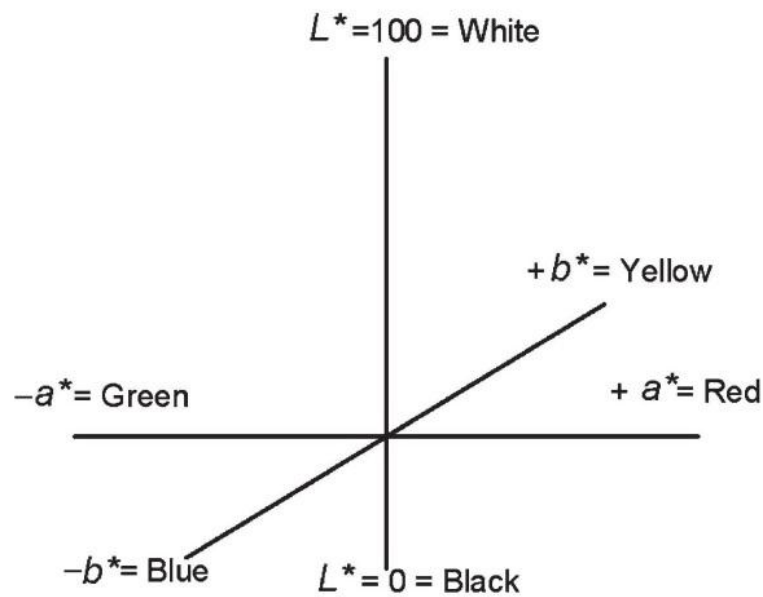


Figure 3.8: 3-D $L^*a^*b^*$ colour space.

Two parameters can be derived from the L^* , a^* , and b^* parameters: the C^* (chroma) and h (hue angle). They are defined as follows:

$$C^* = (a^{*2} + b^{*2})^{1/2} \quad (3.4)$$

$$h = \arctan (b^*/a^*) \quad (3.5)$$

Total colour difference, ΔE between colour pairs is defined as follows:

$$\Delta E = [(\Delta L^*)^2 + (\Delta a^*)^2 + (\Delta b^*)^2]^{1/2} \quad (3.6)$$

Where ΔL^* is difference of lightness, Δa^* is difference of a^* value, and Δb^* is difference of b^* value between two colours. A value of $\Delta E = 1$ was assumed to be the minimum value of colour difference differentiable by human eye [Gonnet, 1998]. CIELAB colour measurement has been a reliable method in estimating degradation of natural pigments. Sanmartin *et al.* (2011) has reported the effective use of CIELAB in estimating chlorophyll degradation. Degradation of anthocyanins in relation with CIELAB has also been reported by Yang *et al.* (2008) and Marco *et al.* (2011). In this work, colour stability of the coating samples upon exposure to UV radiation of wavelength 312nm for 24 hours at room temperature was determined by comparing changes in colour parameters before exposure and after exposure. Spectroline TVC-312A UV lamp was used to produce UV light of 17.55lx. Standard illuminant D_{65} , which represents average daylight and exhibits correlated colour temperature of 6500K, and 2° standard observer were used for measurement of colour. Avantes AvaSpec-2048 Fiber Optic Spectrometer and AvaSoft Colour Application Software were used to obtain the colour parameters and colour diagrams.

3.3.5 X-Ray Diffraction Measurement

X-ray diffraction is a very important technique that has been used to determine crystal structures and size [Cullity, 1956]. It is based on the diffraction or scattering of x-rays by a material. In the case that a material exhibits ordered crystal patterns, the x-rays would be diffracted and favour a certain direction and hence, constructive interference occurs. X-ray diffraction appears on a diffractogram as a sharp peak. The angle at which

this occurs is the glancing angle, the angle between the incident x-ray and atomic plane.

This occurs when Bragg's condition is satisfied as given in Equation.

$$2d \sin \theta = n\lambda \quad (3.7)$$

Where d is the interplanar distance, θ is the glancing angle, n is the order of diffraction and λ is the x-ray wavelength.

XRD can also be used to characterise polymer materials. Due to the amorphous nature of most polymer materials, broad diffraction halo can be observed in the diffractogram. Amorphousness of a material can be represented by the broadness of the halo, where increase in the broadness of peak leads to increase in the amorphous nature [Hema *et al.*, 2010; Mishra *et al.*, 2006]. Broadness can be measured as the full width at half maximum (FWHM) of the peak. Study in the broadness of a peak can be expanded to study the size of ordered domains, or the crystallite size. Analysis of crystallite size in characterisation of polymer has also been conducted by Khayet and Garc ía-Payo (2009). The crystallite size or Scherrer's column length is given by:

$$L = \frac{K\lambda}{B \cos \theta} \quad (3.8)$$

Where K is Scherrer's constant (0.9 in this study), λ is x-ray wavelength, B is the full width at half maximum in radians, and θ is the glancing angle or Bragg angle.

CHAPTER 4: CHARACTERISATION ON AQUEOUS ANTHOCYANIN

4.1 The pH Differential Method

At pH 1.0, anthocyanins exist primarily as red flavylum cation. This can be shown in Figure 4.1, where maximum absorption in the visible range occurs at 518nm at pH 1.0. It can be noticed also that at pH 4.5, the absorption peak in the visible region shows decrease in absorbance by a large amount, and the solution became almost colourless. This is because at pH 4.5, structural equilibrium is disturbed and anthocyanins are discoloured and exist as colourless carbinol form. Hence, it can be inferred that anthocyanins extracted from *Hibiscus sabdariffa* L. (roselle) plant are also subjected to structural transformation between the two pH values.

Difference in absorbance values at the maximum absorption in visible wavelength, $\lambda_{\text{vis-max}}$ between the two spectra after correcting for haze at 700nm can be used to estimate anthocyanin concentration. It yields an absorbance value of 1.1246. By using the modified Beer-Lambert equation, total anthocyanin content expressed as cyanidin-3-glucoside was calculated as 187.8 mg/l. This value falls within the appropriate range from 20 to 3000 mg/l, according to Lee *et al.* (2005). Value of molecular weight was taken as 449.2g/mol, dilution factor employed was 10, molar absorptivity value was taken as 26900 $\text{l mol}^{-1}\text{cm}^{-1}$. In conducting pH differential method to estimate anthocyanin content, selection of solvent is crucial as it will affect the position of the absorption band [Giusti & Wrolstad, 2001].

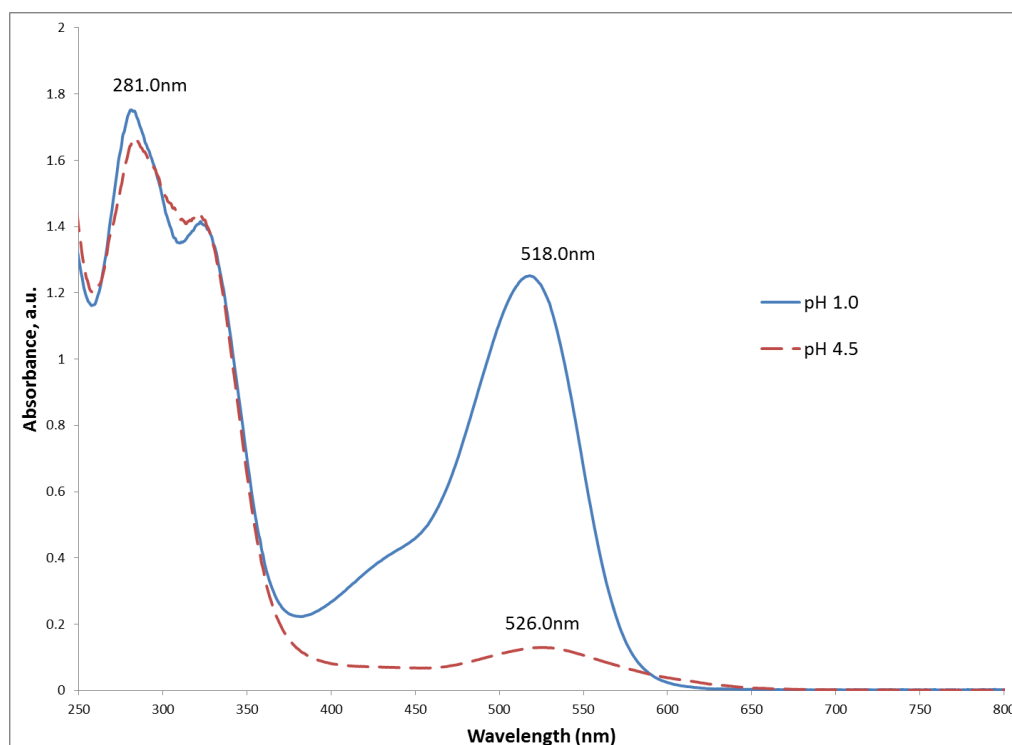


Figure 4.1: UV-visible absorption spectra of anthocyanins at pH 1.0 and pH 4.5.

4.2 UV-Visible Absorption Spectroscopy

Absorption spectra of anthocyanin displayed two bands of absorption: one in the UV region with maximum peak at around 283.5nm and another in the visible region with maximum peak at around 518.0nm. These two bands are spectral characteristics of anthocyanin and can be used to identify it. Giusti and Wrolstad (2001) reported that absorption band in the UV region was around 260-280nm, while that in the visible region was around 490-550nm. Eder (2000) reported that maximum absorption bands of anthocyanin fall in 270-280nm (UV region) and 465-550nm (visible region). Effect of additives on the aqueous anthocyanin can be examined by UV-visible absorption spectroscopy. Figure 4.2 and 4.3 shows the effect of acid and salt respectively on the UV-visible spectrum of aqueous anthocyanin. Relative intensities of the maximum peaks at UV and visible range were studied to reveal masked information. In this work,

relative intensity studies were conducted by taking the ratio of the absorbance of the maximum peak at the visible region to that of the UV region. Table 4.1 lists the relative peak intensities.

It can be seen that addition of 5wt% citric acid and 1wt% hydrochloric acid affected the anthocyanins the most. Hyperchromic effect is observed in those two spectra, where absorption intensity at maximum visible peak shows a large increase. This is shown in the relative peak study where ratios of A_{vis} to A_{uv} increase to 0.6803 and 0.7128 compared to pure roselle anthocyanin's 0.4204. Addition of 5wt% acetic acid however, shows minimal change as the relative intensity of visible to UV absorbance is 0.4220, close to that of roselle anthocyanins. The hyperchromic shift is due to the increase in the π - π electrons system responsible for absorption in the visible range [Yawadio & Morita, 2007]. However, not much change in peak position at both visible and UV regions can be observed.

For samples with 5wt% calcium nitrate, magnesium nitrate and zinc nitrate, an increase in peak intensity at the UV region can be detected. This increase can be attributed to the presence of nitrate anions in all three solutions [Gvozdić *et al.*, 2009; Tomišić *et al.*, 2005]. The absorption maximum at the UV region has changed to around 300nm. Due to changes in position and shape of the maximum peak at UV region, comparison cannot be made between the anthocyanin sample and samples with salts. However, ratios of the visible to UV peak intensity are greatly reduced to 0.1889, 0.1999 and 0.2384 for solution with calcium nitrate, magnesium nitrate, and zinc nitrate, respectively, due to the addition of nitrate salts. It has been reported that the strong absorption at the UV region was due to the $\pi^* \leftarrow n$ transition of nitrate ions [Gvozdić *et*

al., 2009]. No change in the visible peak position can be observed, as shown in Table 4.1, where the maximum wavelength remained the same.

Table 4.1: Relative intensities of maximum peaks at UV and visible range.

Sample	$\lambda_{\text{uv-max}}$ (nm)	Absorbance, A_{uv}	$\lambda_{\text{vis-max}}$ (nm)	Absorbance, A_{vis}	Ratio (A_{vis} to A_{uv})
Antho	283.5	1.7459	518.0	0.7340	0.4204
AAce	283.0	1.6653	518.0	0.7027	0.4220
ACit	282.5	1.7715	519.5	1.2051	0.6803
AHyd	282.0	1.8083	518.0	1.2890	0.7128
ACal	299.0	3.1346	518.0	0.5920	0.1889
AMag	300.0	3.2666	518.0	0.6530	0.1999
AZin	299.5	2.9896	518.0	0.7128	0.2384

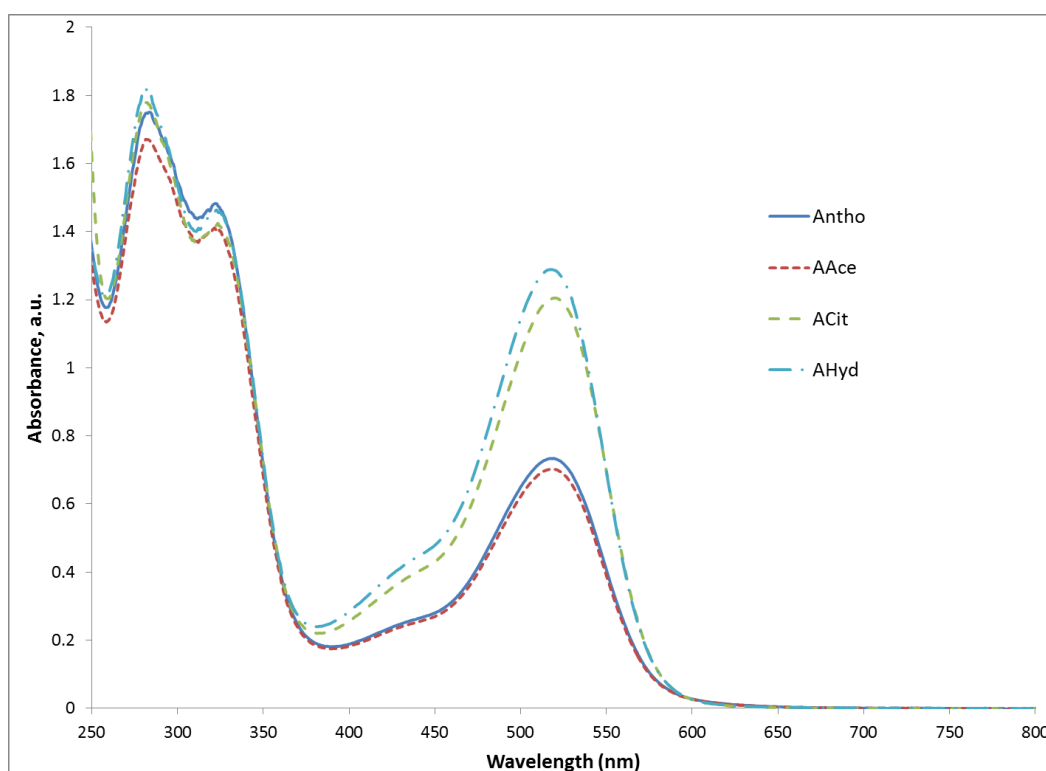


Figure 4.2: Effect of acid on the absorption peak of aqueous anthocyanins.

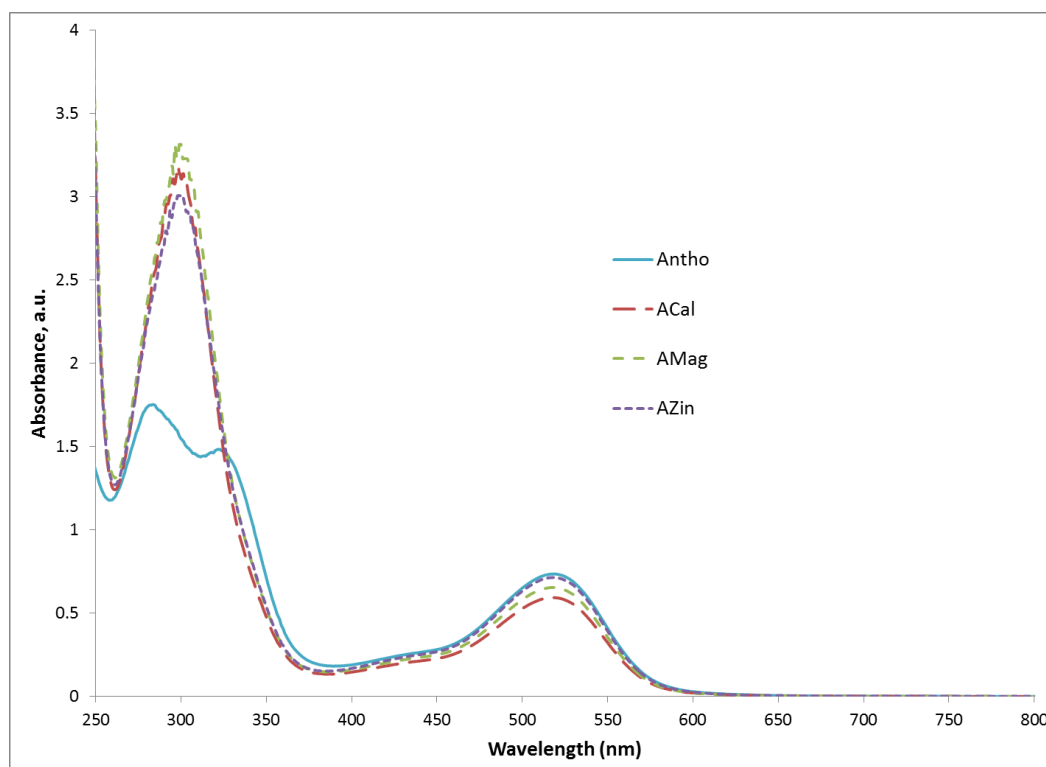


Figure 4.3: Effect of nitrate salt on the absorption peak of aqueous anthocyanins.

4.3 UV Stability of Anthocyanins with Additives

UV-visible absorption spectra of aqueous anthocyanins and anthocyanin extracts with additives exposed to UV radiation for 8 hours are depicted in Figures 4.4 – 4.10. UV radiation has been reported to cause photodegradation of anthocyanins, further causing discolouration effect [Pala & Toklucu, 2011]. From the absorption spectra, degradation of anthocyanins can be associated as drop in the absorption intensity, or the hypochromic effect. It has been reported that degradation of anthocyanin follows first order kinetics [Ahmed *et al.*, 2004; Ozale *et al.*, 2007; Yang *et al.*, 2008]. In first order kinetics, degradation of anthocyanins follows exponential decay and depends only on the initial value. The reaction rate and half-life of first order kinetics are as follows:

$$\ln(A/A_0) = -kt \quad (4.1)$$

$$t_{1/2} = 0.693/k \quad (4.2)$$

Where A is absorbance at time t , A_0 is the initial absorbance, k is the rate constant, and $t_{1/2}$ is the half-life. Initial absorbance values of the samples before UV irradiation (absorbance values at 0th hour) were taken as A_0 . In kinetic analysis of all samples, absorbance data at visible range peak obtained from absorption spectra was fitted to the first order kinetics model using the equations above. In degradation study, absorbance value, A_{vis} of the maximum peak at the visible region ($\lambda_{\text{vis-max}}$) was used as it is indicative of anthocyanin in the flavylium cation form. Plots of $\ln(A/A_0)$ versus t for samples with acid and salt were plotted and illustrated respectively in Figure 4.11 and 4.12. The degradation rate and half-life were calculated and tabulated in Table 4.2.

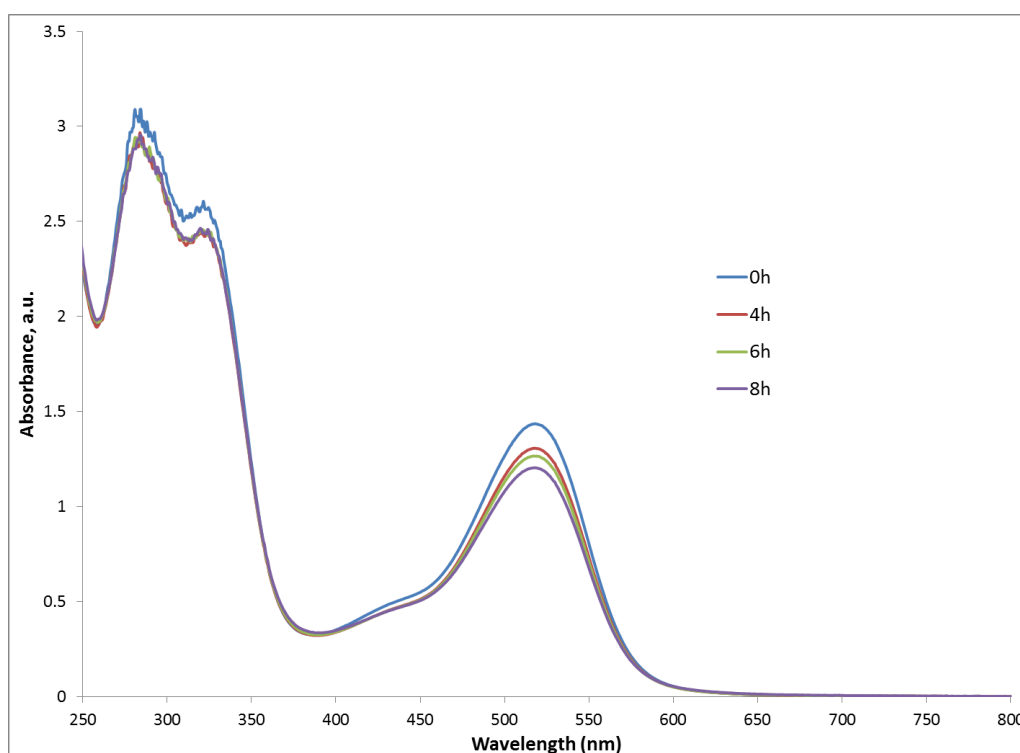


Figure 4.4: UV degradation of Antho.

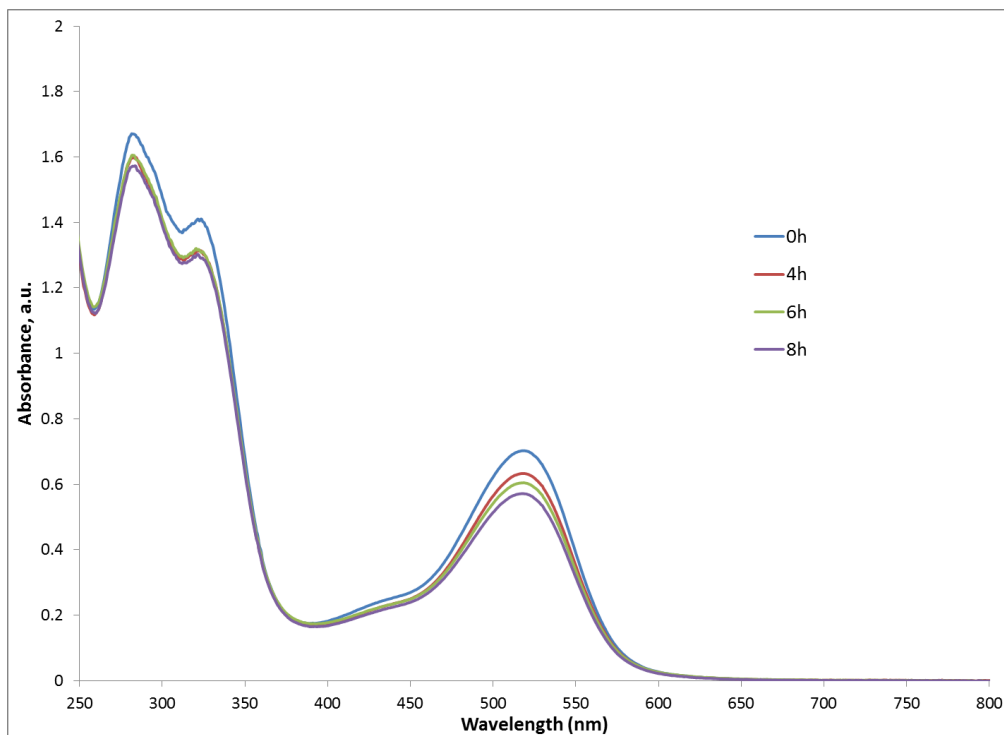


Figure 4.5: UV degradation of AAc.

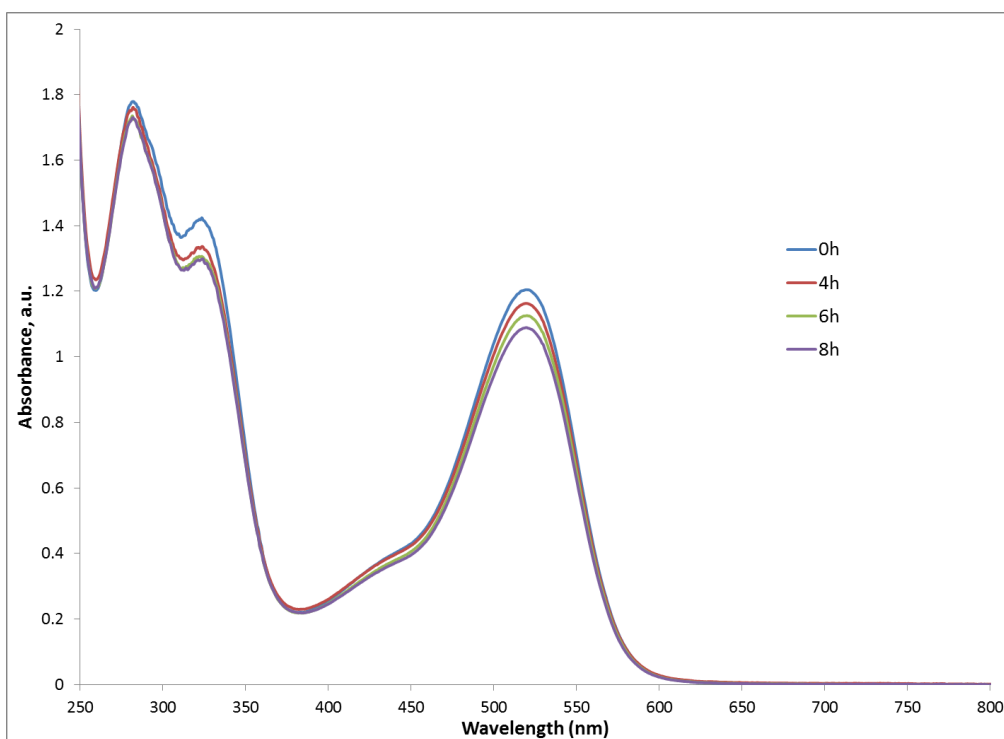


Figure 4.6: UV degradation of ACit.

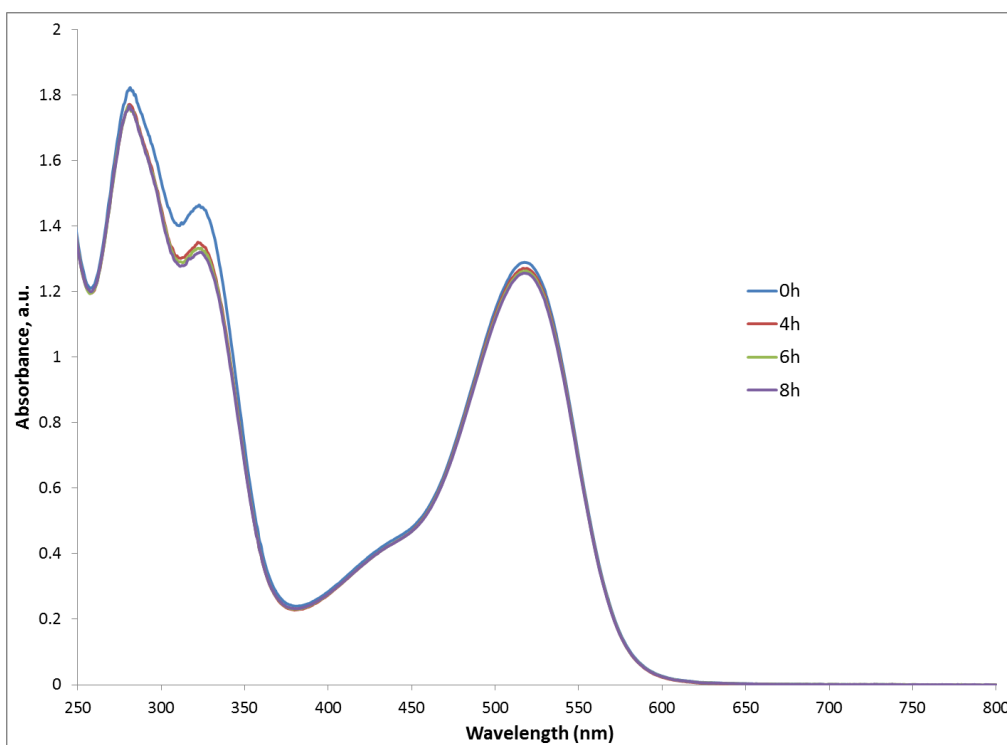


Figure 4.7: UV degradation of AHyd.

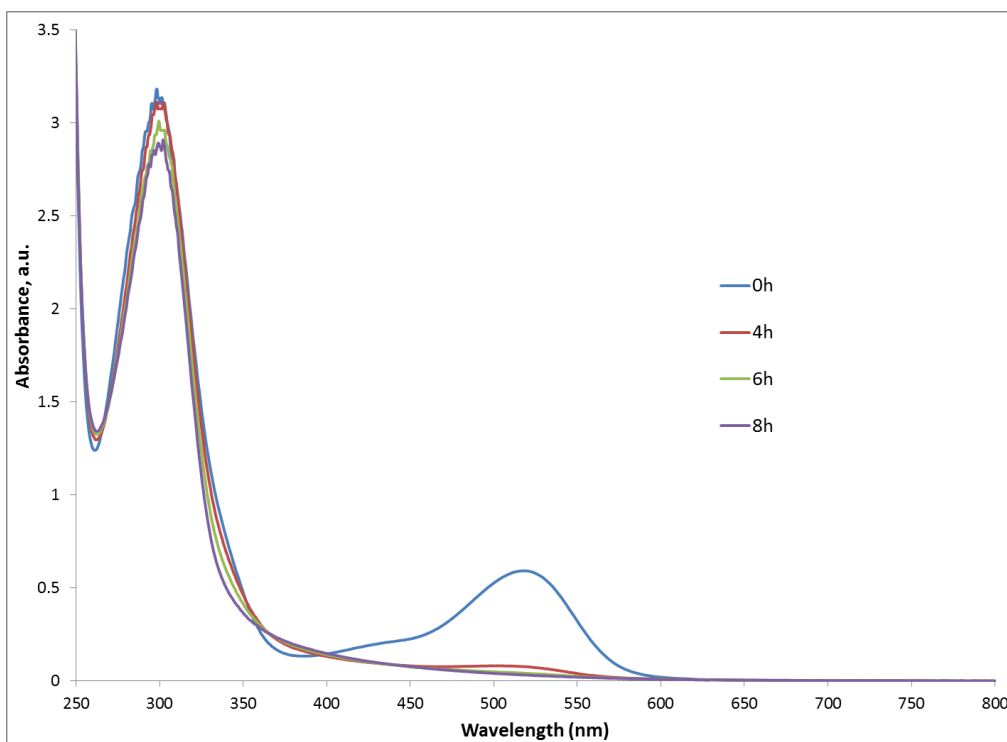


Figure 4.8: UV degradation of ACal.

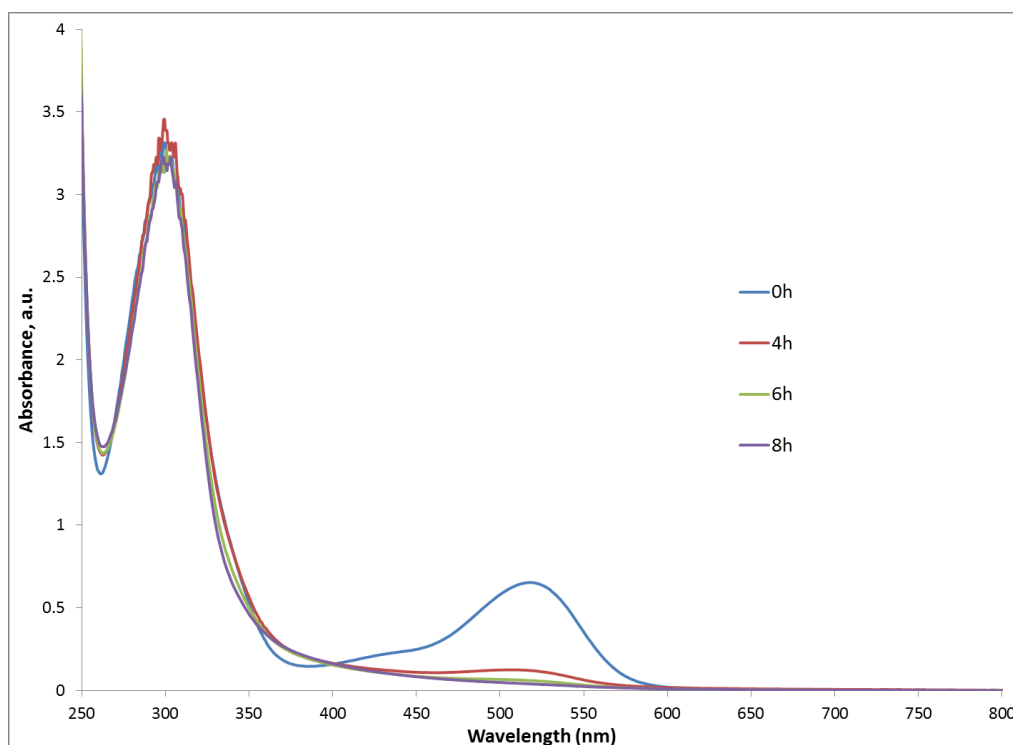


Figure 4.9: UV degradation of AMag.

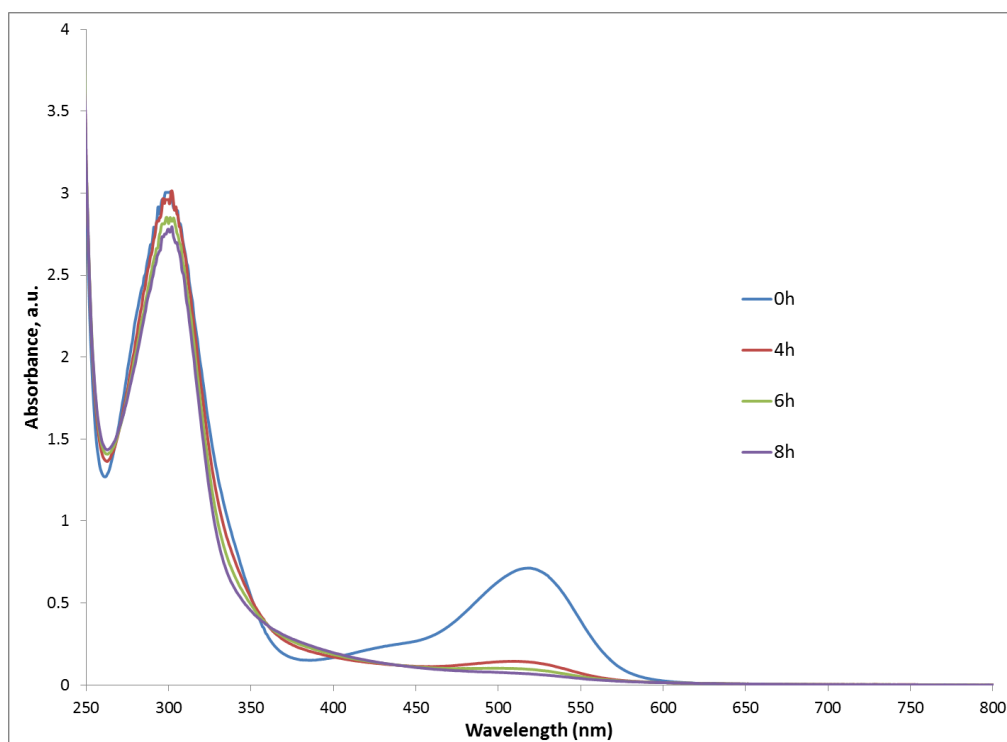


Figure 4.10: UV degradation of AZin.

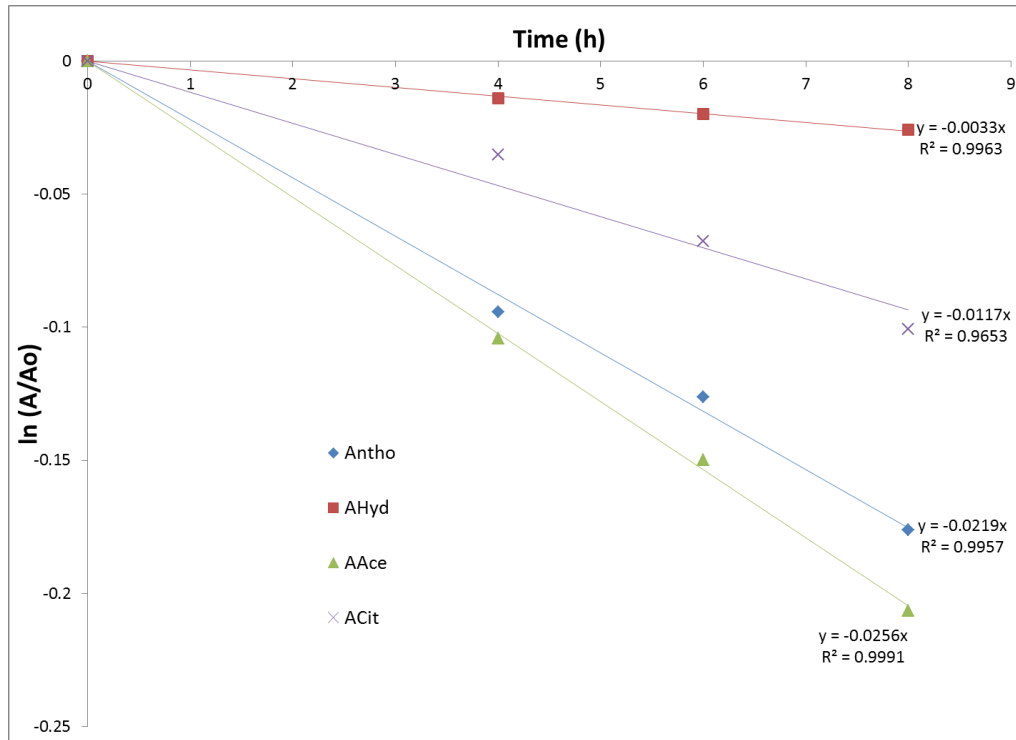


Figure 4.11: Fitted first order kinetics of anthocyanin samples with acid.

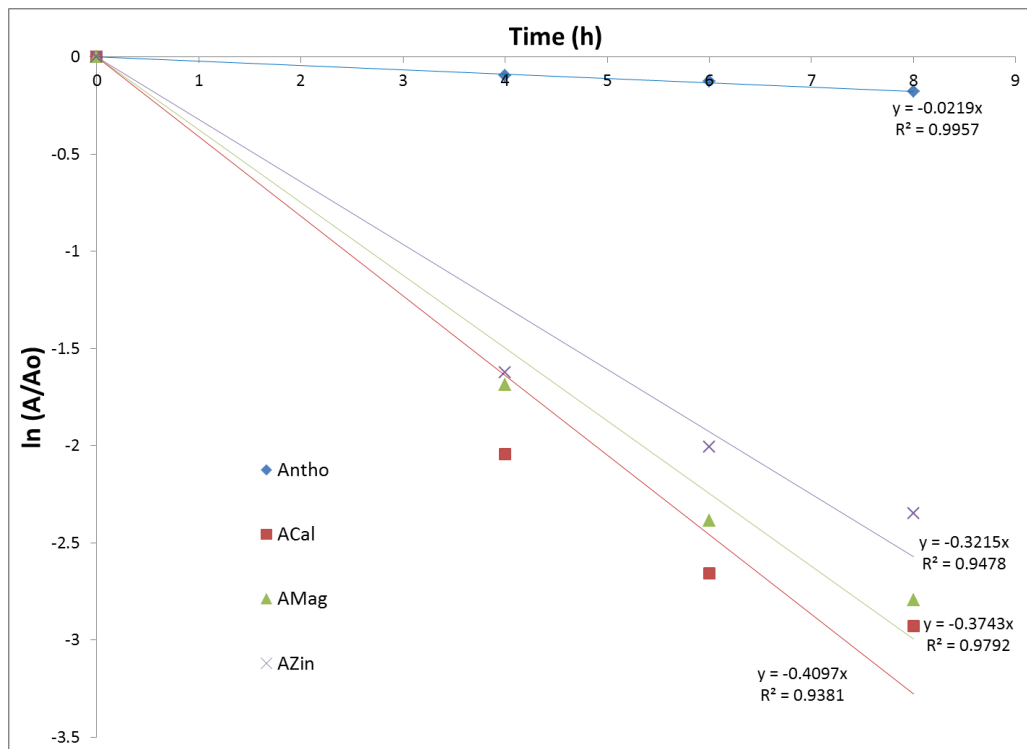


Figure 4.12: Fitted first order kinetics of anthocyanin samples with salt.

Table 4.2: Degradation rates and half-lives of aqueous samples.

Sample	k (h ⁻¹)	t _{1/2} (h)	R ²
Antho	0.0219	31.6	0.9957
AAce	0.0256	27.1	0.9991
ACit	0.0117	59.2	0.9653
AHyd	0.0033	210	0.9963
ACal	0.4097	1.69	0.9381
AMag	0.3743	1.85	0.9792
AZin	0.3215	2.16	0.9478

From Figure 4.4 – 4.10, it can be noted that all samples show hypochromic effect (decrease in absorbance) after irradiation by UV light after 8 hours. According to Marco *et al.* (2011), when anthocyanins are exposed to UV radiation, transformation of the red flavylum cations into colourless cabinol and quinonoidal base occurs. From Figure 4.11 and 4.12, it can be shown that UV degradation of anthocyanins, and anthocyanins with acid and salt is a close fit to the first order kinetics, with R² value close to 1. Degradation rate and half-life of roselle anthocyanins were calculated as 0.0219h⁻¹ and 31.6h, respectively. Comparatively, samples with lower degradation rate and subsequently longer half-life exhibit better anthocyanin retention properties in exponential degradation. A longer half-life indicates that more time is required for a material in study to reach half of its initial amount, and therefore, better stability.

Sample AHyd showed good UV inhibition properties with lowest degradation rate and longest half-life at 0.0033h⁻¹ and 210h respectively, a 7-fold increase from half-life of pure aqueous anthocyanins. Sample ACit also showed improved UV stability with 59.2h. Performance of AAce was similar to that of pure anthocyanins, with half-life

27.0h, slightly lower than that of pure anthocyanins. All samples with salt added (ACal, AMag, and AZin) showed increased degradation rates and decreased half-lives by a large amount. The performance in UV inhibition dropped by 15-fold, to a few hours as compared to pure anthocyanins. Since UV degradation of anthocyanins is related to the structural transformation, it is possible that the salts disturbed the equilibrium and facilitate transformation to colourless carbinol and quinonoidal base.

4.4 Degradation of Anthocyanins by Fungi

In the study of fungal degradation, aspect of interest under study is the observation and detection of presence of fungi, not fungi growth rate. In line of this, visual comparison on day 0 and day 35 of samples kept at room temperature and unexposed to light is tabulated in Table 4.3. Visual inspection of the samples can be supported and improved by CIELAB colourimetric measurement and change in colour of the samples on day 0 and day 35 as indication of degradation. Figures 4.13-4.19 show the colour difference of samples on 0th day and 35th day of storage. Physical measurement of dry weight of the fungi can further support the presence of fungi in both visual inspection and CIELAB colourimetry. Table 4.4 lists the colour parameters and dry weights of all samples.

Table 4.3: Visual comparison of samples on day 0 and day 35.

Sample	Day 0	Day 35
Antho		
AAce		
ACit		
AHyd		
ACal		
AMag		
AZin		

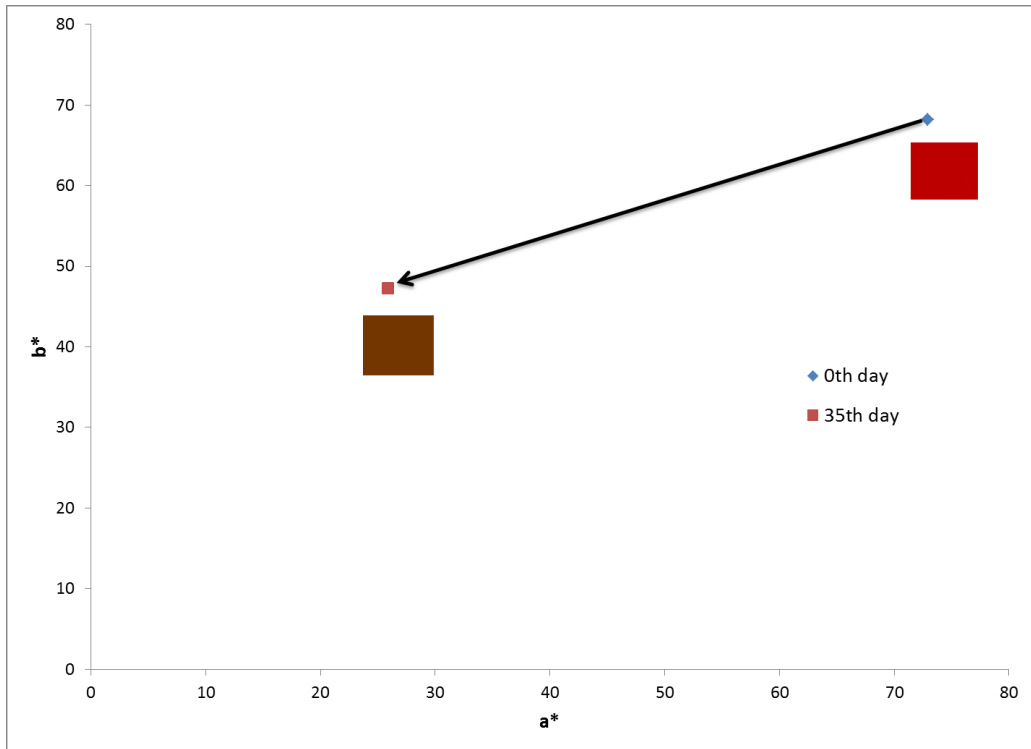


Figure 4.13: Colour degradation of Antho sample by fungi.

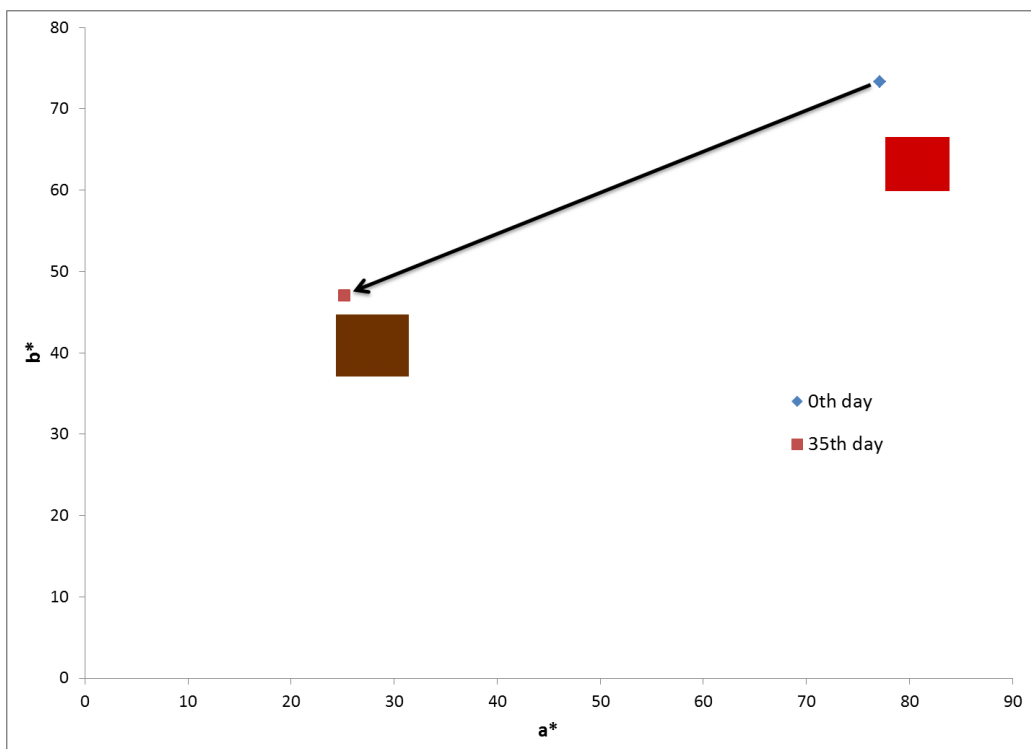


Figure 4.14: Colour degradation of AAce sample by fungi.

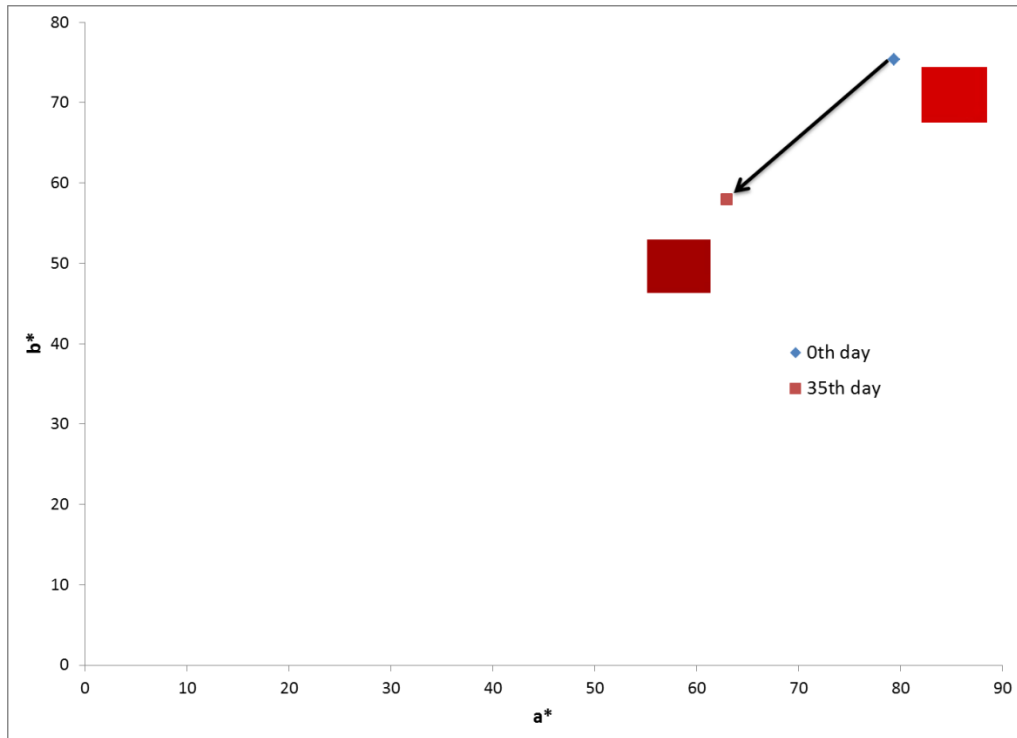


Figure 4.15: Colour degradation of ACit sample by fungi.

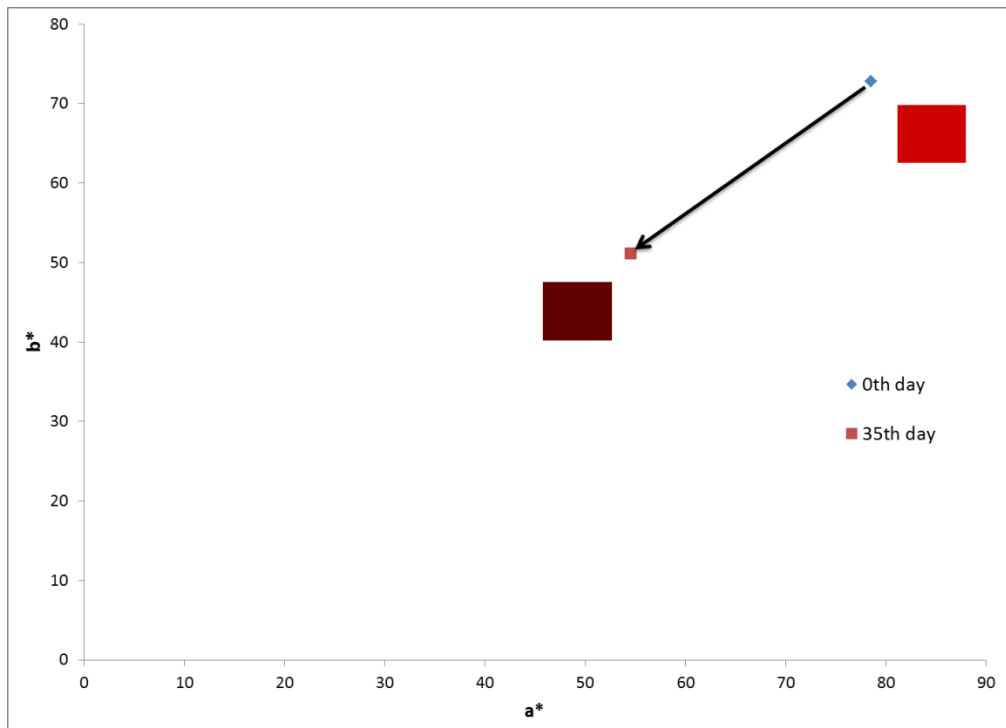


Figure 4.16: Colour degradation of AHyd sample by fungi.

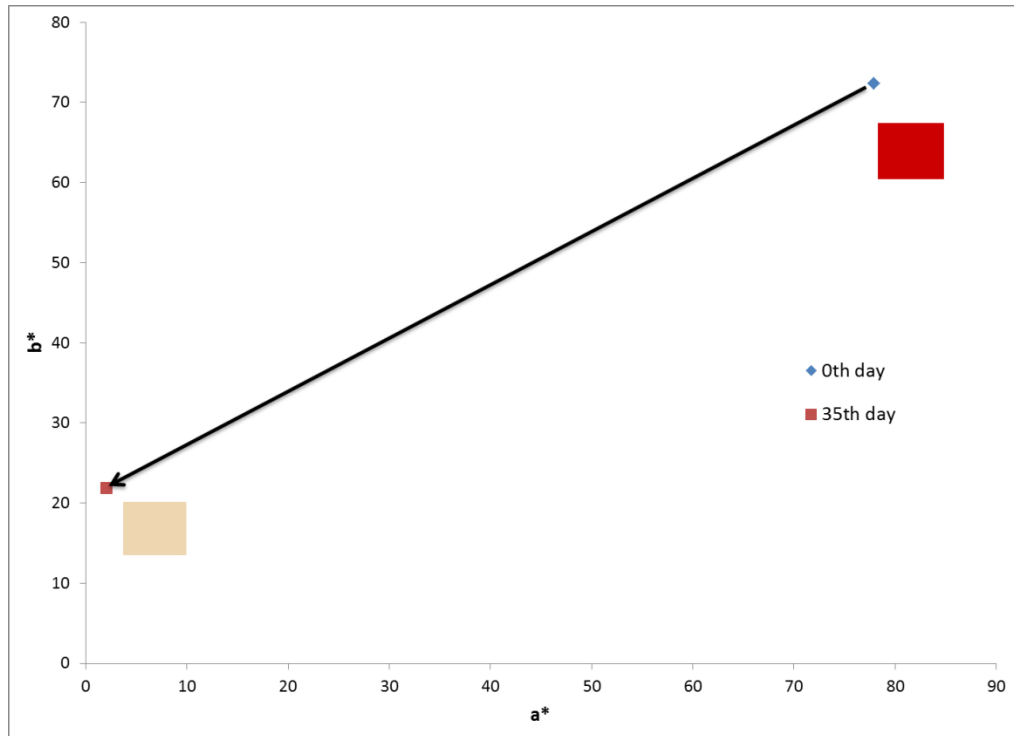


Figure 4.17: Colour degradation of ACal sample by fungi.

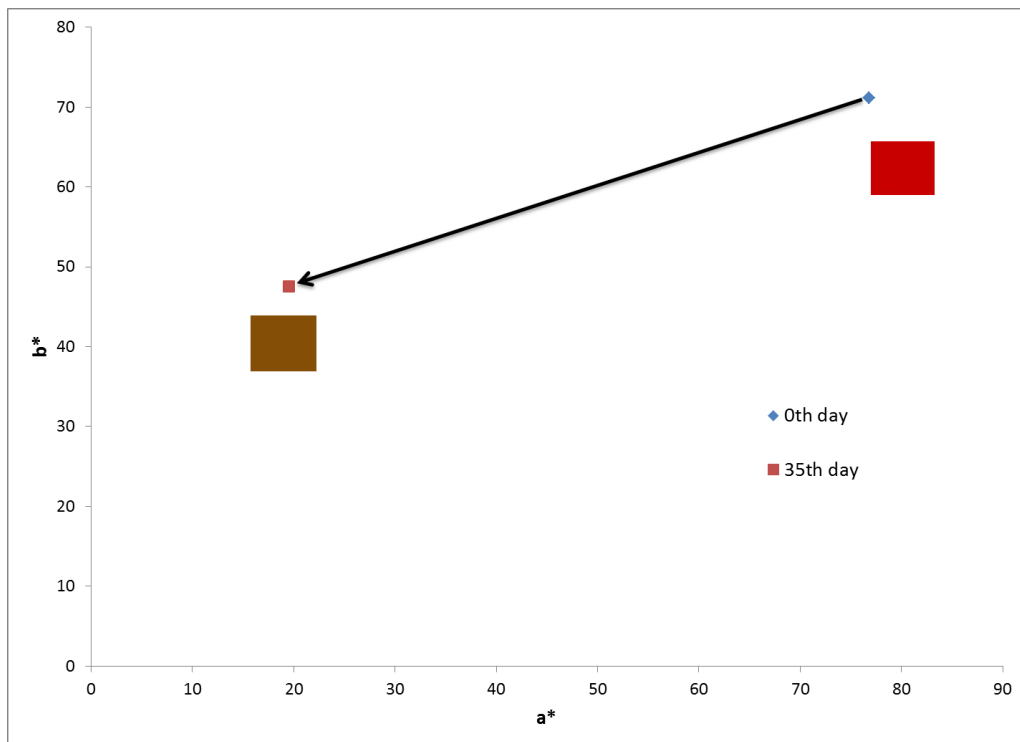


Figure 4.18: Colour degradation of AMag sample by fungi.

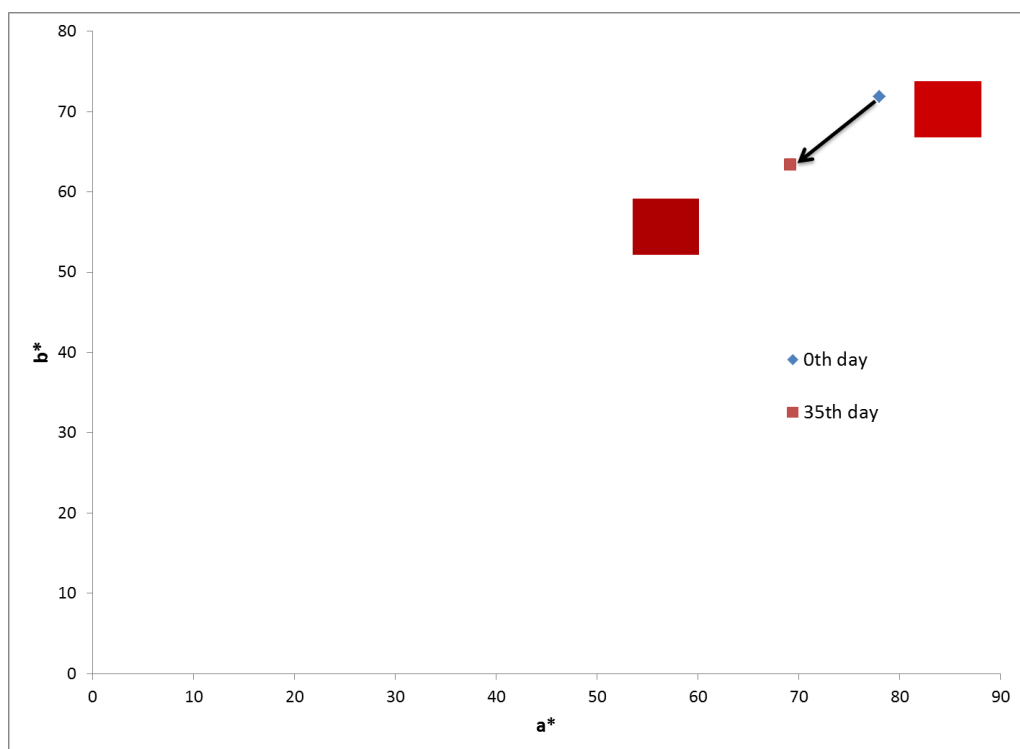


Figure 4.19: Colour degradation of AZin sample by fungi.

Table 4.4: Colour parameters of samples on 0th day and 35th day and fungi dry weight.

Sample	0 th Day			35 th Day			Total colour difference, ΔE	Fungi dry weight, g
	L*	a*	b*	L*	a*	b*		
Antho	35.99	72.92	68.16	29.00	25.88	47.30	51.93	0.030
AAce	39.84	77.11	73.32	27.01	25.19	47.03	55.59	0.024
ACit	41.07	79.37	75.35	31.48	62.95	58.01	25.73	0.022
AHyd	39.28	78.50	72.79	23.18	54.51	51.18	36.08	0.014
ACal	39.05	77.88	72.36	87.04	2.03	21.89	102.97	0.122
AMag	38.37	76.78	71.16	37.92	19.54	47.55	61.92	0.111
AZin	38.91	78.00	71.85	32.91	69.17	63.43	13.60	-

From visual inspection, it can be observed that fungi colonies are detected in Antho, ACit, ACal, and AMag samples. In AAce and AHyd samples, fungi colony is not observed visually, but presence of sedimentary material can be noticed. Presence of sediments could indicate fungi or microbial activity. No fungi colony or sedimentary materials are observed in AZin sample, hence, no data on dry weight can be obtained.

In the study of colour, all samples showed colour change towards b-axis or a-axis from day 0 to day 35 as shown in Figure 4.13- 4.19. This is an indication of colour degradation in all samples. The amount of change can be represented by the length of the arrows. All samples showed decreased values of a^* and b^* , which means colourfulness or saturation of the colour has decreased. Decrease in a^* value indicates the samples are becoming less red in appearance while decrease in b^* value indicates they are becoming less yellow in colour. Antho, AAce, ACal, and AMag samples showed distinctive change towards y-axis, i.e. the yellow zone. This indicated degradation of a larger amount of anthocyanin, as anthocyanins can be associated with red colour (positive a^*) in the flavylium cation form. Direction of colour change towards yellow zone also indicated that degradation products constitute a higher amount than anthocyanins after 35 days. ACit, AHyd, and AZin samples showed direction of colour change towards the origin (grey zone). Decrease in a^* and b^* values is almost the same. It can be shown from the fungi dry weight measurement and visual inspection that fungi growth is less favoured in these samples.

Relationship between the colour degradation and dry weight of the fungi can be established. Generally, the higher the total colour difference before and after 35 days, the higher the dry weight of fungi harvested. However, the dry weight measured included weight of degradation products, such as sediments. In AAce sample, total

colour difference obtained was 55.59, higher than Antho sample. However, the dry weight obtained was lower, at 0.024g. This could be due to the absence of fungi colony on the surface of the sample, but weight of the sediments was included. In AHyd sample, total colour change was lower compared to Antho sample. Presence of sediments gave a dry weight of 0.014g, even though no fungi colony can be observed.

ACit and AHyd samples showed better fungi activity inhibition compared to pure anthocyanin sample. This can be deduced from the smaller values of total colour difference, ΔE and fungi dry weight. AAce sample did not show improvement as the total colour difference was almost the same and the dry weight obtained high. Samples with the least fungi activity inhibition were ACal and AMag. Both samples showed high value of total colour difference at 102.97 and 61.92 respectively, compared to 51.93 of Antho sample. Both samples also yielded large amount of fungi, at 0.122g for ACal sample and 0.111g for AMag sample. This indicates that both samples exhibited increased rate of fungi activity, which could be due to the role of calcium and magnesium as macronutrients required for fungi growth and enzyme activation [Griffin, 1994]. Sample with the best fungal inhibition property was AZin, which showed the smallest colour difference at 13.60 with neither fungi colony nor sediments observed. Hence, the zinc nitrate additive exhibits the potential as fungi inhibitor. Even though zinc is identified as a micronutrient for fungi growth [Griffin, 1994], it has also been reported to be toxic and inhibitory to fungi growth [Babich & Stotzky, 1978]. Since no fungi growth can be observed, the difference in colour can be attributed to the natural degradation of anthocyanins in the sample.

CHAPTER 5: CHARACTERISATION ON PVA-ANTHOCYANIN COATINGS

5.1 Fourier Transform Infrared (FTIR) Spectroscopy

Fourier Transform Infrared spectra of coating with acid and salt as additives are shown in Figure 5.1 and 5.2 respectively. Table 5.1 lists the peaks and their position assignment in pure PVA sample. For pure PVA sample, the bands assigned are characteristic functional groups presence in poly(vinyl alcohol) and can be used as reference. Presence of broad band observed from 3100 cm^{-1} to 3500 cm^{-1} may be assigned to O-H stretching due to strong intramolecular and intermolecular hydrogen bonds [Costa *et al.*, 2008; Andrade *et al.*, 2006]. Presence of bands at 1090.11 cm^{-1} , 1240.54 cm^{-1} and 1732.32 cm^{-1} can be attributed to the C-O stretching, C-C-O stretching and C=O stretching vibrations of non-hydrolysed residual vinyl acetate groups of PVA polymer.

Table 5.1: Band assignment of peaks in pure PVA sample.

Wave number (cm^{-1})	Band assignment	References
844.74	Symmetric C-C-O	Smith (1999)
1090.11	C-O stretch	Linga Raju <i>et al.</i> (2007) Costa <i>et al.</i> (2008)
1240.54	Acetate C-C-O stretch	Smith (1999)
1329.25	OH bend	Costa <i>et al.</i> (2008)
1373.61	Symmetric C-CH ₃ bend	Smith (1999)
1424.72	CH ₂ bend	Costa <i>et al.</i> (2008)
1732.32	C=O stretch (acetate)	Costa <i>et al.</i> (2008) Smith (1999)
2870-2960	CH stretch	Costa <i>et al.</i> (2008)
3100-3500	OH stretch	Costa <i>et al.</i> (2008)

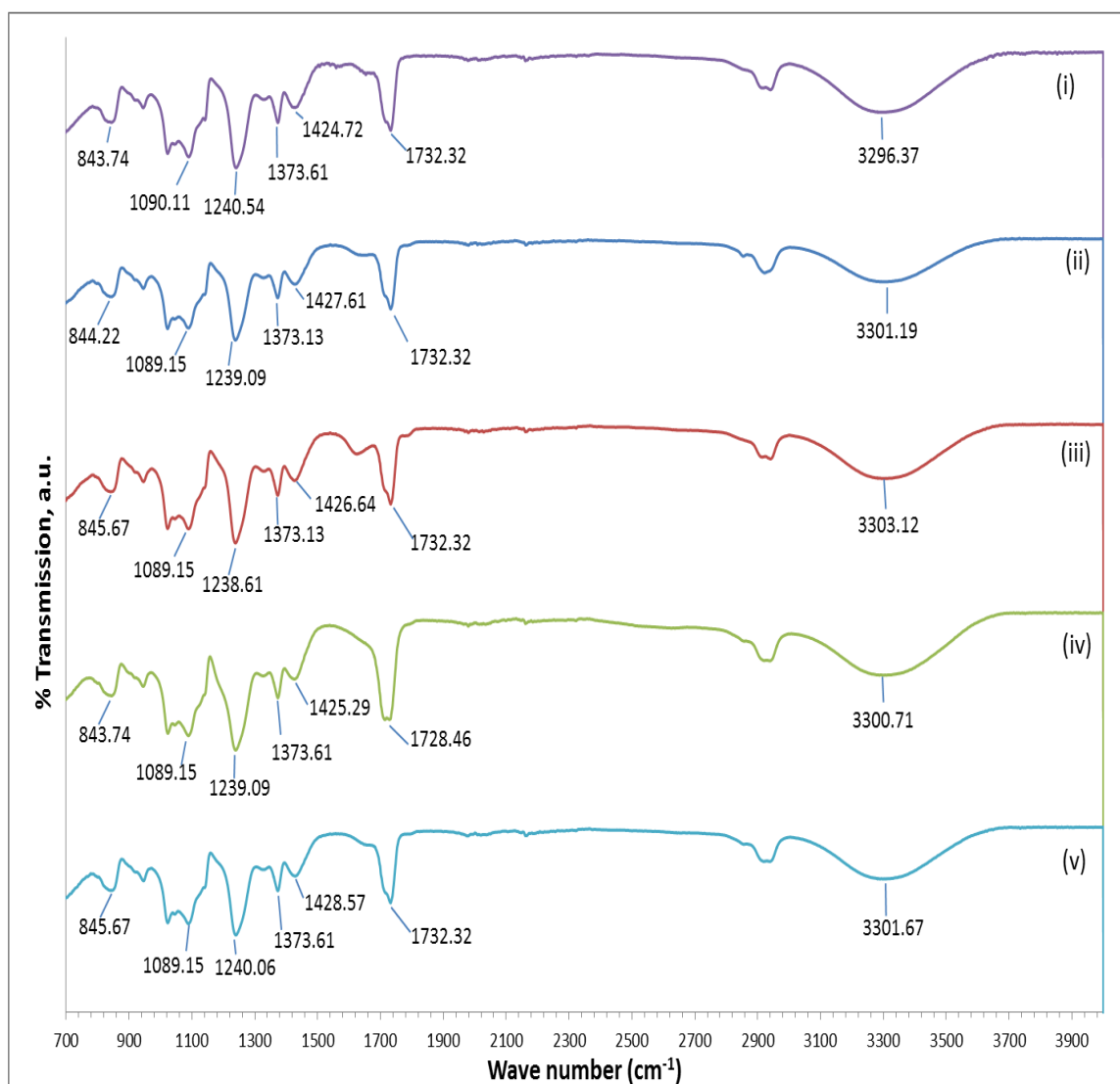


Figure 5.1: FTIR spectra of PVA coatings with acid as additive: (i) PurePVA, (ii) PAntho, (iii) PAAce, (iv) PACit, and (v) PAHyd.

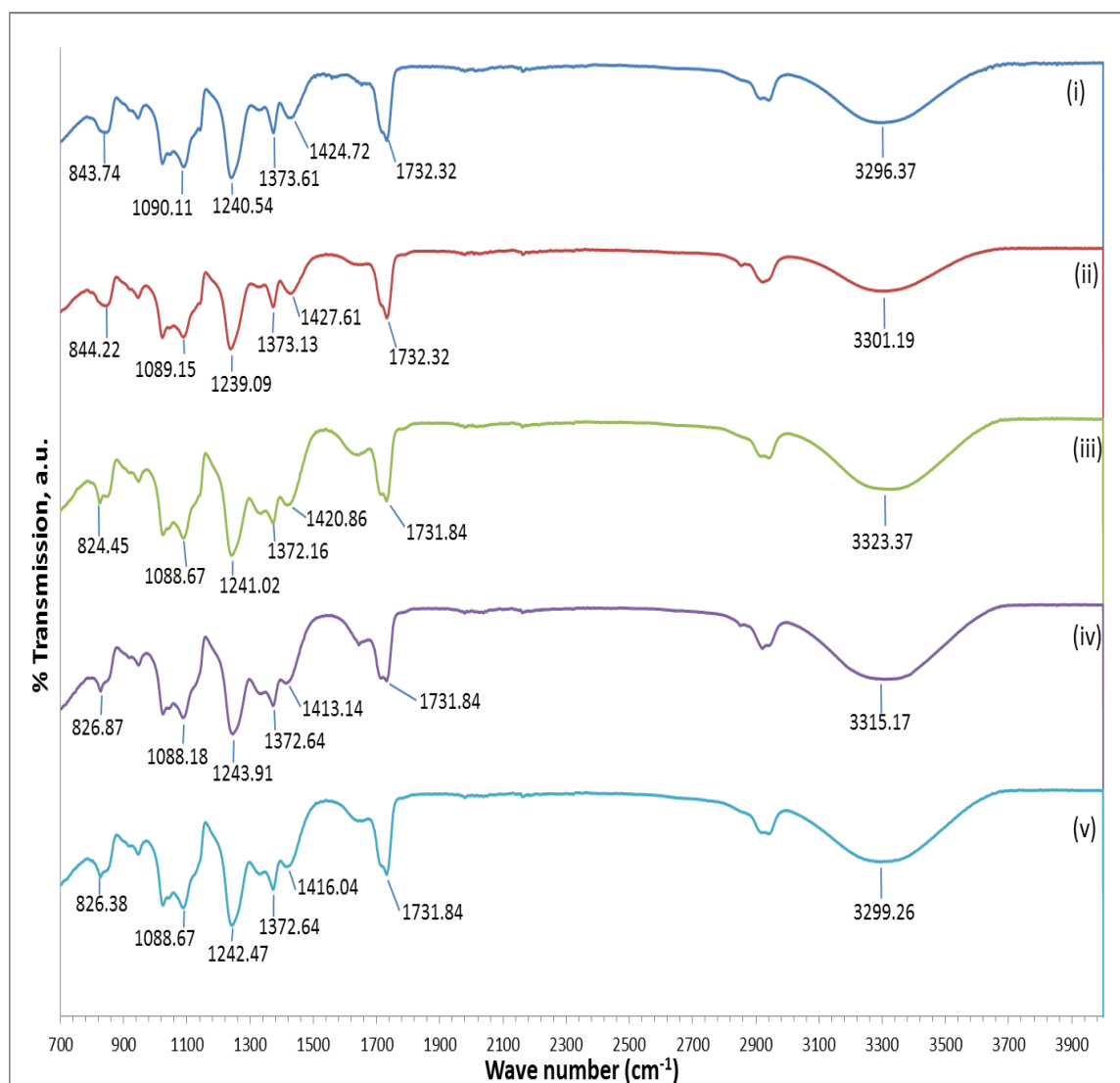


Figure 5.2: FTIR spectra of PVA coatings with nitrate salt as additive: (i) PurePVA, (ii) PAntho, (iii) PACal, (iv) PAMag, and (v) PAZin.

Since the spectra of the samples appeared similar, relative intensities and positions of the peaks were studied to reveal information masked. Lambert-Beer's law states that concentration of a species is proportional to its absorbance, transmission intensities were converted to absorbance values. In relative intensity studies, absorbance of a specific functional group of a sample was compared to absorbance of the same functional group from another sample, and a ratio was obtained between the two. By

comparing the ratio with that for another functional group, information regarding relative amount of the functional group between the two samples can be determined. Relative intensities of the major peaks for all samples are tabulated in Table 5.2 - 5.8.

Table 5.2: Relative peak intensities between sample PurePVA and PAntho.

Sample				Ratio of A_{PAntho} to A_{PurePVA}
PAntho		PurePVA		
Peak Wave Number (cm^{-1})	Absorbance, A_{PAntho}	Peak Wave Number (cm^{-1})	Absorbance, A_{PurePVA}	
844.22	0.0894	843.74	0.1234	0.7243
1089.15	0.1443	1090.11	0.1988	0.7256
1239.09	0.1659	1240.54	0.2258	0.7349
1326.84	0.0573	1329.25	0.0798	0.7182
1373.13	0.0888	1373.61	0.1239	0.7167
1427.61	0.0667	1424.72	0.0943	0.7071
1732.32	0.1058	1732.32	0.1399	0.7563
3301.19	0.0634	3296.37	0.1035	0.6127

Table 5.3: Relative peak intensities between sample PAntho and PAAce.

Sample				Ratio of A_{PAAce} to A_{PAntho}
PAAce		PAntho		
Peak Wave Number (cm^{-1})	Absorbance, A_{PAAce}	Peak Wave Number (cm^{-1})	Absorbance, A_{PAntho}	
845.67	0.1158	844.22	0.0894	1.2953
1089.15	0.1967	1089.15	0.1443	1.3634
1238.61	0.2319	1239.09	0.1659	1.3976
1329.73	0.0775	1326.84	0.0573	1.3523
1373.13	0.1235	1373.13	0.0888	1.3905
1426.64	0.0947	1427.61	0.0667	1.4202
1732.32	0.1415	1732.32	0.1058	1.3378
3303.12	0.0910	3301.19	0.0634	1.4347

Table 5.4: Relative peak intensities between sample PAntho and PACit.

Sample				Ratio of A_{PACit} to A_{PAntho}
PACit		PAntho		
Peak Wave Number (cm^{-1})	Absorbance, A_{PACit}	Peak Wave Number (cm^{-1})	Absorbance, A_{PAntho}	
843.74	0.1107	844.22	0.0894	1.2381
1089.15	0.1812	1089.15	0.1443	1.2562
1239.09	0.2077	1239.09	0.1659	1.2515
1327.32	0.0717	1326.84	0.0573	1.2518
1373.61	0.1113	1373.13	0.0888	1.2534
1425.19	0.0830	1427.61	0.0667	1.2449
1728.46	0.1314	1732.32	0.1058	1.2418
3300.71	0.1104	3301.19	0.0634	1.7417

Table 5.5: Relative peak intensities between sample PAntho and PAHyd.

Sample				Ratio of A_{PAHyd} to A_{PAntho}
PAHyd		PAntho		
Peak Wave Number (cm^{-1})	Absorbance, A_{PAHyd}	Peak Wave Number (cm^{-1})	Absorbance, A_{PAntho}	
845.67	0.1071	844.22	0.0894	1.1980
1089.15	0.1741	1089.15	0.1443	1.2069
1240.06	0.2004	1239.09	0.1659	1.2077
1325.87	0.0702	1326.84	0.0573	1.2260
1373.61	0.1091	1373.13	0.0888	1.2285
1428.57	0.0820	1427.61	0.0667	1.2291
1732.32	0.1311	1732.32	0.1058	1.2389
3301.67	0.0887	3301.19	0.0634	1.3992

Table 5.6: Relative peak intensities between sample PAntho and PACal.

Sample				Ratio of A_{PACal} to A_{PAntho}
PACal		PAntho		
Peak Wave Number (cm^{-1})	Absorbance, A_{PACal}	Peak Wave Number (cm^{-1})	Absorbance, A_{PAntho}	
824.45	0.1535	844.22	0.0894	1.7176
1088.67	0.2371	1089.15	0.1443	1.6437
1241.02	0.2846	1239.09	0.1659	1.7151
1332.63	0.1763	1326.84	0.0573	3.0774
1372.16	0.1992	1373.13	0.0888	2.2435
1420.86	0.1570	1427.61	0.0667	2.3541
1731.84	0.1487	1732.32	0.1058	1.4061
3323.37	0.1244	3301.19	0.0634	1.9622

Table 5.7: Relative peak intensities between sample PAntho and PAMag.

Sample				Ratio of A_{PAMag} to A_{PAntho}
PAMag		PAntho		
Peak Wave Number (cm^{-1})	Absorbance, A_{PAMag}	Peak Wave Number (cm^{-1})	Absorbance, A_{PAntho}	
826.87	0.1597	844.22	0.0894	1.7862
1088.18	0.2222	1089.15	0.1443	1.5401
1243.91	0.2654	1239.09	0.1659	1.5996
1333.11	0.1654	1326.84	0.0573	2.8880
1372.64	0.1927	1373.13	0.0888	2.1700
1413.14	0.1424	1427.61	0.0667	2.1354
1731.84	0.1377	1732.32	0.1058	1.3019
3315.17	0.1342	3301.19	0.0634	2.1157

Table 5.8: Relative peak intensities between sample PAntho and PAZin.

Sample				Ratio of A_{PAZin} to A_{PAntho}
PAZin		PAntho		
Peak Wave Number (cm^{-1})	Absorbance, A_{PAZin}	Peak Wave Number (cm^{-1})	Absorbance, A_{PAntho}	
826.38	0.1610	844.22	0.0894	1.8013
1088.67	0.2355	1089.15	0.1443	1.6325
1242.47	0.2837	1239.09	0.1659	1.7098
1331.66	0.1545	1326.84	0.0573	2.6977
1372.64	0.1892	1373.13	0.0888	2.1311
1416.04	0.1390	1427.61	0.0667	2.0831
1731.84	0.1555	1732.32	0.1058	1.4700
3299.26	0.1284	3301.19	0.0634	2.0254

Infrared spectra of PurePVA and PAntho samples have similar shape. Changes in the position of the peaks are minimal. Addition of anthocyanins into PVA does not cause significant change in the position of peaks. However, study into the relative peak intensity reveals some changes. For PAntho sample, there has been small increase in the C=O and C-O functional groups relative to PurePVA, as can be seen in the increased ratios of 0.7563 and 0.7349 at 1732.32 and 1239.09 cm^{-1} respectively, compared to PurePVA. The increase in these functional groups could be due to the anthocyanins.

For samples with acid as additive, shape and peak positions of the spectra are very similar to PAntho, which does not contain additive. For PAAce, no significant shift can be observed in the peak position. Increase in the relative intensities of O-H stretch, CH_2 , CH_3 , and C-O detected respectively at 3303.12 cm^{-1} , 1426.64 cm^{-1} , 1373.13 cm^{-1} , and 1238.61 cm^{-1} , can be attributed to acetic acid. Increased O-H and C-O relative intensities could suggest that hydrogen bonding occur between acetic acid and PVA.

For PACit and PAHyd samples, the position, shape and relative intensities of peaks are also very similar to that of without acid. For PACit sample, small shift detected at 1728.46 cm^{-1} , which corresponds to C=O bond, could be due to the effect of C=O vibration in citric acid. Presence of relatively higher ratio of C-O, O-H bend and O-H stretch peaks respectively at 1089.15 cm^{-1} , 1327.32 cm^{-1} and 3300.71 cm^{-1} compared to that of PAntho suggests that hydrogen bonding occurs between citric acid with PVA coating. For PAHyd sample, small increase in the relative intensity ratios of CH₂, CH₃, O-H bend, and O-H stretch can be observed at 1428.57 cm^{-1} , 1373.61 cm^{-1} , 1325.87 cm^{-1} , and 3301.67 cm^{-1} respectively. Due to the molecular structure of hydrochloric acid which consists of a hydrogen atom and a chlorine atom, increased intensities of these groups indicate more hydrogen bonding with PVA.

For samples with salt as additive, more obvious changes in peak position, shape and relative intensities can be observed. For all PACal, PAMag, and PAZin samples, a new peak appears at 824.45 cm^{-1} , 826.27 cm^{-1} , and 826.38 cm^{-1} respectively. This vibrational band can be assigned as N-O out-of-plane bending for nitrates [Smith, 1999]. Shifts are detected at 1326.84 cm^{-1} and 1427.61 cm^{-1} , which are assigned as O-H and CH₂ bending vibrations in PAntho sample. For O-H bending vibration, the peaks shifted to 1332.63 cm^{-1} , 1333.11 cm^{-1} and 1331.66 cm^{-1} while for CH₂ bending vibration, the peaks shifted to 1420.86 cm^{-1} , 1413.14 cm^{-1} , and 1416.04 cm^{-1} for PACal, PAMag and PAZin respectively. Shifts in O-H stretching vibration can also be noted. PACal, PAMag, and PAZin samples showed shifts to 3323.37 cm^{-1} , 3315.17 cm^{-1} , and 3299.26 cm^{-1} respectively. Increase in relative intensities and shifts in the O-H stretch, O-H bending, CH₂, and CH₃ vibrations can be observed for the PACal, PAMag and PAZin samples compared to PAntho sample. This indicated an increase of amount in these functional groups in the three samples. Shifts in the O-H and CH₂ bands and appearance of nitrate

groups could suggest that interaction occurred in the form of hydrogen bonding between nitrate functional group and PVA.

5.2 Thermogravimetric Analysis (TGA)

Results of thermogravimetric analysis and derivative TGA (DTG) are shown in thermograms in Figures 5.3 – 5.10. Overlapped thermograms of all samples are illustrated in Figure 5.11. Table 5.9 lists the remaining percent weight of the samples at 300 °C, while Table 5.10 lists temperature of the samples when they are at 70% weight. Thermogravimetric analysis and its derivative analysis are very important technique in determining thermal stability of coating materials. In addition to that, these techniques can also be used to study the degradation of coating materials including their degradation products.

From the thermogram of PurePVA sample, it is noticeable that poly(vinyl alcohol) undergoes three degradation steps. The first weight loss at temperature below 100 °C is due to the water content. This degradation step was also observed in all other samples, which indicated evaporation of moisture. Second degradation step at 200 °C - 400 °C, which accounts for the highest percent change in weight, is due to the thermal degradation of PVA molecule. The third weight loss from 400 °C - 500 °C was due to PVA byproducts [Chen *et al.*, 2008].

PAntho sample, in which anthocyanins are added, showed an additional small degradation step of about 5.35% and a DTG peak at 200 °C - 250 °C, as shown in Figure 5.4. By comparing this with pure PVA sample, the additional step can be attributed to the degradation of anthocyanin, or its degradation byproducts. Thermogram of PAAce sample is similar to that of PAntho and addition of acetic acid has minimal effect on the

degradation of PVA. For PACit sample, appearance of large weight loss steps and DTG bands of peaks at 200 °C - 250 °C and 400 °C - 450 °C as shown in Figure 5.6 can be attributed to the fragments or decomposition products of citric acid [Hardy *et al.*, 2003]. For PAHyd sample, degradation at 400 °C - 450 °C was also enhanced, which could be due to the evolution of hydrochloric acid.

For PACal, PAMag, and PAZin samples, in which nitrate salt was added as additive, additional steps can also be observed. From Figures 5.7 -5.9, small degradation steps and DTG peaks observed at temperature 150 °C - 200 °C can be attributed to evolution of water and fragments of nitrates such as NO and NO₂ gasses [Malecka *et al.*, 2003]. Besides, appearance of weight loss steps and DTG peaks can also be detected at temperature 300 °C - 400 °C in the three samples. These decomposition steps are due to NO, NO₂ and O₂ gasses, which are the decomposition byproducts of nitrates [Malecka *et al.*, 2003; Madarasz *et al.*, 2007; Migdal-Mikuli *et al.*, 2004]. It can also be observed from Figures 5.8-5.10 that PACal, PAMag, and PAZin samples which respectively contained calcium, magnesium and zinc metal cation showed higher residue content at temperature higher than 600 °C. This could be due to the formation of the respective metal oxides which are thermally stable after the liberation of NO, NO₂ and O₂ gasses [Malecka *et al.*, 2003; Migdal-Mikuli *et al.*, 2004; Brockner *et al.*, 2007].

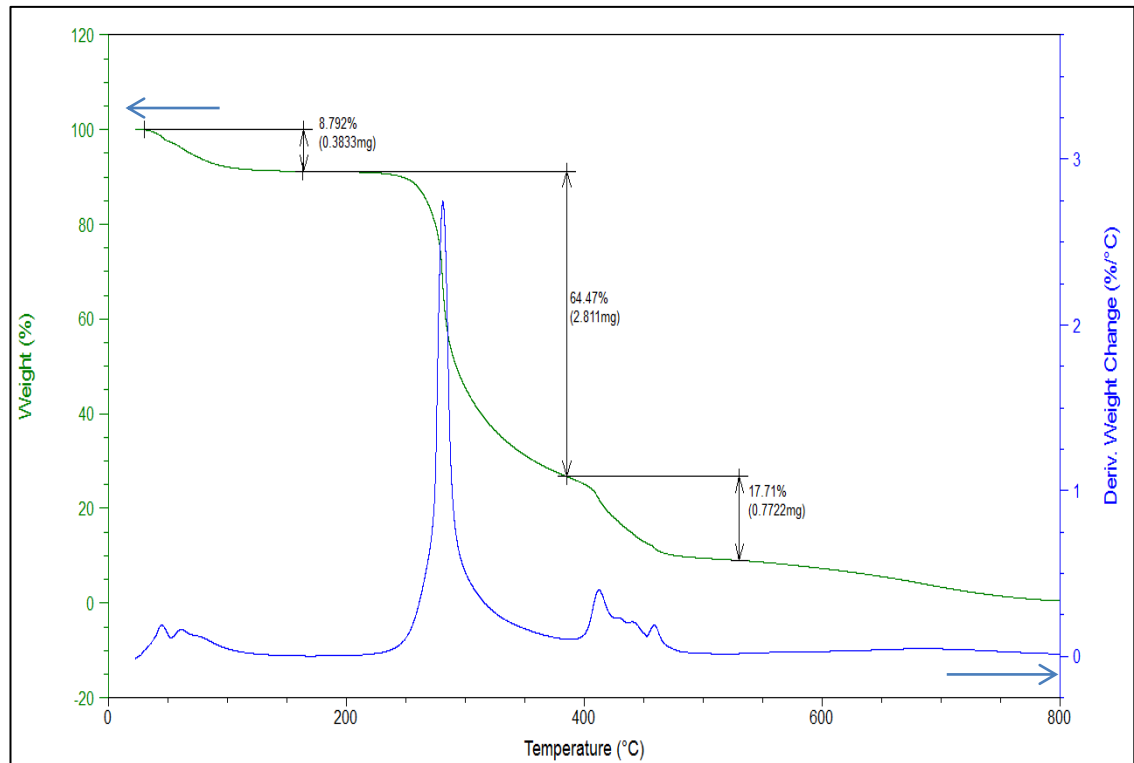


Figure 5.3: Thermogram and DTG of Pure PVA sample.

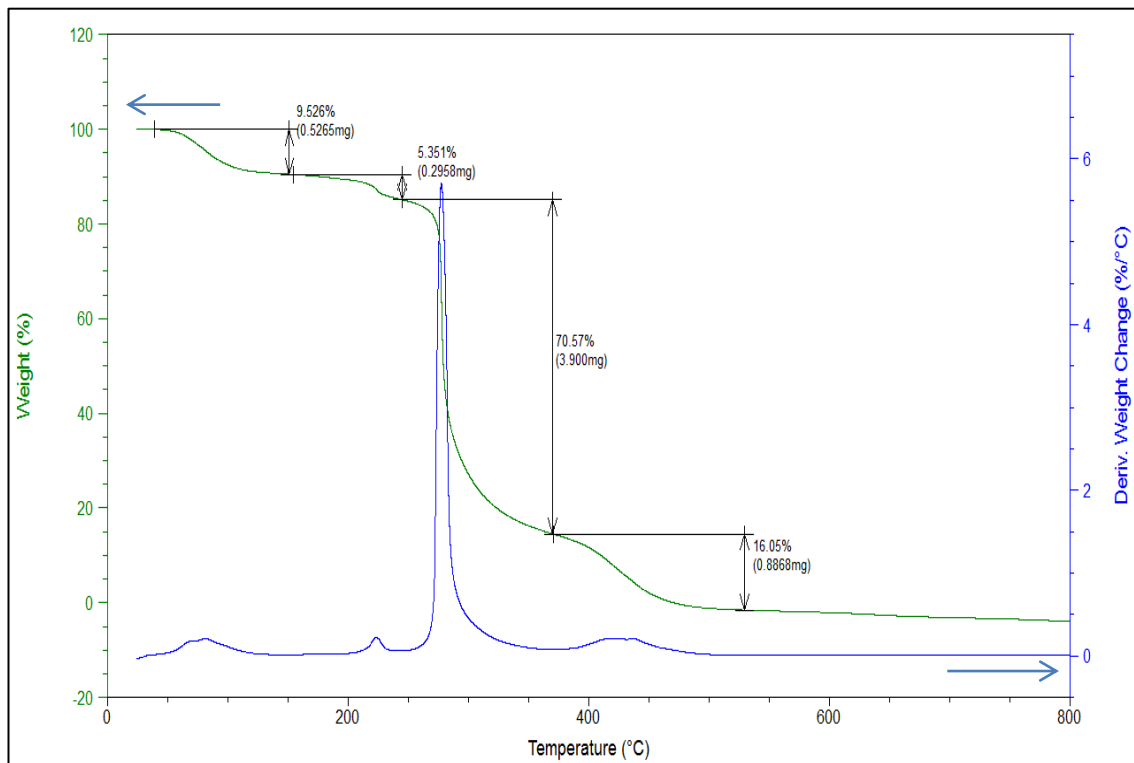


Figure 5.4: Thermogram and DTG of PAntho sample.

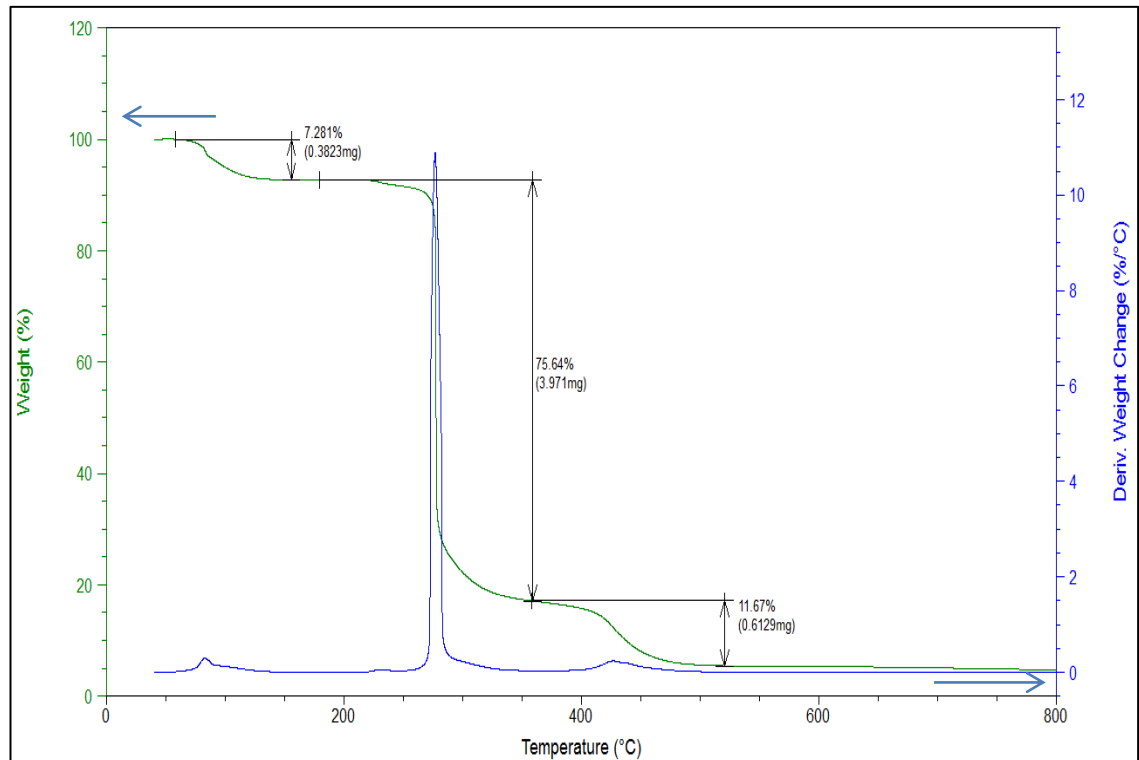


Figure 5.5: Thermogram and DTG of PAAce sample.

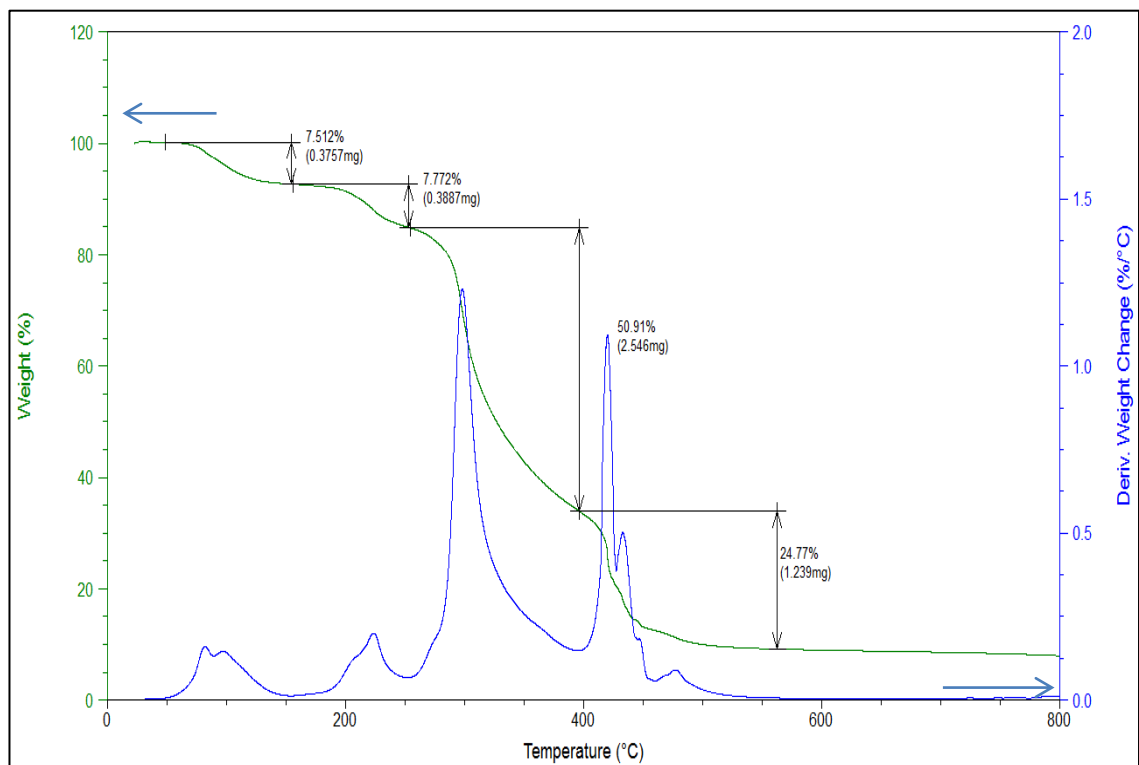


Figure 5.6: Thermogram and DTG of PACit sample.

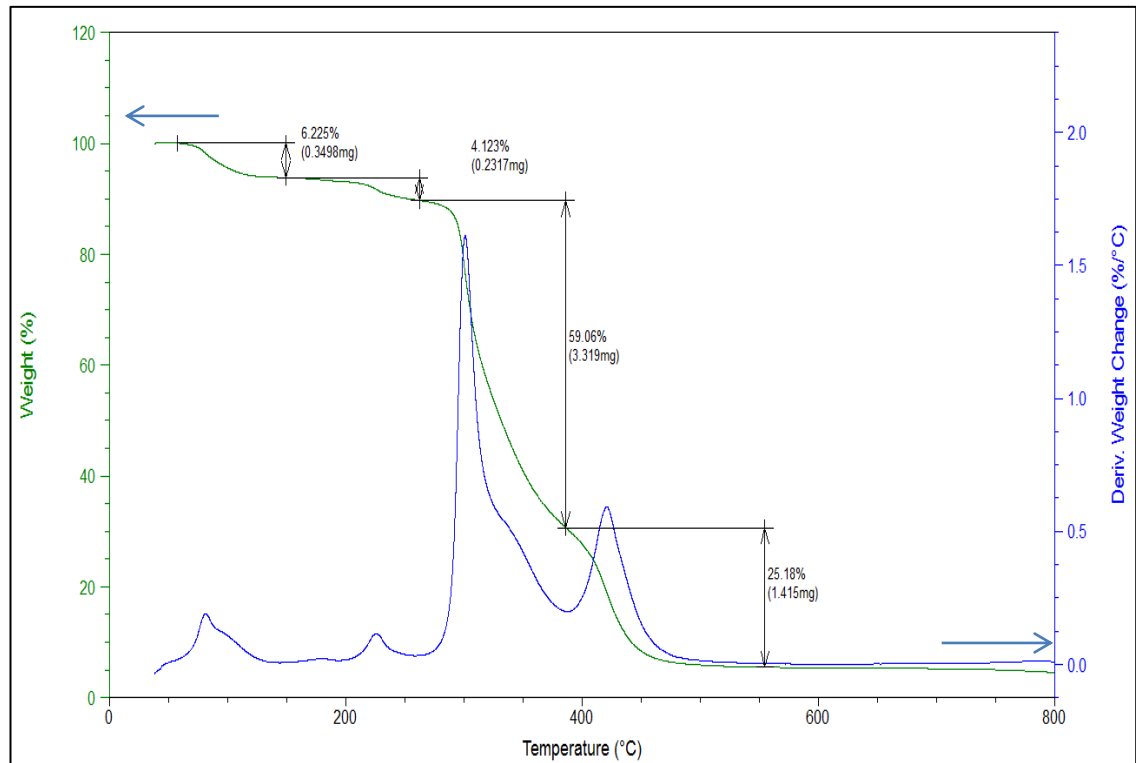


Figure 5.7: Thermogram and DTG of PAHyd sample.

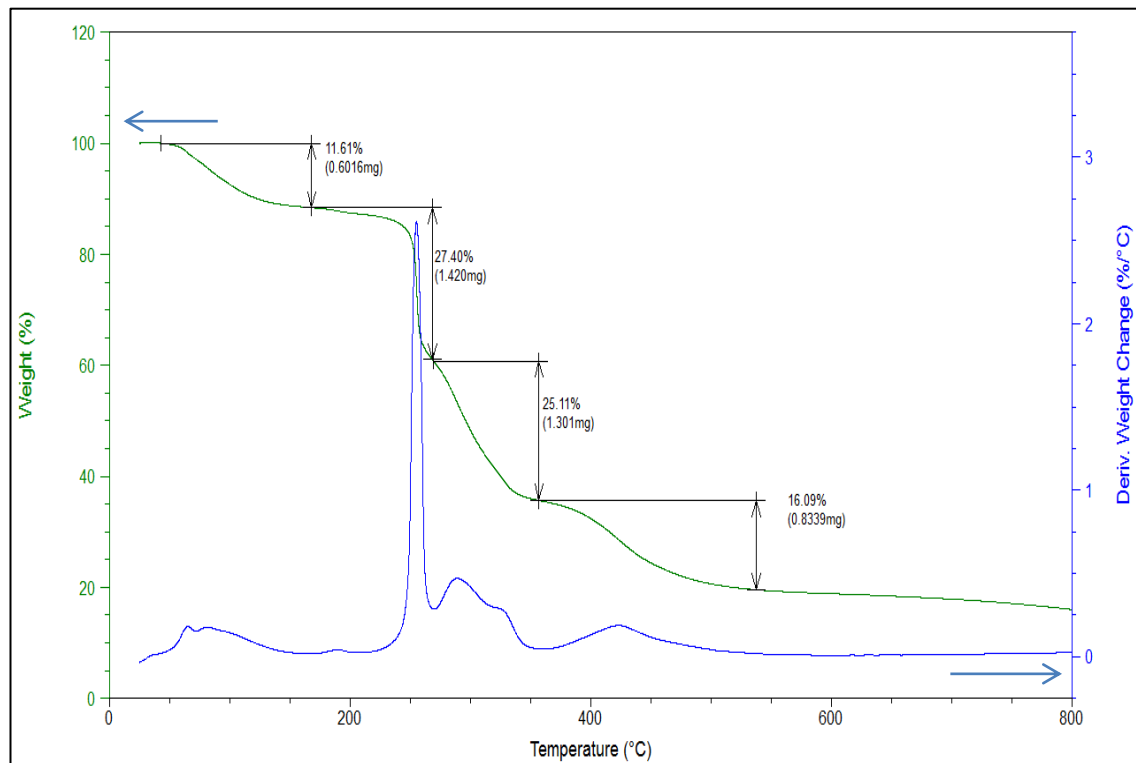


Figure 5.8: Thermogram and DTG of PACal sample.

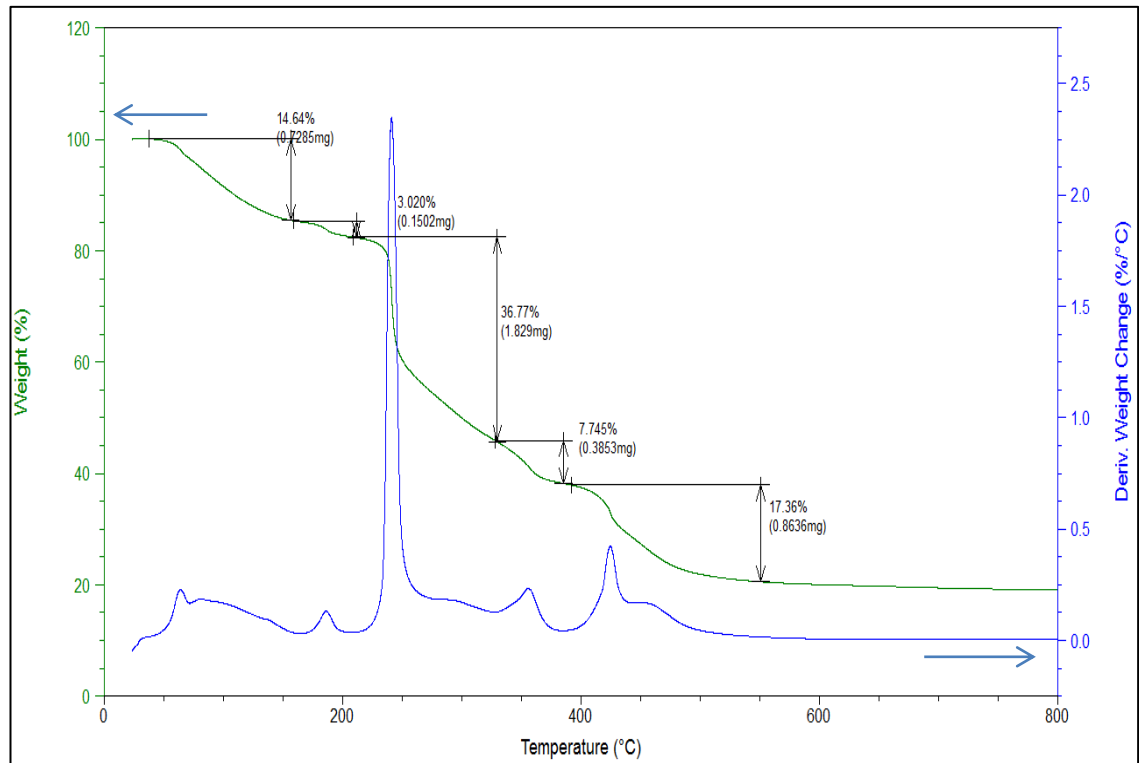


Figure 5.9: Thermogram and DTG of PAMag sample.

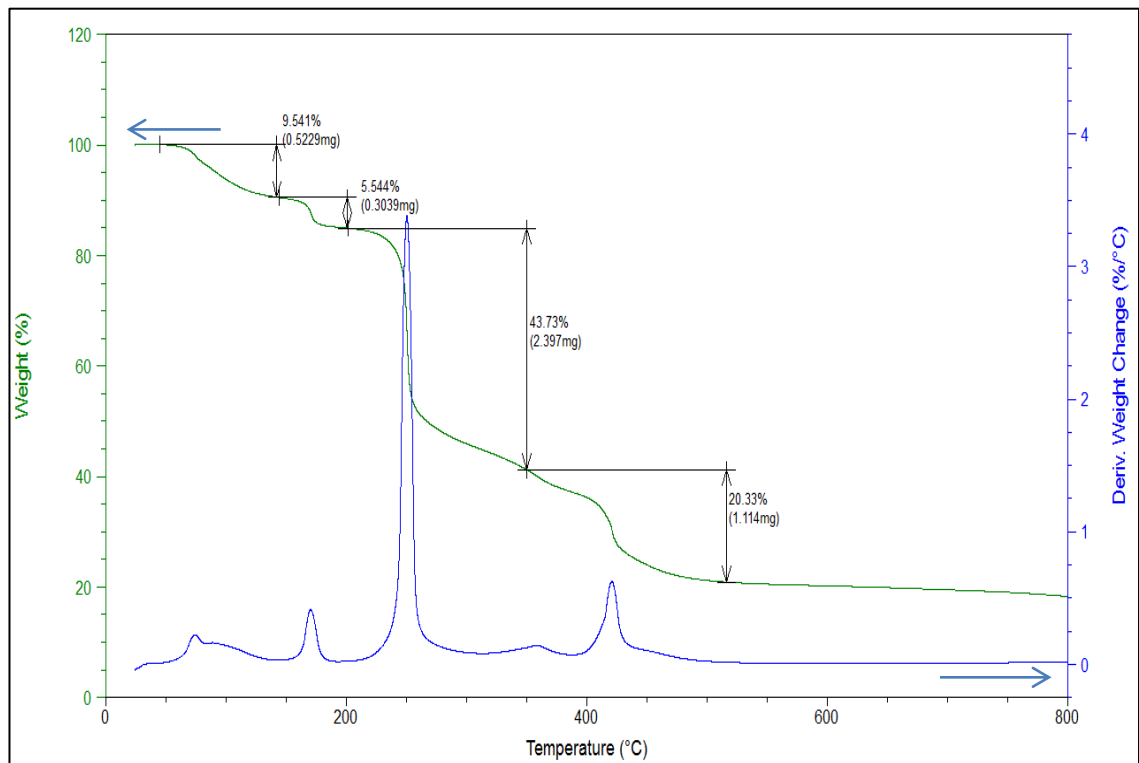


Figure 5.10: Thermogram and DTG of PAZin sample.

Addition of anthocyanin into the PVA does not alter much the thermal stability of PVA, as decomposition of PVA main chain (degradation with the largest step) occur almost at the same temperature as shown in Figure 5.11. This can also be shown in Table 5.10 where degradation temperatures of PurePVA and PAntho at 70% weight are close, at 280.70 °C and 277.33 °C respectively. Addition of acetic acid has minimal effect on the thermal stability of the coating, as can be shown from the close values of percent weight at 300 °C and temperature at 70% weight from Table 5.9 and 5.10 respectively. Addition of citric acid and hydrochloric acid shifts the degradation of PVA to higher temperature, at 300 °C - 350 °C as compared to 250 °C - 300 °C in PurePVA, PAntho and PAAce, hence enhancing thermal stability of PACit and PAHyd samples. This can also be seen in Table 5.9, where weight percentages of PACit and PAHyd are respectively 67.69% and 78.60%, higher than PurePVA and PAntho with only 45.61% and 27.21% left. From Table 5.10, PACit and PAHyd has also displayed higher temperature at 298.16 °C and 305.37 °C respectively compared to PAntho at 277.33 °C.

On the other hand, addition of salt shifts PVA decomposition to lower temperature at 220 °C - 270 °C, causing the samples to be less thermally stable. This is also shown from Table 5.10 where samples with nitrate salts as additive displayed lower temperature at 70% weight compared to PurePVA and PAntho. As can be noticed from DTG curves of samples with salts, decomposition at lower temperature could be initiated by evolution of NO and NO₂ gasses. However, at 300 °C, their weight percentages are higher than that of PurePVA and PAntho as observed in Table 5.9. This could be due to the presence of more thermally stable nitrate salts in these samples [Malecka *et al.*, 2003; Migdal-Mikuli *et al.*, 2004]. Referring to the thermograms of PACal, PAMag, and PAZin, it is observed that decomposition of the material is continuous due to the presence of more decomposition products and fragments of the additives, as opposed to

sharp drop in weight in PurePVA and PAntho samples. Hence, it can be deduced that thermal stability of PVA coating can be influenced by the addition of additives and thermal stability of the additives.

Table 5.9: Percent weight of all coating samples at 300 °C.

Sample	Weight at 300 °C (%)
PurePVA	45.61
PAntho	27.21
PAAce	22.26
PACit	67.69
PAHyd	78.60
PACal	48.35
PAMag	50.00
PAZin	45.94

Table 5.10: Temperature of coating samples at 70% weight.

Sample	Temperature at 70% weight (°C)
PurePVA	280.70
PAntho	277.33
PAAce	277.74
PACit	298.16
PAHyd	305.37
PACal	256.27
PAMag	247.87
PAZin	250.01

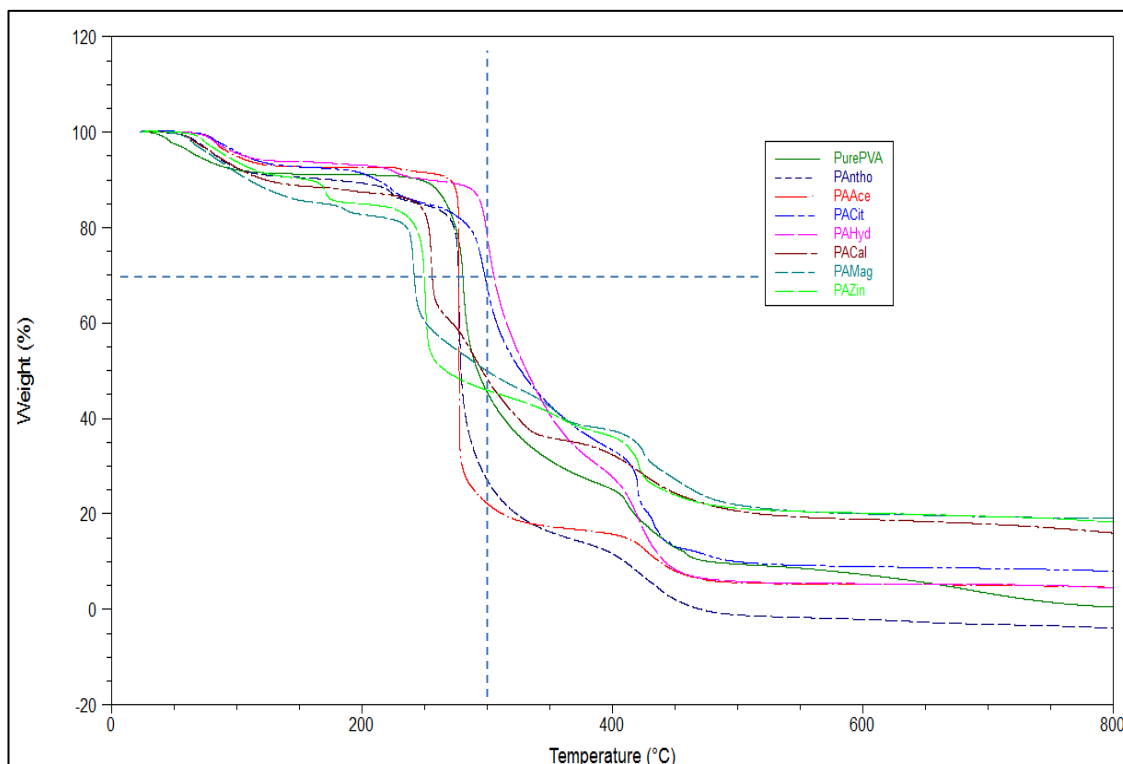


Figure 5.11: Overlapped thermograms of all coating samples.

5.3 Glass Transition Temperature by DSC

Glass transition temperatures of the all samples are shown in Figure 5.12 – 5.19. It can be observed that glass transition temperature of pure PVA is found to be 62.97 °C. It has been reported that glass transition temperature of PVA ranges from 70 - 80 °C [Malathi *et al.*, 2010; Sudhamani *et al.*, 2003]. Anthocyanins do not seem to have significant effect on PVA. The recorded T_g of PAntho sample is 61.46 °C, which is close to that of pure PVA. Addition of additives into PVA could affect its glass transition temperature. Increase in glass transition temperature indicates less chain mobility and more intramolecular and intermolecular hydrogen bonding [Nugent *et al.*, 2005]. On the other hand, lower glass transition temperature causes higher segmental motion of polymer chain due to plasticization [Malathi *et al.*, 2010].

Addition of acid has minimal effect on the glass transition temperature of PVA. This can be seen in Figures 5.14 - 5.16. Addition of acetic acid increases the T_g to 62.34 °C, which is close to the value of 61.46 °C for PAntho. Addition of hydrochloric acid has also increased the T_g by a small amount to 64.28 °C. Addition of citric acid causes a small drop in T_g value of PVA from 61.46 °C to 59.37 °C. On the other hand, addition of nitrate salts into PVA causes large increase in the T_g of the PVA sample. PACal, PAMag, and PAZin samples recorded high T_g values at 83.10 °C, 83.76 °C and 74.46 °C, respectively, at least a 13 °C increase, as compared to 61.46 °C of PAntho. The large increase could be attributed to the interaction between nitrate functional group and PVA through hydrogen bonding. Formation of the hydrogen bonding in these samples can be observed in the increase intensity and shift in O-H, CH₂ and CH₃ bonds in the infrared spectra of these samples, as discussed in Section 5.1. There has been report that presence of hydrogen bonding could increase glass transition temperature [Lin *et al.*, 2010; Xu *et al.*, 2002]. Increase in glass transition temperature upon addition of inorganic salt has also been reported by Kim *et al.* (2003), Every *et al.* (1998), and Belfiore *et al.* (1992).

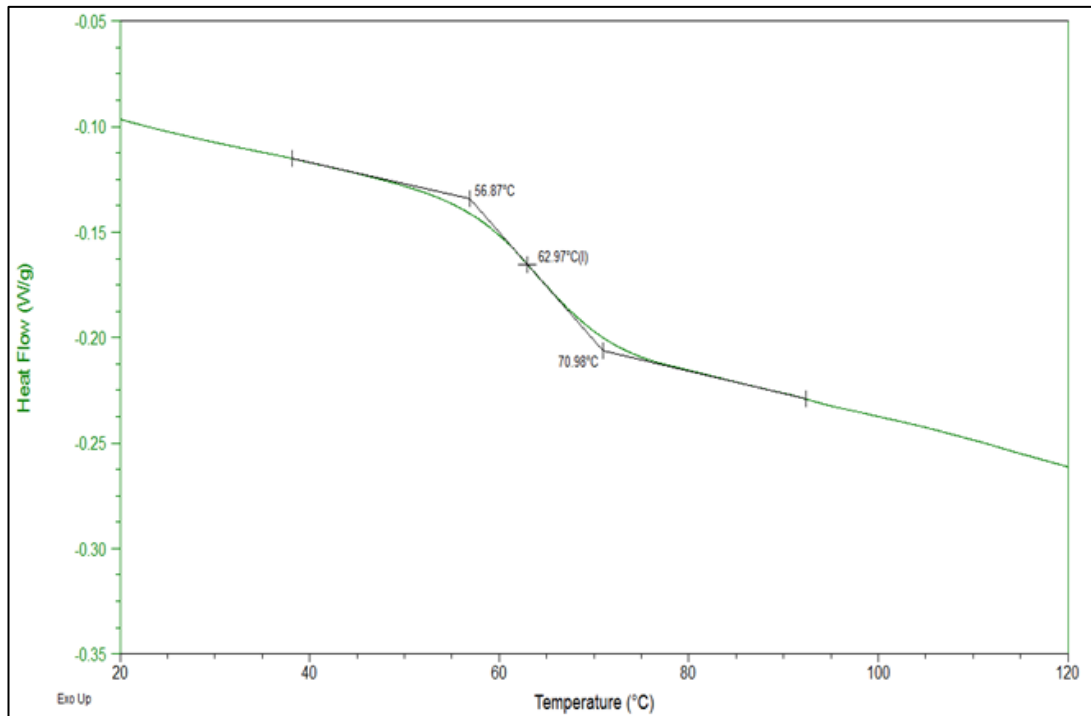


Figure 5.12: Glass transition temperature of PurePVA sample.

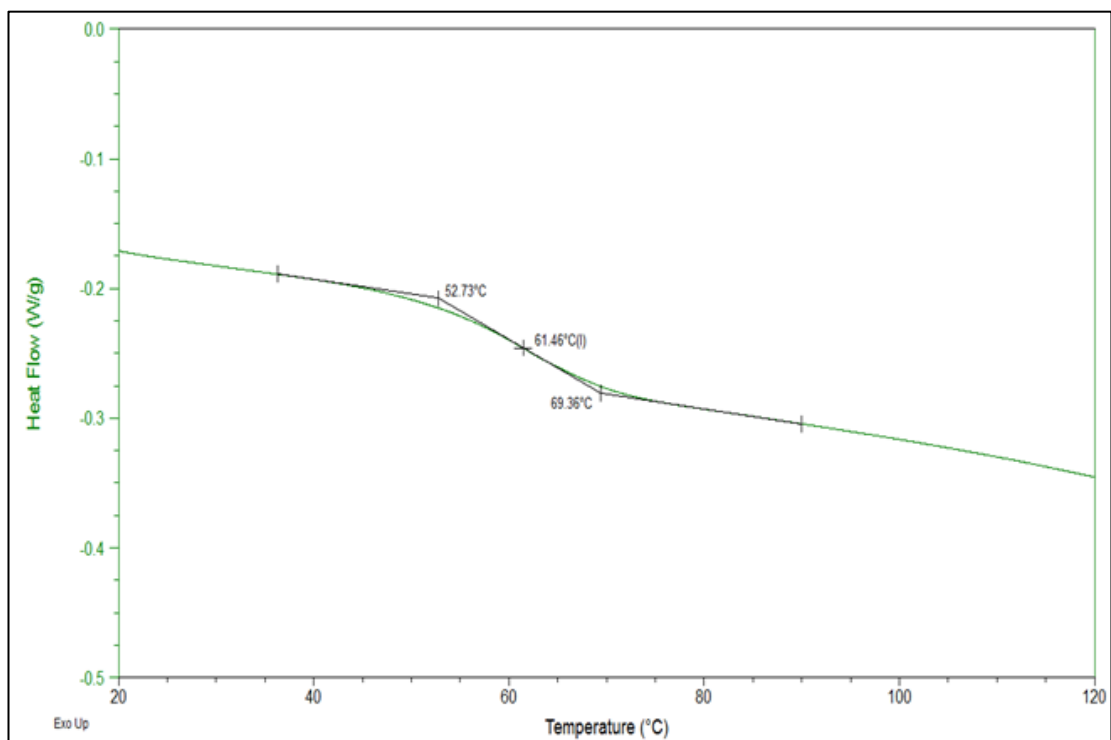


Figure 5.13: Glass transition temperature of PAntho sample.

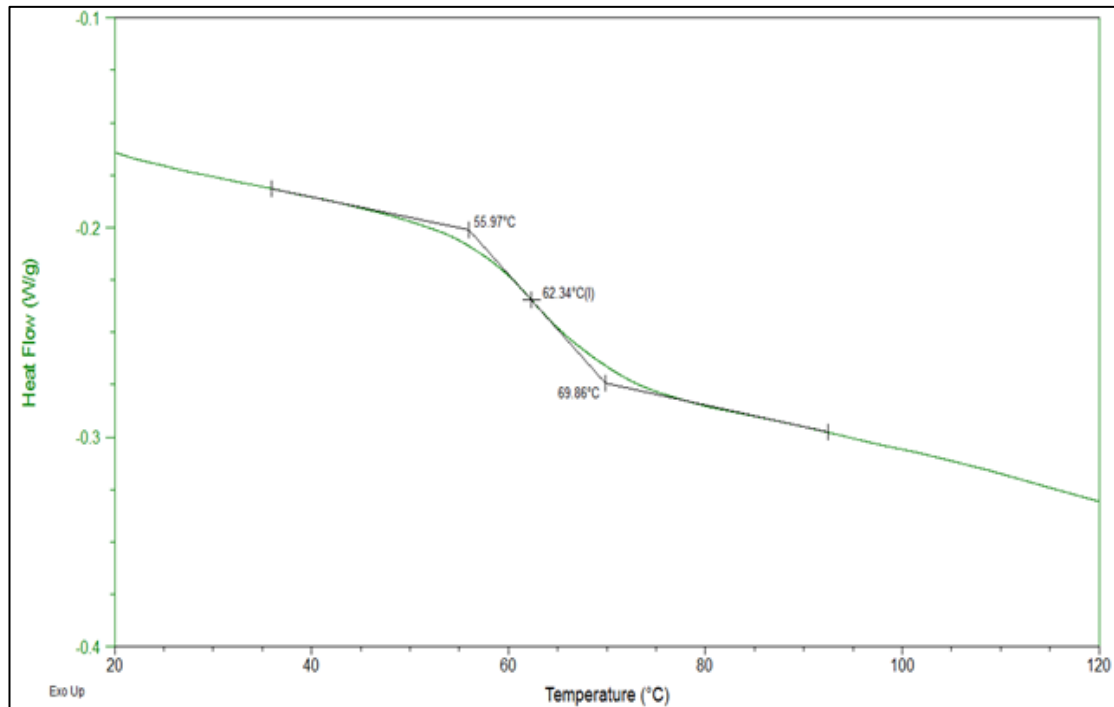


Figure 5.14: Glass transition temperature of PAce sample.

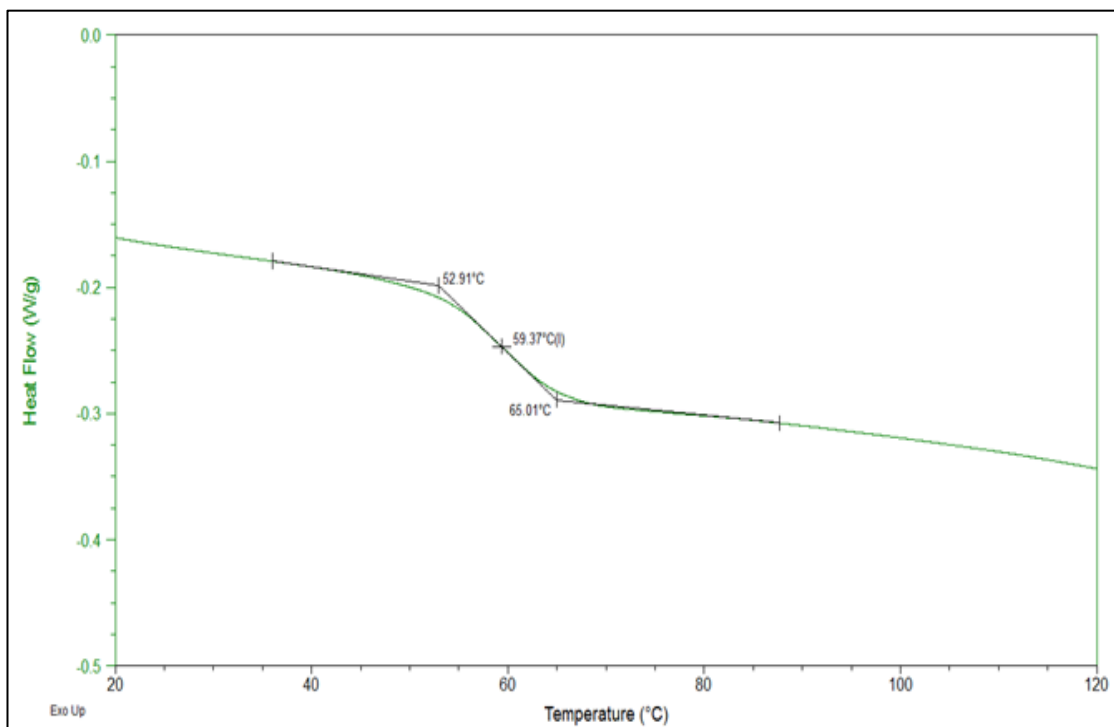


Figure 5.15: Glass transition temperature of PACit sample.

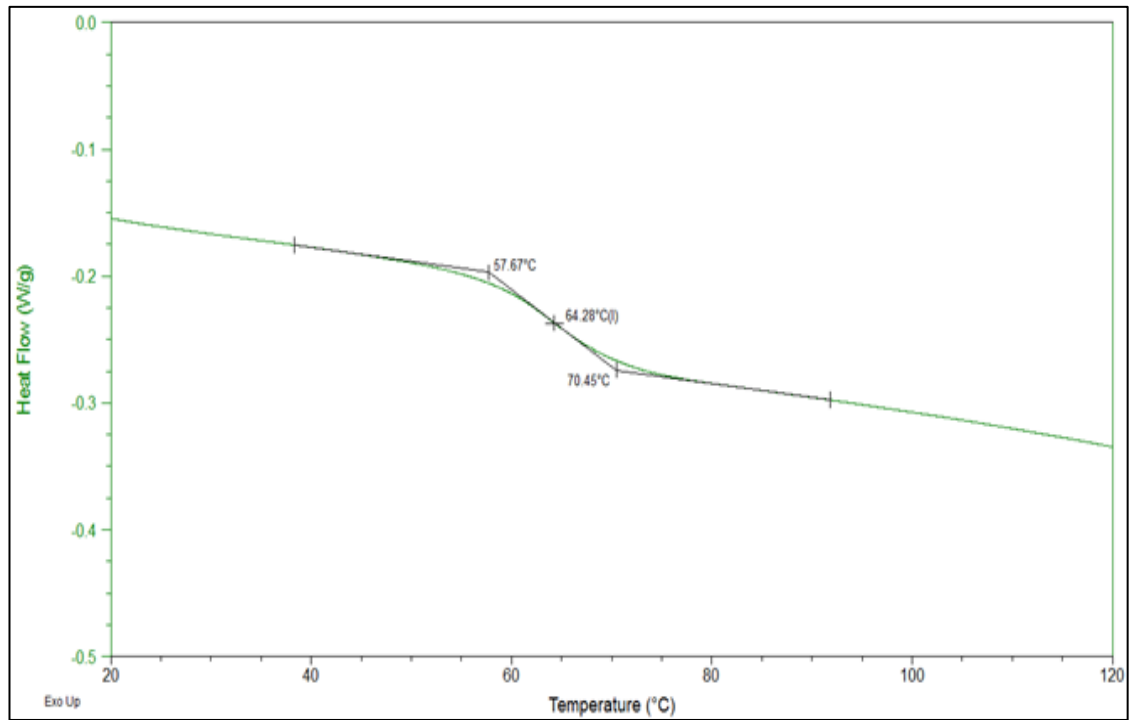


Figure 5.16: Glass transition temperature of PAHyd sample.

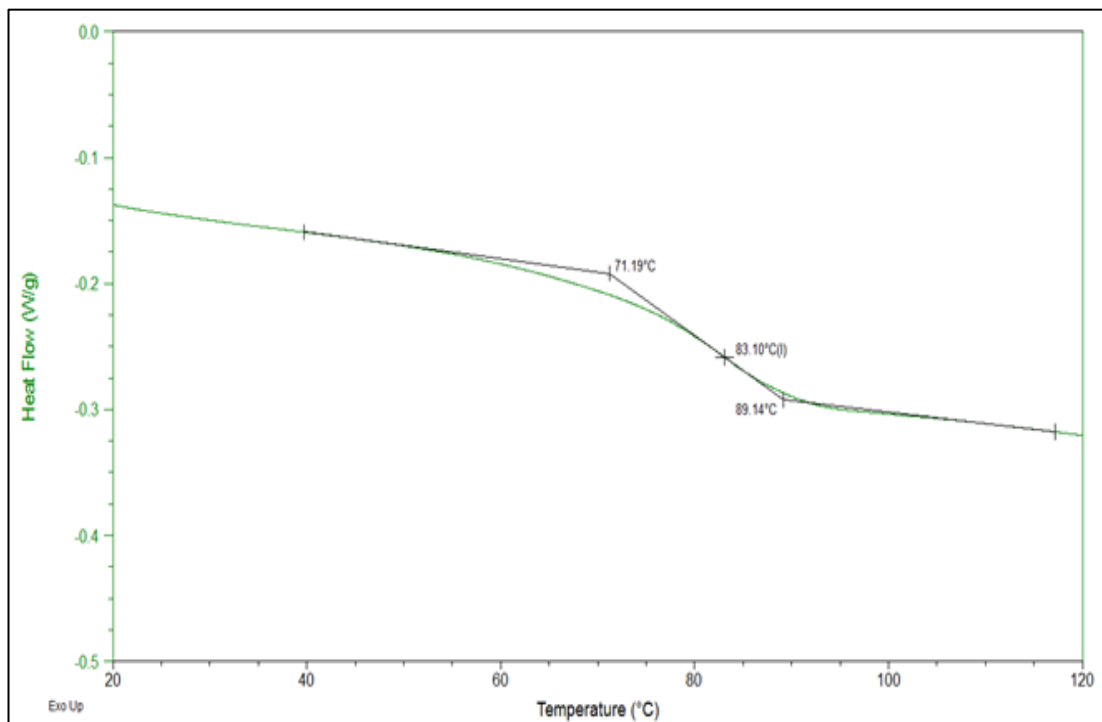


Figure 5.17: Glass transition temperature of PACal sample.

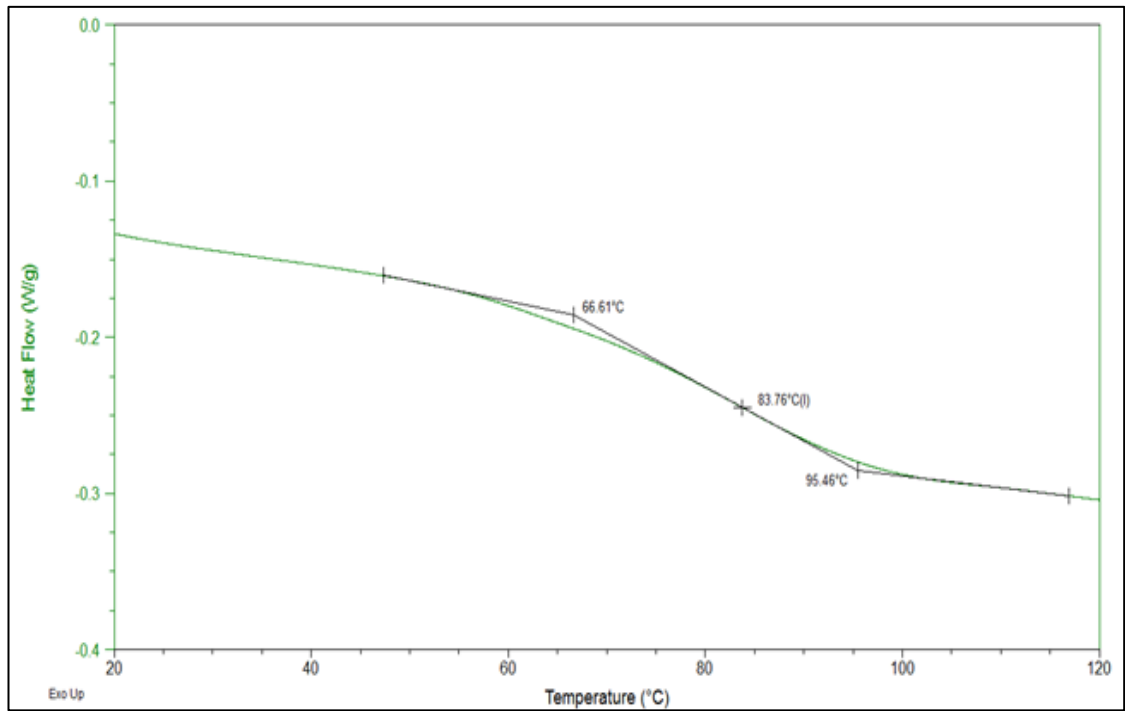


Figure 5.18: Glass transition temperature of PAMag sample.

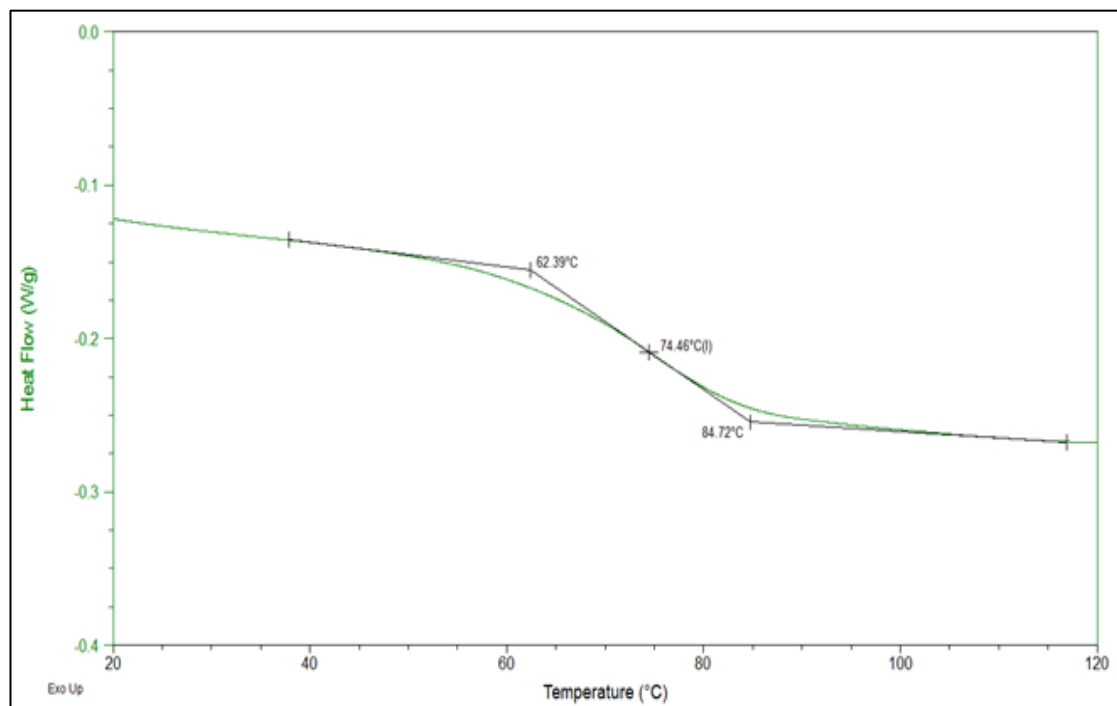


Figure 5.19: Glass transition temperature of PAZin sample.

5.4 UV Degradation by CIELAB Colourimetry

According to ASTM D4329, length of exposure to UV radiation should be that enough to cause substantial change in property of interest. In assessing performance of the coating, comparison is made after 24 hours of exposure to UV radiation. Colour changes of all samples before and upon UV irradiation are depicted in Figure 5.20 – 5.26. Table 5.11 lists the CIELAB colour parameters at the 0th and 24th hour of UV exposure and the respective colour differences of all samples. From Figure 5.20 – 5.26, it can be observed that colour degradation occurs in all samples upon UV exposure. Length of the arrow indicates the amount of change in chroma (C*) values of the samples, which indicates the colour degradation. Chroma is a measure of colourfulness or vividness [Ohta & Robertson, 2005]. The colour of all samples moves towards origin or the a/-b axis. This indicates that colour changes from the red (positive a*) and blue (negative b*) region towards green (negative a*) and yellow (positive b*) region. PAntho, PAAce, and PACit samples showed direction of colour change towards or approaching origin, i.e. the grey zone. However, no correlation can be established with the amount of colour change. PACal, PAMag, and PAZin samples showed distinctive change towards the red and further to the yellow zone. This indicated a significant change in the b* values and yellowing of the samples.

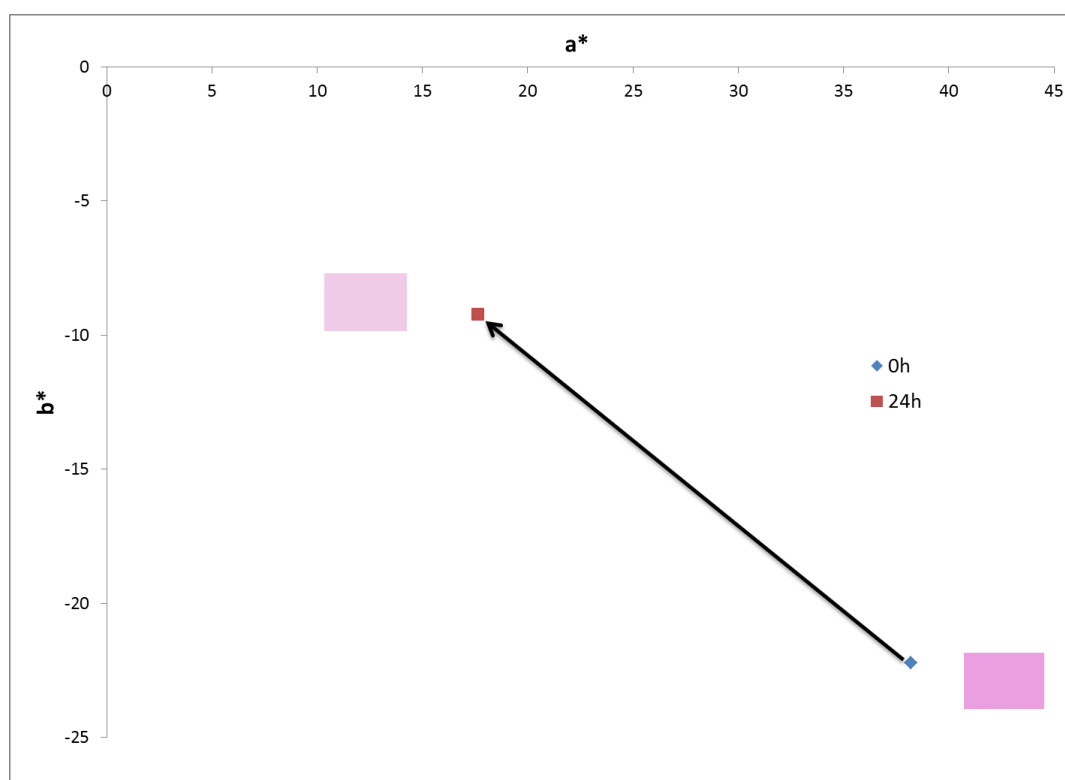
From Table 5.11, it is noticeable that all samples showed increase in lightness, L* and b* values and decrease in a* and C* values. It can be deduced that UV irradiation increases lightness and lowers redness and blueness of all samples, in which the change could be due to the degradation of anthocyanins in the samples, as the colour is due to the presence of anthocyanins. Yang *et al.* (2008) has reported that decrease in a* value could be attributed to degradation of monomeric anthocyanins, while increase in b* value indicated the formation of yellow chalcone species. Colour degradation can also

be assessed by the total colour difference, ΔE . A minimum of $\Delta E = 1$ was assumed to be the basis for colour difference noticeable by human eye [Gonnet, 1998].

Total colour difference of PAntho sample was calculated to be 26.67. Addition of acetic acid and hydrochloric acid enhanced the UV stability of the coating. This can be seen from the lower total colour difference of 8.95 and 16.89 in the PAAce and PAHyd samples respectively. Although total colour difference of PAAce sample is the lowest, its colour was not vivid, as indicated by the low C^* value initially and after UV irradiation. For PAHyd sample, however, the C^* value before and after UV exposure was very high, and hence the vivid colour even after UV irradiation. However, addition of citric acid causes faster UV degradation as indicated by the higher total colour difference. On the other hand, addition of salt accelerated the UV degradation of anthocyanins in coating. This is observed from the high ΔE values of 31.83, 47.22 and 31.20 of PACal, PAMag, and PAZin samples respectively. As observed in the UV degradation of aqueous anthocyanins, in which the ACal, AMag, and AZin samples also showed increased degradation rate, it can be deduced that all the nitrate salts in this study caused faster UV degradation of anthocyanins.

Table 5.11: CIELAB parameters of all samples upon UV irradiation for 24 hours.

Sample	0 th hour				24 th hour				ΔE
	L*	a*	b*	C*	L*	a*	b*	C*	
PAntho	74.85	38.21	-22.23	44.21	85.71	17.62	-9.21	19.88	26.67
PAAce	84.24	15.35	-15.15	21.57	87.34	9.89	-8.77	13.22	8.95
PACit	74.76	43.31	-19.91	47.67	88.12	15.07	-7.22	16.71	33.72
PAHyd	60.91	58.96	-24.77	63.96	67.02	43.95	-20.01	48.29	16.89
PACal	83.81	41.73	-16.84	45.00	92.69	15.52	-1.11	15.56	31.83
PAMag	75.95	53.67	-22.12	58.05	88.97	15.29	2.12	15.44	47.22
PAZin	72.07	45.60	-21.77	50.53	78.74	20.95	-3.85	21.30	31.20

**Figure 5.20: Colour change of PAntho sample upon exposure to UV for 24 hours.**

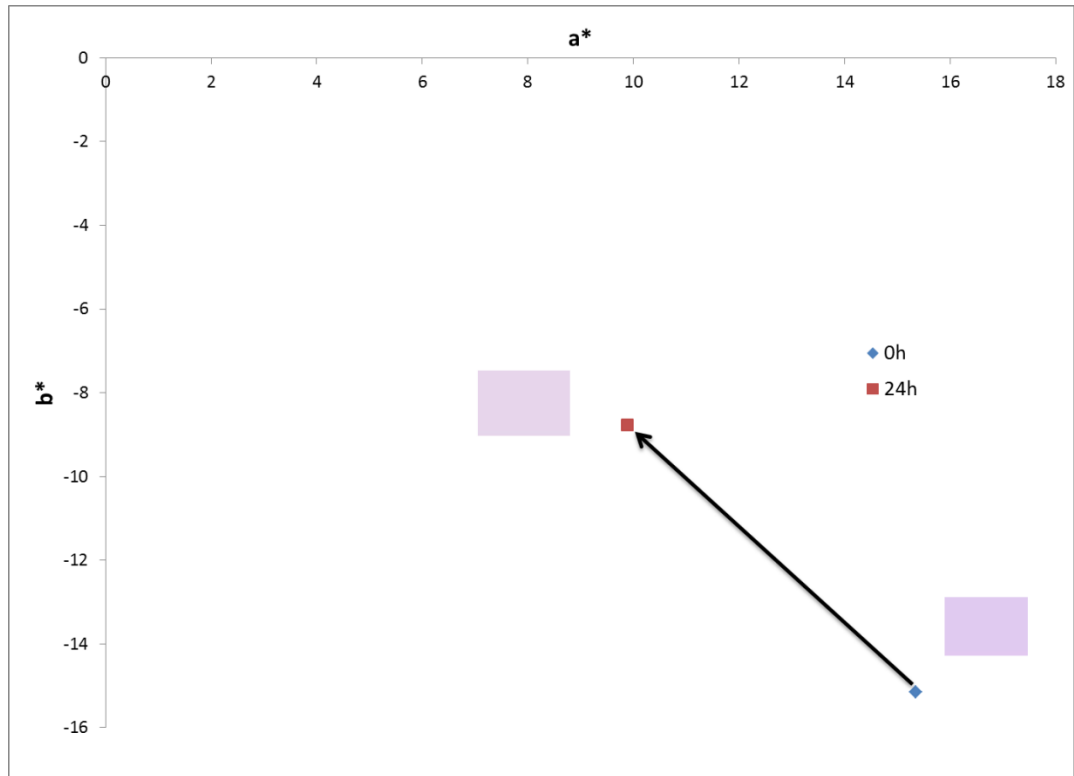


Figure 5.21: Colour change of PAAce sample upon exposure to UV for 24 hours.

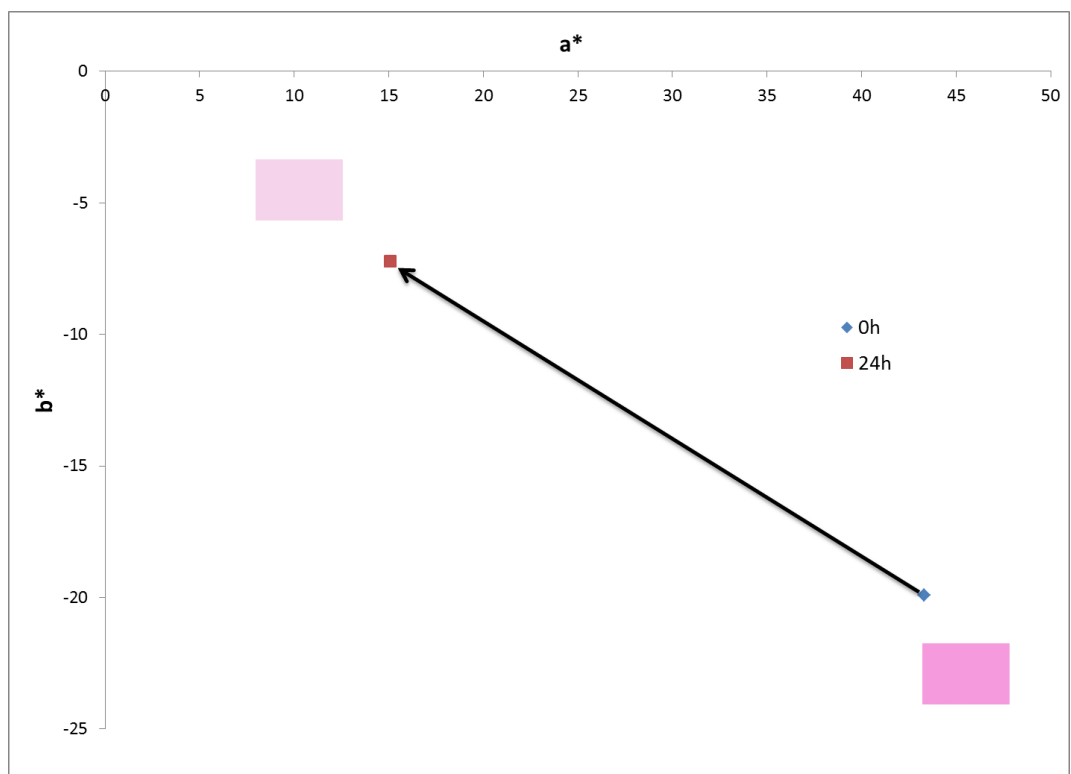


Figure 5.22: Colour change of PACit sample upon exposure to UV for 24 hours.

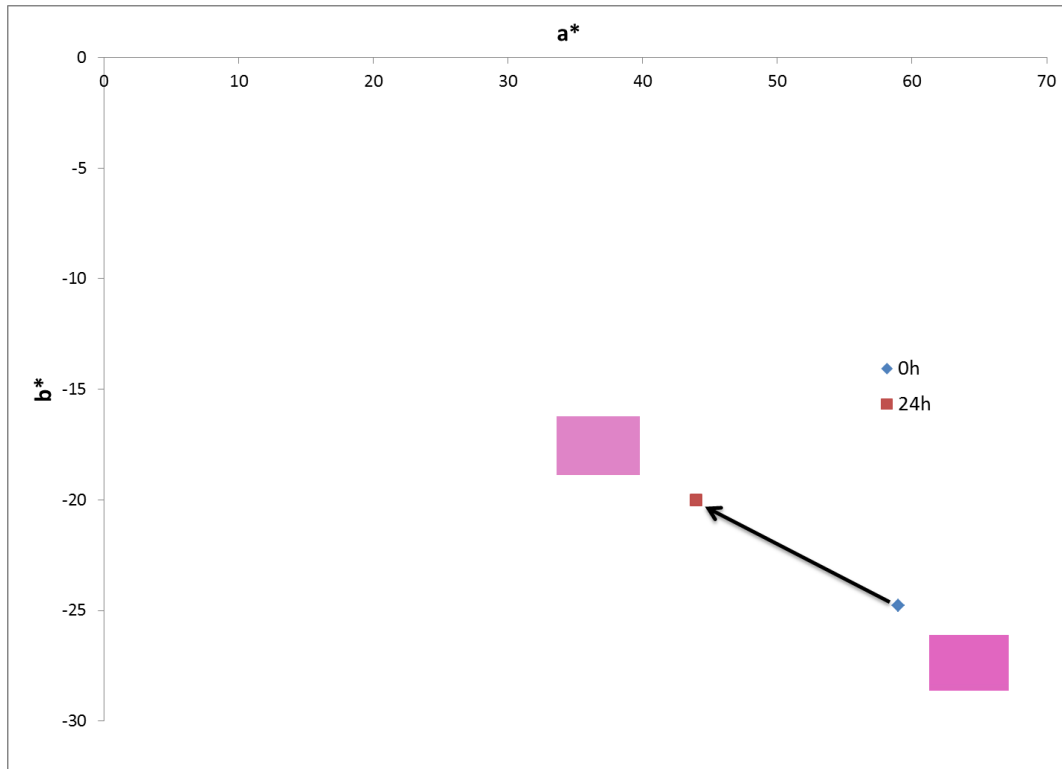


Figure 5.23: Colour change of PAHyd sample upon exposure to UV for 24 hours.

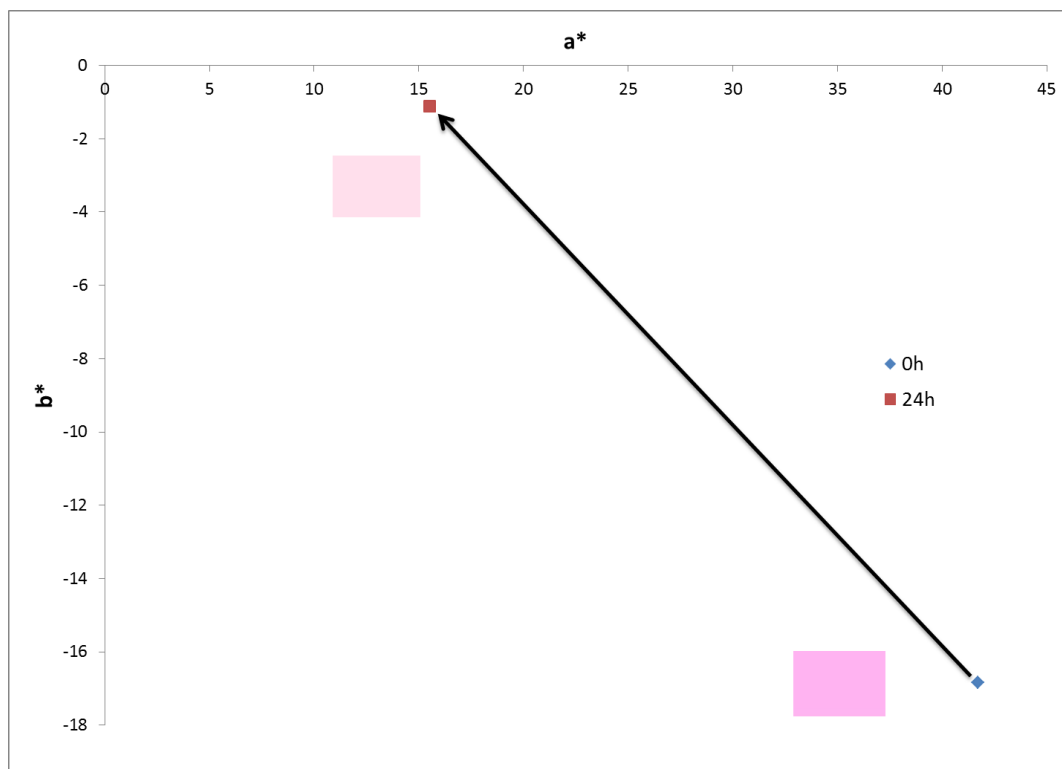


Figure 5.24: Colour change of PACal sample upon exposure to UV for 24 hours.

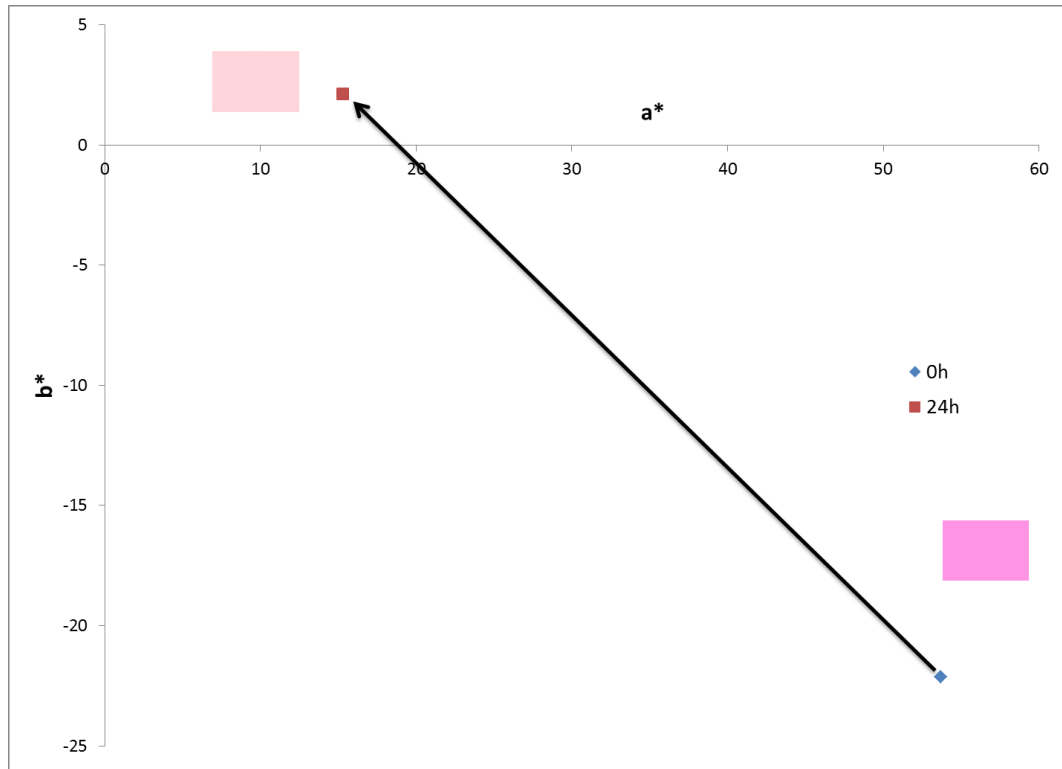


Figure 5.25: Colour change of PAMag sample upon exposure to UV for 24 hours.

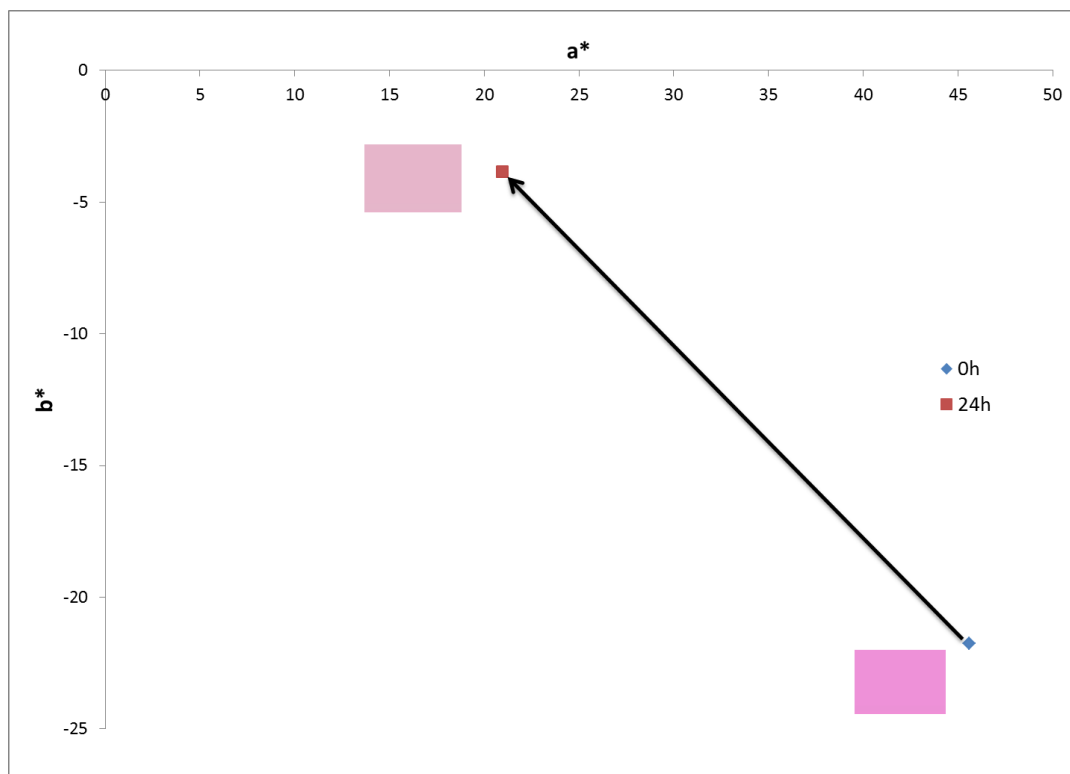


Figure 5.26: Colour change of PAZin sample upon exposure to UV for 24 hours.

5.5 X-Ray Diffraction (XRD)

Results of X-ray diffraction of coating samples are shown in Figures 5.27 - 5.28. The diffractograms of all samples were smoothed in the Origins Pro 8.0 software. Table 5.12 lists the measured 2θ and FWHM and the calculated d-spacing and Scherrer length. From the diffractograms of all samples, it is obvious that all the samples exhibited amorphous characteristics, with the presence of a broad diffraction halo. From the diffractogram of PurePVA sample, the halo peak is located at 19.5° which is the same as obtained by Hema *et al.* (2010). This halo indicates that the d-spacing for all samples is in the range 4.53-4.55 Å. The d-spacing can be related to the interchain distance of a polymer (Huang *et al.*, 2006). The almost preserved d-spacing tells that the interaction between all additives and PVA gives insignificant effect on the interchain distance between PVA molecules. The full width at half maximum (FWHM) of PurePVA sample was measured to be 8.0° and the Scherrer length was calculated to be 10.08 Å. Addition of anthocyanins reduced the FWHM to 6.7° and hence reduced the broadness of the halo. This consequently improved the size of the ordered structures that give the halo peak as shown by the increased Scherrer column length. It can be said that the amorphous nature of the sample becomes less dominant upon addition of anthocyanins.

Addition of acetic acid has minimal effect on the amorphous properties of the sample. This is shown in the FWHM of 6.4° , which is close to 6.7° of PAntho. Addition of citric, however, increased the amorphousness of the coating, as can be shown in the increase in FWHM to 8.8° and decrease in crystallite size to 9.16 Å. For PAHyd sample, the FWHM and Scherrer value is close to that of PAntho, at 6.6° and 12.21 Å, respectively. It can be inferred that addition of hydrochloric acid has minimal effect on the structural characteristics of the PVA-anthocyanin coating. On the other hand, addition of nitrate salts significantly increased the FWHM values of the coating to 9.5° , 11.5° , and 8.7° for

the PACal, PAMag, and PAZin samples respectively. The corresponding Scherrer column length for PACal, PAMag and PAZin has also been reduced compared to PAntho, indicating that the size of the ordered structure has been reduced. Hence, it can be deduced that addition of nitrate salts disturbed the ordered structure and caused the coating to become more amorphous. This interaction can be deduced from hydrogen bonding between nitrates with OH bonds from PVA. Presence of hydrogen bonding has been discussed in Section 5.1 and 5.3. Hema *et al.* (2010) has also reported that addition of salt could increase the amorphous nature of PVA.

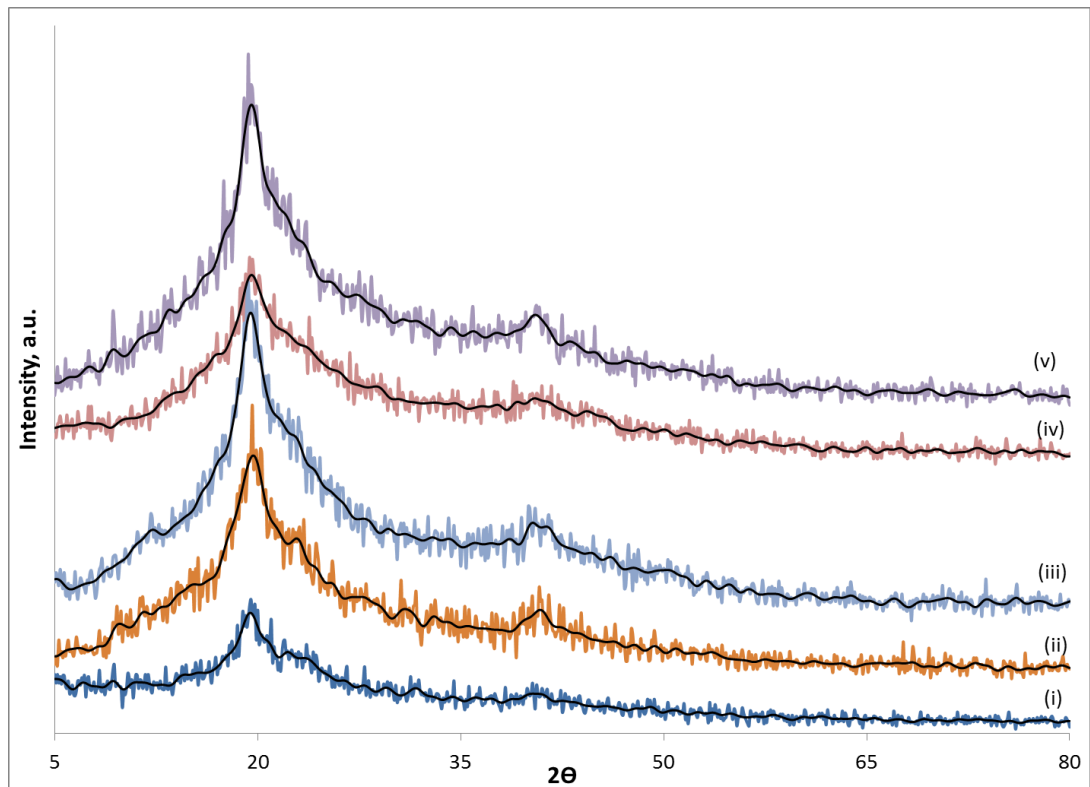


Figure 5.27: X-ray diffractograms of coating samples (i) PurePVA, (ii) PAntho, (iii) PAAce, (iv) PACit, (v) PAHyd.

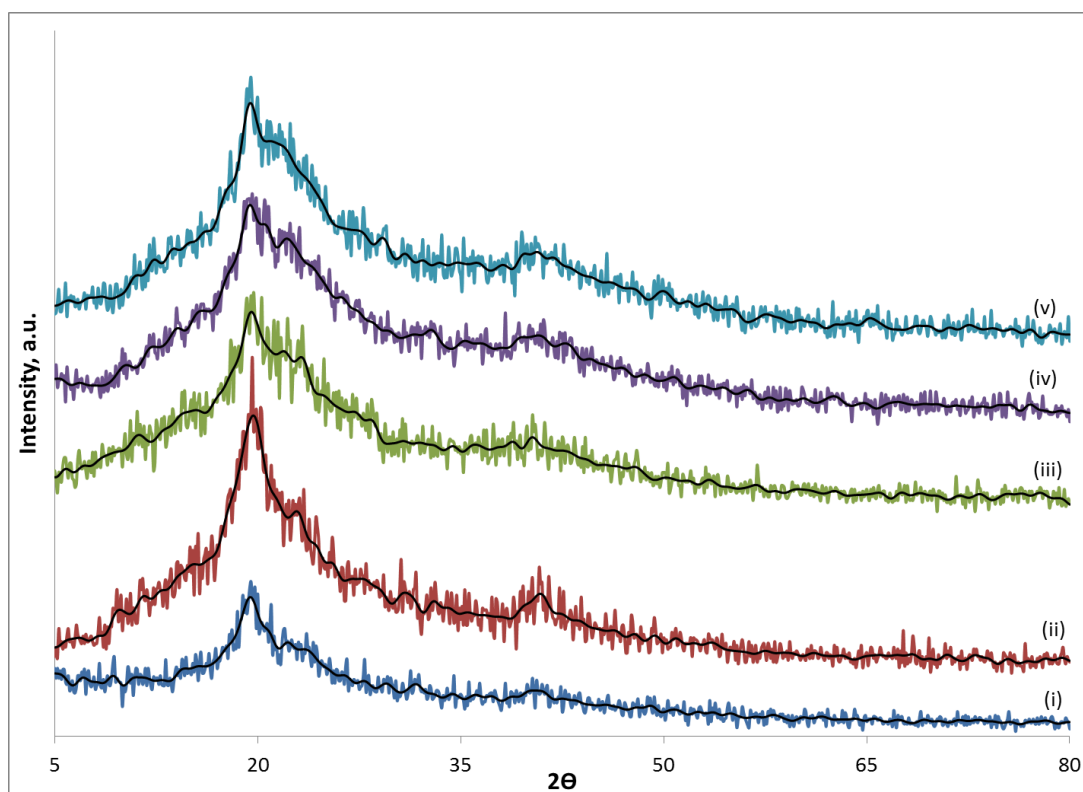


Figure 5.28: X-ray diffractograms of coating samples (i) PurePVA, (ii) PAntho, (iii) PACal, (iv) PAMag, (v) PAZin.

Table 5.12: FWHM values from XRD diffraction halo for all PVA coating samples.

Sample	2θ	d-spacing (\AA)	FWHM	Scherrer length, L (\AA)
PurePVA	19.5°	4.55	8.0°	10.08
PAntho	19.6°	4.53	6.7°	12.03
PAAce	19.5°	4.55	6.4°	12.60
PACit	19.6°	4.53	8.8°	9.16
PAHyd	19.5°	4.55	6.6°	12.21
PACal	19.6°	4.53	9.5°	8.49
PAMag	19.6°	4.53	11.5°	7.01
PAZin	19.5°	4.55	8.7°	9.27

CHAPTER 6: DISCUSSION

From the pH differential method, it can be shown that the maximum peak in the visible region has diminished at pH 4.5, as compared to pH 1.0. At pH 1.0, a high absorption band is noticeable in the green to yellow region, including a portion of the blue region, hence giving anthocyanins red colour. At pH 4.5, the band has diminished, causing the anthocyanins to appear colourless. This is an indication that structural transformation has occurred in the anthocyanins structure, from the red flavylium cation at pH 1.0 to the colourless carbinol at pH 4.5 [Giusti & Wrolstad, 2001]. From the UV-Vis absorption spectroscopy of the anthocyanins and anthocyanins with added additives, it can be seen that addition of acids generally enhances the absorption band in the visible range. On the other hand, addition of nitrate salts enhances the absorption in the UV range, which could be due to the nitrates [Gvozdić *et al.*, 2009 and Tomišić *et al.*, 2005].

In the study of UV degradation of aqueous anthocyanins and anthocyanins with additives, all the samples are shown to follow first order degradation kinetics, in which degradation occurs exponentially. Addition of hydrochloric acid has greatly enhanced the UV inhibition properties of the aqueous anthocyanins, increasing the half-life 7 times higher to 210 h. Addition of nitrate salts, however, accelerates the degradation process. This could be due to the change in the equilibrium, since the discolouration is due to the transformation of flavylium cation to the colourless carbinol.

In the study of natural degradation by fungi, AZin sample shows the best performance in terms of fungi inhibition, where no fungi growth can be observed in the sample. This is supported by CIELAB colourimetry, in which a minimal change in the total colour difference (ΔE) of 13.60 is noted, which can be due to the natural degradation of anthocyanins rather than by fungi. There is a vast potential for zinc nitrate to be used as fungi inhibitor, if aqueous anthocyanins are to be stored for a prolonged period. In all other samples, a certain degree of degradation by fungi can be noticeable. Samples that did not fare very well are ACal and AMag, where calcium nitrate and magnesium nitrate are respectively added as additives. In both samples, fungi growth is visible and can be confirmed by the high values of measured fungi dry weight, as well as the high values of total colour difference.

From the FTIR spectra of the coating samples, major vibrational bands are assigned. Relative intensity studies were conducted to reveal information in comparing samples with similar spectra shapes and peak positions. Addition of anthocyanins into PVA causes small increase in the C-O and C=O functional groups from the study of relative intensity. Increase in the C-O and O-H bands relative intensity in PACit sample and CH₂, CH₃, and O-H bands relative intensity in PAHyd sample compared to PAntho could suggest the presence of hydrogen bonding in these samples. On the other hand, appearance of new peaks at 824.45 cm⁻¹, 826.27 cm⁻¹, and 826.38 cm⁻¹ in PACal, PAMag, and PAZin samples respectively can be assigned to N-O out-of-plane bending due to the nitrates. Large increase and shifts in the relative intensity of O-H bending, CH₂, and CH₃ bands could suggest the occurrence of more hydrogen bonds between nitrate salts and PVA.

In thermogravimetric analysis, degradation of individual compounds or their fragments can be identified from the thermogram as a weight loss step and from DTG as a peak. In PACit sample, presence of large weight loss steps at 200 °C - 250 °C and 400 °C - 450 °C can be due to the decomposition of citric acid. In PACal, PAMag, and PAZin samples, presence of weight loss steps at temperature 300 °C - 400 °C are due to NO, NO₂ and O₂ gasses [Malecka *et al.*, 2003, Madarasz *et al.*, 2007, Migdal-Mikuli *et al.*, 2004], which are the decomposition byproducts of nitrates. In thermal stability study, position of a degradation step and percent weight loss can be used to assess thermal stability of a material. Addition of hydrochloric acid and citric acid enhances thermal stability of the coating samples. This can be seen in the main thermal degradation at higher temperature (300 °C - 350 °C) compared to that of PAntho (250 °C - 300 °C). By comparing the weight percentage at 300 °C, it can also be shown that PACit and PAHyd samples recorded weight percent of 67.69% and 78.60% respectively, higher than other samples. This indicates that thermal stability of these coating samples is higher than others at 300 °C.

In the glass transition temperature study, large increase in the glass transition temperature of PACal, PAMag, and PAZin samples can be seen. The increase indicates that the amount of hydrogen bonding in the samples has increased, which could be due to the interaction of nitrates with PVA. This can be related to the FTIR study, where large increase in the relative intensity of N-O, O-H stretching, O-H bending, CH₂, and CH₃ bands are observed in these samples. Presence of these groups, which could also indicate presence of more hydrogen bonding, could lead to less free volume, hence increasing the glass transition temperature. Increase in glass transition temperature due to hydrogen bonding has been reported by Lin *et al.* (2010). Higher glass transition temperature leads to more glassy and hard structure.

All the coating samples exhibited colour degradation upon exposure to UV radiation. This can be seen in the decrease in a^* values and increase in b^* values and colour change direction towards yellow-green region in the colour space. Addition of acetic acid and hydrochloric acid inhibited the colour degradation of anthocyanins in the coatings by UV, as can be seen from the lower values of total colour difference. It is possible that hydrochloric acid interacts with anthocyanin and stabilizes it in the flavylium form. On the other hand, PACal, PAMag and PAZin did not perform well as these samples exhibit larger values of colour change. In the UV degradation study of aqueous anthocyanins, ACal, AMag, and AZin samples have shown to exhibit the lowest UV stability. Hence, it can be inferred that calcium nitrate, magnesium nitrate and zinc nitrate increase the UV degradation rate in both aqueous solution and coating.

Presence of broad diffraction halo indicates that all coating samples are amorphous. The amorphousness is due to the poly(vinyl alcohol), and the peak at 19.5° confirms this. It has been reported that salt could increase the amorphousness of PVA [Hema *et al.*, 2010]. Upon addition of calcium nitrate, magnesium nitrate and zinc nitrate into the coating sample, broadness of the amorphous halo in X-ray diffractogram of these samples increases, as can be noted from the increase in FWHM values. In addition, calculated Scherrer length for these samples has increased. This shows that the size of the ordered domains has decreased due to interaction of PVA with nitrate.

CHAPTER 7: CONCLUSIONS AND SUGGESTIONS FOR FUTURE WORKS

Integration of anthocyanins as red colourant into poly(vinyl alcohol) coating has been achieved. The integration is made possible due to the use of water as common solvent. Anthocyanin is water soluble pigment; hence water can be used to extract anthocyanin from cell vacuole. Poly(vinyl alcohol) is a water soluble non-toxic polymer. Therefore, the extract containing anthocyanins can also be used to dissolve poly(vinyl alcohol). Coating prepared from mixture of poly(vinyl alcohol) and anthocyanin is environmental friendly. Anthocyanin, a natural dye obtained from plant source is used instead of artificial colourant. Poly(vinyl alcohol), a water soluble, non-toxic and biodegradable polymer, is one of the safest sources to be used as binder in coating. In addition, no organic solvent is used in the preparation and formulation of the coating. This further reduces the harmful effect of VOC towards environment and also the coating applicator.

In terms of performance, the anthocyanin dye and coating did not fare well. Anthocyanin is susceptible to UV degradation upon exposure to UV radiation, in both extract and coating. Being extracted by water, anthocyanin is susceptible to attack by fungi. This affected storage properties of the paint. Thermal stability of the coating is dependent on the thermal stability poly(vinyl alcohol) as the binder in the coating. Upon addition of additive, the performance in different aspects of the extract and coating can be enhanced. However, there is no universal additive that can enhance every aspect of a coating's performance in the coating industrial. Different additive is used to achieve specific functions and effects on the coating, which is why additive is functional specific.

In this work, hydrochloric acid has shown to affect the properties and performance of anthocyanins and coating. Addition of hydrochloric acid enhanced the UV stability of the anthocyanins extract to 210h, a 7 fold increase compared to the anthocyanin extract without additive. In the colour degradation study of coating upon exposure to UV radiation, addition of hydrochloric reduced the total colour difference before and after UV irradiation, compared to that of coating without additive. Hydrochloric acid enhanced thermal stability of the coating, evident from the shifting of the main degradation towards higher temperature in thermogravimetric analysis. However, it did not fare well in storage stability and risked infested by fungi.

In study of degradation by fungi, zinc nitrate has shown to enhance the fungi inhibition properties of the extract, where no fungi growth can be observed visually and supported by the small colour difference obtained in CIELAB colourimetry. Addition of zinc nitrate caused the coating to become hard and glassy due to increase in cross-link density, as seen in the increase in glass transition temperature, and appearance of nitrate functional group and hydrogen bonding from FTIR study. Addition of zinc nitrate, however, reduced the UV stability of anthocyanin in both extract and coating.

From these evidences, it can be concluded that hydrochloric acid exhibits potential as colour stabilizer of anthocyanins in extract and coating, and thermal stabilizer in anthocyanin-PVA coating up to 300 °C. On the other hand, zinc nitrate exhibits potential as fungi inhibitor and enhances storage stability of the anthocyanin extract.

For further works, it is suggested that anthocyanin dye be extended to other coating applications. More additives can also be explored to enhance the performance of not only the coating, but also properties and stability of the natural dye. Selection of natural

colourants can also be extended, though stability and compatibility with coating has to be assessed. More characterisation techniques not included in this work could also be employed to assess the performance of the coating.

REFERENCES

- Abidin, Z.H.Z. (2005). Electrochemical and Mechanical Studies of Acrylic Resin Mixed with Natural Compounds. PhD Thesis, University of Malaya, Kuala Lumpur.
- Abidin, Z.H.Z., Taha, R.M., Puteh, R. & Arof, A.K. (2006). Characteristics of paints prepared from lawsonia pigment and dammar from *Dipterocarpus Grandifolius*. *Materials Science Forum*, 517, 290-293.
- Ahmed, J., Shivhare, U.S., Raghavan, G.S.V. (2004). Thermal degradation kinetics of anthocyanin and visual colour of plum puree. *European Food and Research Technology*, 218 (6), 525-528.
- Andersen, Ø. M., & Jordheim, M. (2006). The anthocyanins. In Ø. M. Andersen & K. R. Markham (Eds.), *Flavonoids: chemistry, biochemistry and applications* (pp. 164-187). Boca Raton, Flin: CRC Press.
- Andrade, G., Barbosa-Stancioli, E.F., Piscitelli Mansur, A.A., Vasconcelos, W.L., & Mansur, H.S. (2006). Design of novel hybrid organic-inorganic nanostructured biomaterials for immunoassay applications. *Biomedical Materials*, 1, 221-234.
- Babich, H. & Stotzky, G. (1978). Toxicity of zinc to fungi, bacteria, and coliphages: influence of chloride ions. *Applied and Environmental Microbiology*, 36, 906-914.
- Bakowska, A., Kucharska, A.Z., & Oszmianski, J. (2003). The effects of heating, UV irradiation, and storage on the stability of the anthocyanin-polyphenol copigment complex. *Food Chemistry*, 81, 349-355.
- Belfiore, L.A., Pires, A.T.N., Wang, Y., Graham, H., & Ueda, E. (1992). Transition-metal coordination in polymer blends and model systems. *Macromolecules*, 25, 1411-1419.
- Borkowski, T., Szymusiak, H., Gliszczynska-Swiglo, A., & Tyrakowska, B. (2005). The effect of 3-o-beta-glycosylation on structural transformations of anthocyanins. *Food Research International*, 38, 1031-1037.
- Bridle, P., & Timberlake, C.F. (1997). Anthocyanins as natural food colours-selected aspects. *Food Chemistry*, 58 (1), 103-109.

- Britton, G. (1983). *The biochemistry of natural pigments*. London: Cambridge University Press.
- Brockner, W., Ehrhardt, C., & Gjikaj, M. (2007). Thermal decomposition of nickel nitrate hexahydrate, $\text{Ni}(\text{NO}_3)_2 \cdot 6\text{H}_2\text{O}$, in comparison to $\text{Co}(\text{NO}_3)_2 \cdot 6\text{H}_2\text{O}$ and $\text{Ca}(\text{NO}_3)_2 \cdot 4\text{H}_2\text{O}$. *Thermochimica Acta*, 456, 64-68.
- Brouillard, R. & Dubois, J-E. (1977). Mechanism of the structural transformations of anthocyanins in acidic media. *Journal of the American Chemical Society*, 99, 1359-1364.
- Brown, M.E. (2004). *Introduction to thermal analysis: techniques and applications 2th edition*. New York: Kluwer Academic Publishers.
- Bruce Prime, R., Bair, H.E., Vyazovkin, S., Gallagher, P.K., & Riga, A. (2009). Thermogravimetric analysis (TGA). In J.D. Menczel & R. Bruce Prime (Eds.), *Thermal analysis of polymers: fundamentals and applications* (pp.241-317). New Jersey: John Wiley & Sons Inc.
- Chang, I.S., Kim, C.I., & Nam, B.U. (2005). The influence of poly-vinyl-alcohol (PVA) characteristics on the physical stability of encapsulated immobilization media for advanced wastewater treatment. *Process Biochemistry*, 40, 3050-3054.
- Chen, C.H., Wang, F.Y., Mao, C.F., Liao, W.T., & Hsieh, C.D. (2008). Studies of chitosan: II. Preparation and characterization of chitosan/poly(vinyl alcohol)/gelatin ternary blend films. *International Journal of Biological Macromolecules*, 43, 37-42.
- Chew, K.W., Arof, A.K., & Puteh, R. (2007). Chemical and heat resistance of silicone-acrylic-based binder and paint system on mild steel panels. *Pigment and Resin Technology*, 36, 286-292.
- Chuang, W.Y., Young, T.H., Yao, C.H., & Chiu, W.Y. (1999). Properties of the poly(vinyl alcohol)/chitosan blend and its effect on the culture of fibroblast in vitro. *Biomaterials*, 20, 1479-1487.
- Chumsri, P., Sirichote, A., & Itharat, A. (2008). Studies on the optimum conditions for the extraction and concentration of roselle (*Hibiscus sabdariffa* Linn.) extract. *Songklanakarin Journal of Science and Technology*, 30, 133-139.
- Costa, H.S., Rocha, M.F., Andrade, G.I., Barbosa-Stancioli, E.F., Pereira, M.M., Orefice, R.L., et al. (2008). Sol-gel derived composite from bioactive glass-polyvinyl alcohol. *Journal of Materials Science*, 43 (2), 494-502.

Cullity, B.D. (1956). *Elements of X-ray diffraction*. Massachusetts: Addison-Wesley Publishing.

Deroles, S. (2009). Anthocyanin biosynthesis in plant cell cultures: a potential source of natural colourants. In K. Gould, K. Davies & C. Winefield (Eds.), *Anthocyanins: biosynthesis, functions and applications* (pp. 107-168). New York: Springer.

Du, C.T. & Francis, F.J. (1973). Anthocyanins of roselle (*Hibiscus sabdariffa* L.). *Journal of Food Science*, 38 (5), 810-812.

Eder, R. (2000). Pigments. In L.M.L. Nollet (Ed.), *Food analysis by HPLC* (pp. 845-880). Monticello, NY: Marcel Dekker.

Every, H.A., Zhou, F., Forsyth, M., & MacFarlane, D.R. (1998). Lithium ion mobility in poly(vinyl alcohol) based polymer electrolytes as determined by ^7Li NMR spectroscopy. *Electrochimica Acta*, 43 (10-11), 1465-1469.

Forsgren, A. (2006). *Corrosion control through organic coating*. Boca Raton: Taylor & Francis.

Francis, F.J. & Markakis, P.C. (1989). Food colorants: anthocyanins. *Critical Reviews in Food Science and Nutrition*, 28 (4), 273-314.

Fuller, C.W. (1973). Colored Iron Oxide Pigments, Synthetic. In T.C. Patton (Ed.), *Pigment Handbook* (pp. 333). New York: John Wiley.

Gabbott, P. (2008). A practical introduction to differential scanning calorimetry. In P. Gabbott (Ed.), *Principles and applications of thermal analysis* (pp. 1-50). Oxford, U.K.: Blackwell Publishing.

Gempeler, H., & Schneider, W. (1998). Epoxy Coatings. In D. Stoye & W. Freitag (Eds.), *Paints, coatings and solvents* (pp. 69-78). Burghausen, Germany: Wiley-VCH.

Gilman, W.S. (2006). Thermal analysis for coatings characterizations. In A.A. Tracton (Ed.), *Coatings technology handbook* (pp. 1-4). Boca Raton: CRC Press.

Giusti, M.M. & Wallace, T.C. (2009). Flavonoids as natural pigments. In T. Bechtold & R. Mussak (Eds.), *Handbook of natural colourants* (pp. 257-275). West Sussex, UK: John Wiley & Sons, Inc.

- Giusti, M.M., & Wrolstad, R.E. (2001). Characterization and measurement of anthocyanins by UV-visible spectroscopy. *Current Protocols in Food Analytical Chemistry*, F1.2.1 - F1.2.13.
- Gonnet, J.F. (1998). Colour effects of co-pigmentation of anthocyanins revisited - I. A calorimetric definition using the CIELAB scale. *Food Chemistry*, 63, 409-415.
- Griffin, D.H. (1994). *Fungal Physiology*. New York: Wiley-Liss, Inc.
- Gvozdić, V., Tomišić, V., Butorac, V., & Simeon, V. (2009). Association of nitrate ion with metal cations in aqueous solution: a UV-Vis spectrometric and factor-analytical study. *Croatica Chemica Acta*, 82, 553-559.
- Harborne, J.B.(1998). Phenolic compounds. In J.B. Harborne (ed), *Photochemical methods - a guide to modern techniques of plant analysis* (pp. 66-74). New York: Chapman & Hall.
- Hardy, A., Van Werde, K., Vanhoyland, G., Van Bael, M.K., Mullens, J., & Van Poucke, L.C. (2003). Study of the decomposition of an aqueous metal–chelate gel precursor for $(\text{Bi,L a})_4\text{Ti}_3\text{O}_{12}$ by means of TGA–FTIR, TGA–MS and HT-DRIFT. *Thermochimica Acta*, 397, 143-153.
- He, J., & Giusti, M.M. (2010). Anthocyanins: natural colorants with health-promoting properties. *Annual Review of Food Science and Technology*, 1, 163-187.
- Heiling, P. (1998). Poly(vinyl alcohol). In D. Stoye & W. Freitag (Eds.), *Paints, coatings and solvents* (pp. 33). Burghausen, Germany: Wiley-VCH.
- Hema, M., Selvasekarapandian, S., Hirankumar, G., Sakunthala, A., Arunkumar, D., & Nithya, H. (2010). Laser Raman and ac impedance spectroscopic studies of PVA: NH_4NO_3 polymer electrolyte. *Spectrochimica Acta Part A: Molecular and Biomolecular Spectroscopy*, 75 (1), 474-478.
- Huang, H.T. (1955). Decolorization of anthocyanins by fungal enzymes. *Agricultural and Food Chemistry*, 3 (2), 141-146.
- Igarashi, K., Takanashi, K., Makino, M., & Yasui, T. (1989). Antioxidative activity of major anthocyanin isolated from wild grapes (*Vitis coignetiae*). *Nippon Shokuhin Kogyo Gakkaishi*, 36, 852-856.

- Ihms, E.C. & Brinkman, D.W. (2004). Thermogravimetric analysis as a polymer identification technique in forensic applications. *Journal of Forensic Sciences*, 49 (3), 1-6.
- Kadir, M.F.Z., Majid, S.R., & Arof, A.K. (2010). Plasticized chitosan-PVA blend polymer electrolyte based proton battery. *Electrochimica Acta*, 55, 1475-1482.
- Kendall, D.S. (2006). Infrared Spectroscopy of Coatings. In A.A. Tracton (Ed.), *Coatings technology handbook* (pp. 1-8). Boca Raton: CRC Press.
- Kim, J.H., Min, B.R., Won, J., & Kang, Y.S. (2003). Analysis of the glass transition behavior of polymer-salt complexes: an extended configurational entropy model. *The Journal of Physical Chemistry B*, 107 (24), 5901-5905.
- Kohler, K. (1998). Inorganic Pigments. In D. Stoye & W. Freitag (Eds.), *Paints, coatings and solvents* (pp. 143-147). Burghausen, Germany: Wiley-VCH.
- Kong, J., Chia, L., Goh, N., Chia, T., & Brouillard, R. (2003). Analysis and biological activities of anthocyanins. *Phytochemistry*, 64, 923-933.
- Koutchma, T. (2009). Advances in ultraviolet light technology for non-thermal processing of liquid foods. *Food Bioprocess Technology*, 2, 138-155.
- Larkin, P.J. (2011). *Infrared and Raman spectroscopy: principles and spectral interpretation*. Oxford, UK: Elsevier Inc.
- Lee, J., Durst, R.W., & Wrolstad, R.E. (2005). Determination of total monomeric anthocyanin pigment content of fruit juices, beverages, natural colorants, and wines by the pH differential method: collaborative study. *Journal of AOAC International*, 88, 1269-1277.
- Lin, C., Kuo, S., Huang, C., & Chang, F. (2010). Glass transition temperature enhancement of PMMA through copolymerization with PMAAM and PTCM mediated by hydrogen bonding. *Polymer*, 51 (4), 883-889.
- Linga Raju, C.H., Rao, J.L., Reddy, B.C.V., & Veera Brahmam, K. (2007). Thermal and IR studies on copper doped polyvinyl alcohol. *Bulletin of Materials Science*, 30 (3), 215-218.

- Madarasz, J., Varga, P.P., & Pokol, G. (2007). Evolved gas analyses (TG/DTA–MS and TG–FTIR) on dehydration and pyrolysis of magnesium nitrate hexahydrate in air and nitrogen. *Journal of Analytical and Applied Pyrolysis*, 79 (No. 1-2), 475-478.
- Mahadevan, N., Kamboj, S., & Kamboi, P. (2009). Hibiscus sabdariffa Linn. – an overview. *Natural Product Radiance*, 8, 77-83.
- Malathi, J., Kumaravadivel, M., Brahmanandhan, G.M., Hema, M., Baskaran, R., & Selvasekarapandian, S. (2010). Structural, thermal and electrical properties of PVA–LiCF₃SO₃ polymer electrolyte. *Journal of Non-Crystalline Solids*, 356 (43), 2277-2281.
- Malecka, B., Gajerski, R., Malecki, A., Wierzbicka, M., & Olszewski, P. (2003). Mass spectral studies on the mechanism of thermal decomposition of Zn(NO₃)₂ · nH₂O. *Thermochimica Acta*, 404 (No. 1-2), 125-132.
- Marco, P.H., Poppi, R.J., Scarminio, I.S., & Tauler, R. (2011). Investigation of the pH effect and UV radiation on kinetic degradation of anthocyanin mixtures extracted from *Hibiscus acetosella*. *Food Chemistry*, 125 (3), 1020-1027.
- Mateus, N., & de Freitas, V. (2009). Anthocyanins as Food Colorants. In K. Gould, K. Davies & C. Winefield (Eds.), *Anthocyanins: biosynthesis, functions and applications* (pp. 283-304). New York: Springer.
- Melo, M.J., Pina, F., & Andary, C. (2009). Anthocyanins : nature's glamorous palette. In T. Bechtold & R. Mussak (Eds.), *Handbook of natural colourants* (pp. 135-150). West Sussex, UK: John Wiley & Sons, Inc.
- Menczel, J.D., Judovits, L., Bruce Prime, R., Bair, H.E., Reading, M., & Swier, S. (2009). Differential scanning calorimetry (DSC). In J.D. Menczel & R. Bruce Prime (Eds.), *Thermal analysis of polymers: fundamentals and applications* (pp. 7-240). New Jersey: John Wiley & Sons Inc.
- Migdal-Mikuli, A., Mikuli, E., Dziembaj, R., Majda, D., & Hetmanczyk, L. (2004). Thermal decomposition of [Mg(NH₃)₆](NO₃)₂, [Ni(NH₃)₆](NO₃)₂ and [Ni(ND₃)₆](NO₃)₂. *Thermochimica Acta*, 419 (No. 1-2), 223-229.
- Mishra, S., Bajpai, R., Katare, R., & Bajpai, A.K. (2006). Preparation, characterization and microhardness study of semi interpenetrating polymer networks of polyvinyl alcohol and crosslinked polyacrylamide. *Journal of Materials Science: Materials in Medicine*, 17, 1305-1313.

- Mojiminiyi, F.B.O., Dikko, M., Muhammad, B.Y., Ojobor, P.D., Ajagbonna, O.P., Okolo, R.U., Igbokwe, U.V., & Anga, T.J. (2007). Antihypertensive effect of an aqueous extract of the calyx of *Hibiscus sabdariffa*. *Fitoterapia*, *78*, 292–297.
- Nugent, M.J.D., Hanley, A., Tomkins, P.T., & Higginbotham, C.L. (2005). Investigation of a novel freeze-thaw process for the production of drug delivery hydrogels. *Journal of Materials Science: Materials in Medicine*, *16*, 1149-1158.
- Odigie, I.P., Ettarh, R.R., & Adigun, S.A. (2003). Chronic administration of aqueous extract of *Hibiscus sabdariffa* attenuates hypertension and reverses cardiac hypertrophy in 2K-1C hypertensive rats. *Journal of Ethnopharmacology*, *86*, 181–185.
- Ohta, N., & Robertson, A.R. (2005). *Colorimetry: fundamentals and applications*. West Sussex: John Wiley & Sons, Inc.
- Omar, N.M. & Ahmad, A.H. (2009). Characteristics of paint systems prepared from dammar with the addition of natural pigment. *Polymers Advanced Technologies*, *20*, 161-164.
- Ortelt, M. (1998). Solvents. In D. Stoye & W. Freitag (Eds.), *Paints, coatings and solvents* (pp. 277-373). Burghausen, Germany: Wiley-VCH.
- Ozela, E.F., Stringheta, P.C., & Chauca, M.C. (2007). Stability of anthocyanin in spinach vine (*Basella rubra*) fruits. *Ciencia e Investigacion Agraria*, *34* (2), 115-120.
- Pala, C.U., & Toklucu, A.R. (2011). Effect of UV-C light on anthocyanin content and other quality parameters of pomegranate juice. *Journal of Food Composition and Analysis*, *24*, 790-795.
- Patras, A., Brunton, N.P., O'Donnell, C., & Tiwari, B.K. (2010). Effect of thermal processing on anthocyanin stability in foods; mechanisms and kinetics of degradation. *Trends in Food Science & Technology*, *21*, 3-11.
- Paul, W., & Sharma, C.P. (1997). Acetylsalicylic acid loaded poly(vinyl alcohol) hemodialysis membranes: effect of drug release on blood compatibility and permeability. *Journal of Biomaterials Science: Polymer Edition*, *8*, 755-764.
- Pavia, D.L., Lampman, G.M., Kriz, G.S., & Vyvyan, J.R. (2009). Introduction to Spectroscopy (4th ed.). Belmont, CA: Brooks/Cole.

- Peppas, N.A., Huang, Y., Torres-Lugo, M., Ward, J.H., & Zhang, J. (2000). Physicochemical Foundations and structural design of hydrogels in medicine and biology. *Annual Reviews of Biomedical Engineering*, 2, 9-29.
- Pourciel, M.L., Launay, J., Sant, W., Conélera, V., Martinez, A., & Temple-Boyer, P. (2003). Development of photo-polymerisable polyvinyl alcohol for biotechnological applications. *Sensors and Actuators B*, 94 (3), 330-336.
- Prencesti, E., Berto, S., Daniele, P.G., & Toso, S. (2007). Antioxidant power quantification of decoction and cold infusions of Hibiscus sabdariffa flowers. *Food Chemistry*, 2, 433-438.
- Priyadarshini, E. & Tulpule, P.G. (1978). Relationship between fungal growth and aflatoxin production in varieties of maize and groundnut. *Journal of Agricultural and Food Chemistry*, 26 (1), 249-252.
- Quina, F.H., Moreira Jr., P.F., Vautier-Giongo, C., Rettori, D., Rodrigues, R.F., Freitas, A.A. , et al. (2009). Phytochemistry of anthocyanins and their biological role in plant tissues. *Pure Applied Chemistry*, 82, 1687-1694.
- Ramesh, K., Osman, Z., & Arof, A.K. (2007). Studies on the properties of silicone resin blend materials for corrosion protection. *Anti-Corrosion Methods and Materials*, 54, 99-102.
- Ramesh, K., Osman, Z., Arof, A.K., Vengadaesvaran, B., & Basirun, W.J. (2008). Structural and corrosion analyses of coatings containing silicone-polyester resins. *Pigment and Resin Technology*, 37, 37-41.
- Reeslev, M. & Kjølner, A. (1995). Comparison of biomass dry weights and radial growth rates of fungal colonies on media solidified with different gelling compounds. *Applied and Environmental Microbiology*, 61 (12), 4236-4239.
- Sanmartin, P., Villa, F., Silva, B., Cappitelli, F., & Prieto, B. (2011). Color measurements as a reliable method for estimating chlorophyll degradation to phaeopigments. *Biodegradation*, 22, 763-771.
- Saxena, S.K. (2004). Polyvinyl alcohol (PVA): Chemical and technical assessment (CTA). 61st Joint FAO/WHO Expert Committee on Food Additives, 61, 1-3.
- Schanda, J. (2007). CIE Colorimetry. In J. Schanda (Ed.), *Colorimetry: understanding the CIE system* (pp. 25-78). New Jersey: John Wiley & Sons, Inc.

- Schuman, T., Wikström, M., & Rigdahl, M. (2004). Coating of surface-modified papers with poly(vinyl alcohol). *Surface and coatings technology*, 183 (1), 96-105.
- Schweitzer, P.A. (Eds). (2006). *Paint and coatings: applications and corrosion resistance*. Boca Raton, Finl: CRC Press.
- Setareh, P., Heidari, R., Ghasemifar, E., & Jamei, R. (2007). Effect of heating, UV irradiation and pH on stability of the anthocyanin copigment complex. *Pakistan Journal of Biological Sciences*, 10 (2), 267-272.
- Smith, B.C. (1996). *Fundamentals of Fourier transform infrared spectroscopy*. Boca Raton: CRC Press.
- Smith, B.C. (1999). *Infrared spectral interpretation: a systematic approach*. Boca Raton: CRC Press.
- Sudhamani, S.R., Prasad, M.S., & Udaya Sankar, K. (2003). DSC and FTIR studies on Gellan and Polyvinyl alcohol (PVA) blend films. *Food Hydrocolloids*, 17, 245-250.
- Sutton, L.M. & Starzyk, M.J. (1973). Procedure and analysis of a useful method in determining mycelial dry weights from agar plates. *Applied Microbiology*, 24 (6), 1011-1012.
- Tomišić, V., Butorac, V., Viher, J., & Simeon, V. (2005). Comparison of the temperature effect on the $\pi^* \leftarrow n$ and $\pi^* \leftarrow \pi$ electronic transition bands of $\text{NO}_3^-(\text{aq})$. *Journal of Solution Chemistry*, 34, 613-616.
- Tsai, P. McIntosh, J., Pearce, P., Camden, B., & Jordan, B.R. (2002). Anthocyanin and antioxidant capacity in roselle (*Hibiscus sabdariffa* L.) extract. *Food Research International*, 35 (4), 351-356.
- Tsai, P. & Huang, H. (2004). Effect of polymerization on the antioxidant capacity of anthocyanins in Roselle. *Food Research International*, 37, 313-318.
- Tullo, A.H. (2004). Paints and coatings: Industrial coatings market is beginning to recover as companies mull new markets and technologies. *Chemical Engineering News*, 82(42), 25-31.
- Valeur, B. (2002). *Molecular fluorescence: principles and applications*. Weinheim, Germany: Wiley-VCH.

- Vengadaesvaran, B. (2003). Investigation on the properties of silicone resins blending with acrylic polyol resins. PhD Thesis, University of Malaya, Kuala Lumpur.
- Vengadaesvaran, B., Rau, S.R., Ramesh, K., Puteh, R., & Arof, A.K. (2010). Preparation and characterization of phenyl silicone-acrylic polyol coatings. *Pigment and Resin Technology*, 39, 283-287.
- Wagner, H. (1985). New plant phenolics of pharmaceutical interest. In van Sumere, C.F. & Lea, P.J. (Eds.), *Annual Proceedings of Phytochemical Society of Europe* (pp. 409-425). Oxford: Clarendon Press.
- Wampler, T.P. (2007). Analytical pyrolysis: an overview. In T.P. Wampler (Ed.), *Applied pyrolysis handbook 2ed.* (pp. 1-26). Boca Raton: CRC Press.
- Warnon, J. (2004). Present and Future Coatings Legislation and the Drive to Compliance. In A. Marrion (Ed.), *The Chemistry and Physics of Coatings* (pp. 8-25). Cambridge, UK: The Royal Society of Chemistry.
- Weldon, D.G. (2009). *Failure analysis of paints and coatings*. West Sussex, UK: John Wiley & Sons, Inc.
- Wicks, Z.W. Jr., Jones, F.N., Pappas, S.P., & Wicks, D.A. (2007). *Organic coatings: science and technology*. New Jersey: John Wiley & Sons, Inc.
- Wong, P., Yusof, S., Ghazali, H.M., & Che Man, Y.B. (2002). Physico-chemical characteristics of roselle (*Hibiscus sabdariffa* L.). *Nutrition and Food Science*, 32 (2), 68-73.
- Wrolstad, R.E. (2004). Anthocaynin pigments – bioactivity and coloring properties. *Journal of Food Science*, 69, 419-421.
- Xu, H., Kuo, S., & Chang, F. (2002). Significant glass transition temperature increase based on polyhedral oligomeric silsequioxane (POSS) copolymer through hydrogen bonding. *Polymer Bulletin*, 48, 469-474.
- Yang, Z., Han, Y., Gu, Z., Fan, G., & Chen, Z. (2008). Thermal degradation kinetics of aqueous anthocyanins and visual color of purple corn (*Zea mays* L.) cob. *Innovative Food Science and Emerging Technologies*, 9, 341-347.
- Yawadio, R. & Morita, N. (2007). Color enhancing effect of carboxylic acids on anthocyanins. *Food Chemistry*, 105, 421-427.

Young, T.H., Chuang, W.Y. Yao, N.K., Chen, L.W. (1996). Evaluation asymmetric poly(vinyl alcohol) membranes for use in artificial islets. *Biometaterials*, *17*, 2139-2145.

Yuhas, S.A.Jr. (1995). Solvents. In J.V. Koleske (Ed.), *Paint and Coating Testing Manual: Fourteenth Edition of the Gardner-Sward Handbook* (pp. 125-155). Philadelphia: ASTM.

Zhu, H., Zeng, H., Subramaniam, V., Masarapu, C., Hung, K., & Wei, B. (2008). Anthocyanin-sensitized solar cells using carbon nanotube films as counter electrodes. *Nanotechnology*, *19*, 1-5.